Studying Many-Body Physics through Quantum Coding Theory

by

Beni Yoshida

B.S., The university of Tokyo (2007)

Submitted to the Department of Physics
in partial fulfillment of the requirements for the degree of

Doctor of Philosophy in Physics

at the

MASSACHUSETTS INSTITUTE OF TECHNOLOGY

June 2012

Author .....
Department of Physics
May 2, 2012

Certified by .....
Edward H. Farhi
Cecil and Ida Green Professor of Physics
Thesis Supervisor

Accepted by .....
Krishna Rajagopal
Professor of Physics
Associate Department Head for Education

Studying Many-Body Physics through Quantum Coding Theory

by

Beni Yoshida

Submitted to the Department of Physics
on May 2, 2012, in partial fulfillment of the
requirements for the degree of
Doctor of Philosophy in Physics

Abstract

The emerging closeness between correlated spin systems and error-correcting codes enables us to use coding theoretical techniques to study physical properties of many-body spin systems. This thesis illustrates the use of classical and quantum coding theory in classifying quantum phases arising in many-body spin systems via a systematic study of stabilizer Hamiltonians with translation symmetries.

In the first part, we ask what kinds of quantum phases may arise in gapped spin systems on a D-dimensional lattice. We address this condensed matter theoretical question by giving a complete classification of quantum phases arising in stabilizer Hamiltonians at fixed points of RG transformations for $D = 1, 2, 3$. We found a certain dimensional duality on geometric shapes of logical operators where m-dimensional and $(D - m)$-dimensional logical operators always form anti-commuting pairs (m is an integer). We demonstrate that quantum phases are completely classified by topological characterizations of logical operators where topological quantum phase transitions are driven by non-analytical changes of geometric shapes of logical operators. As a consequence, we argue that topological order is unstable at any non-zero temperature and self-correcting quantum memory in a strict sense may not exist where the memory time is upper bounded by some constant at a fixed temperature, regardless of the system size. Our result also implies that topological field theory is the universal theory for stabilizer Hamiltonians with continuous scale symmetries.

In the second part, we ask the fundamental limit on information storage capacity of discrete spin systems. There is a well-known theoretical limit on the amount of information that can be reliably stored in a given volume of discrete spin systems. Yet, previously known systems were far below this theoretical limit. We propose a construction of classical stabilizer Hamiltonians which asymptotically saturate this limit. Our model borrows an idea from fractal geometries arising in the Sierpinski triangle, and is a rare manifestation of limit cycle behaviors with discrete scale symmetries in real-space RG transformations, which may be beyond descriptions of topological field theory.

Thesis Supervisor: Edward H. Farhi
Title: Cecil and Ida Green Professor of Physics

Acknowledgment

First and foremost, I would like to thank my PhD advisors, Eddie Farhi and Peter Shor. Eddie has been an excellent teacher and mentor with openness to new ideas, and granted me freedom for research, but with an eye toward my growth as a scientist. Peter is the smartest person I have ever met in my life, and his brilliant mathematical insights will have a lasting impact on my career as a researcher. I also want to thank Ike Chuang for encouragement and support during two years when I was at his group. Without his help, none of the work in this thesis would have been possible. Finally, I would like to thank Patrick Lee for being a thesis committee member.

I am deeply grateful to researchers of various fields from all over the world. I would like to thank Sergey Bravyi, Oliver Buerschaper, Ignacio Cirac, Jeongwan Haah, Alioscia Hamma, Patrick Hayden, Isaac Kim, Spiros Michalakis, Fernando Pastawski, John Preskill, Barbara Terhal, Masahito Ueda and Zenghang Wang for everything I learned from them. I have been fortunate to have so many productive travel opportunities during my PhD studies. Thanks to Daniel Gottesman, Michele Mosca and Akimasa Miyake for inviting me to the Perimeter institute. Thanks to Fernando Pastawski and Ignacio Cirac for inviting me to the Max-Planck Institute in Munich. Thanks to John Preskill for inviting me to Caltech and Zhenghan Wang for inviting me to Microsoft Station Q. Special thanks go to Jonas Mlynek, Andreas Wallraff, Yasunobu Nakamura and Hideo Kosaka for all the helps at ETH Zurich.

Among many friends I had the pleasure to meet at MIT, Yusuke Nishida deserves a special comment for encouragement and mentoring. Special thanks go to Sam Ocko for wonderful collaboration and for checking my English writing so many times. I would like to thank all other friends and colleagues at MIT (and Harvard) who made these years memorable, including: Xie Chen, Byron Drury, Shelby Kimmel, Takuya Kitagawa, Chris Laumann, Cedric Lin, Han-Hsuan Lin, Andy Lutomirski, Ramis Movassagh, Haruka Tanji and many others too numerous to mention.

I have been fortunate to have so many wonderful memories at MIT thanks to supports from wonderful mentors, staff and friends. I would like to thank Dave Pritchard for being my academic advisor for five years. I am also deeply thankful to administrative staff in physics department at MIT. I have been financially supported by wonderful people with love for science. I want to thank Riccardo DiCapua for the summer research fellowship and George Elbaum for the Whiteman fellowship. I also want to thank the Nakajima foundation for their support.

Despite living in a foreign city, far from my home town, I have never felt alone thanks to Megumi Matsutani. Without her love, I would not have made it this far.

Contents

Chapter 1

Introduction

In recent years, ideas from quantum information science have become increasingly useful in condensed matter physics. In particular, it has been realized that many interesting physical systems in condensed matter physics may be described in the language of quantum coding schemes such as the stabilizer formalism. Notable examples include ferromagnetic systems, non-chiral topologically ordered systems [1, 2] and spin glasses [3]. What is emerging is a closeness between the two fields, which is a result of the intrinsic similarity between quantum correlations, as studied in condensed matter physics, and entanglement, as studied in quantum information science.

This fascinating similarity between two fields provides us with an exciting new avenue for an application of classical and quantum coding theory;

-*One may address various problems in many-body physics through coding theory.*

This thesis is an attempt to demonstrate the usefulness of coding theory in solving some interesting problems which are at the interface between physics and information science.

1.1 Many-body spin system as a quantum code

The underlying difficulty in quantum information science is the fact that quantum entanglement decays easily, and one needs to protect a qubit from decoherence. A remarkable solution to this problem, proposed by Shor, is to encode a qubit into many-body entangled states such that errors do not destroy an encoded logical qubit [4]. This beautiful art of protecting a qubit from decoherence, called *quantum coding theory*, constitutes the underlying building block for fault-tolerant realizations of quantum information theoretical ideas.

With a hope for physical realizations of quantum codes, one may be naturally led to the following question:

-*What kinds of many-body spin systems work as quantum error-correcting codes?*

The answer to this question is surprisingly simple; in principle, *an arbitrary correlated spin system with degenerate ground states and a finite energy gap can be used as a quantum error-correcting code* (Fig. 1-1). To appreciate this point, consider a pair of degenerate ground states which are separated from other excited states by a finite energy gap Δ. Here, we label one of the ground states as $|\tilde{0}\rangle$ and the other one as $|\tilde{1}\rangle$. Then, a "qubit" can be encoded inside the energy ground space as a superposition state $\alpha|\tilde{0}\rangle + \beta|\tilde{1}\rangle$. Since an encoded qubit is separated from excited states by a finite energy gap Δ, such a quantum memory encodes a qubit securely if $k_B T \ll \Delta$ and some error-correcting procedure is available.

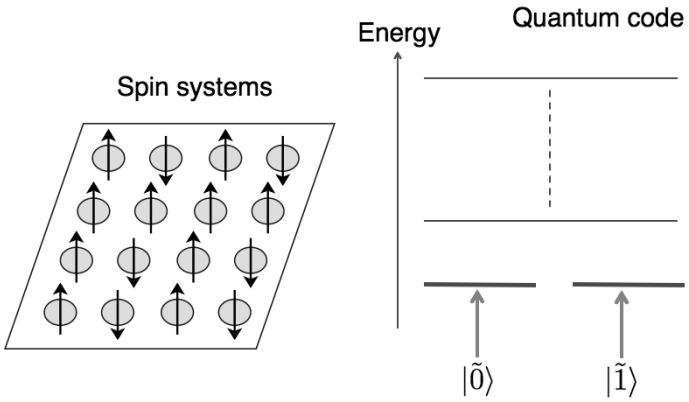

Figure 1-1: Correlated spin systems as quantum codes.

This observation hints the intrinsic closeness between quantum error-correcting codes and correlated spin systems. In condensed matter physics, one wishes to study physical properties of ground states, such as quantum correlations, arising in gapped spin systems. In quantum coding theory, one hopes to study coding properties of ground states, such as quantum entanglement, arising in gapped spin systems. Therefore, one may take a slight liberty and say the following:

-Studying physical properties of correlated spin systems is fundamentally akin to studying coding properties of quantum codes which are physically realized as gapped ground states.

Ferromagnet as a classical code: At this point, one may wonder what exactly quantum codes are. Here, we start by looking at how *classical* codes work. The goal of classical coding theory is to encode bits of information such that encoded logical bits will not be lost even in the presence of noises and errors. The simplest approach of encoding a bit of information is to encode 0 as a repetition of 0s and 1 as a repetition of 1s:

$$0 \ \rightarrow \ 000\cdots0, \qquad 1 \ \rightarrow \ 111\cdots1. \tag{1.1}$$

Now, assume that we initially encode 0 into $000\cdots0$. Then, even if some of the entries are flipped from 0 to 1 due to thermalization or communication error, one can

reliably recover the originally encoded information as long as no more than a half of entries are flipped.

This repetition code is exactly the same as a ferromagnet discussed in condensed matter physics community. Consider the following system Hamiltonian

$$H \;=\; -\sum_j Z_j Z_{j+1} \tag{1.2}$$

where Z_j is a Pauli matrix acting on jth spin. Since the Hamiltonian favors states with aligned spins, ground states are

$$|\uparrow\uparrow\uparrow\cdots\uparrow\rangle, \qquad |\downarrow\downarrow\downarrow\cdots\downarrow\rangle. \tag{1.3}$$

Upon identifying $\uparrow$ as 0 and $\downarrow$ as 1, we notice that this ferromagnetic Hamiltonian is a physical realization of the repetition code.

The repetition code is resilient against errors acting on "codewords" $000\cdots0$ and $111\cdots1$. Then, ground states of a ferromagnet are resilient against what? It turns out that a ferromagnet is stable against *quantum fluctuations*. Consider the following perturbed Hamiltonian:

$$H \;=\; -\sum_j Z_j Z_{j+1} - \epsilon \sum_j X_j \tag{1.4}$$

where the Pauli matrix X_j mixes up $|\uparrow\rangle$ and $|\downarrow\rangle$, and ϵ is meant to be small. As a result of perturbation, a ground state of this Hamiltonian is not $|\uparrow\uparrow\uparrow\cdots\uparrow\rangle$ or $|\downarrow\downarrow\downarrow\cdots\downarrow\rangle$ anymore. Yet, the effect of perturbation is small as seen from a perturbative analysis where the effect of perturbation will be exponentially suppressed since the unperturbed ground states $|\uparrow\uparrow\uparrow\cdots\uparrow\rangle$ and $|\downarrow\downarrow\downarrow\cdots\downarrow\rangle$ are connected only by nth order perturbative contributions where n is the total number of spins. Therefore, physical properties of the perturbed Hamiltonian are close to the unperturbed ones, and a ferromagnetic phase is said to be stable against quantum fluctuations at the thermodynamic limit where n goes to infinity.

The underlying reason why a ferromagnetic phase is stable against quantum fluctuations is because the *distance* between two ground states $|\uparrow\uparrow\uparrow\cdots\uparrow\rangle$ and $|\downarrow\downarrow\downarrow\cdots\downarrow\rangle$ is very large where all of the n entries are different. This is also exactly the reason why the repetition code is resilient against errors. Therefore, in a classical error-correcting code and its physical realization as a ferromagnet, the reliability of encoding and the stability of ground states against quantum fluctuations are essentially the same thing ! This observation may further hint that classifications of error-correcting codes may eventually lead to classification of quantum phases arising in gapped spin systems.

Quantum code: However, the repetition code (or a ferromagnet) does not work as a quantum code in practice. If we were to use the repetition code as a quantum code, one would encode a quantum state $|0\rangle$ as $|000\cdots0\rangle$ and a quantum state $|1\rangle$ as $|111\cdots1\rangle$. Then, a quantum state $\frac{1}{\sqrt{2}}(|0\rangle+|1\rangle)$ would be encoded as a so-called *cat state* $\frac{1}{\sqrt{2}}(|000\cdots0\rangle+|111\cdots1\rangle)$ due to the superposition principle. Yet, this cat

state is known to be fragile against *phase errors*. Indeed, if a phase error, represented as follows

$$|0\rangle \ \rightarrow \ |0\rangle \qquad |1\rangle \ \rightarrow \ -|1\rangle \tag{1.5}$$

occurs, a cat state will change to $\frac{1}{\sqrt{2}}(|000\cdots0\rangle - |111\cdots1\rangle)$ which correspond to $\frac{1}{\sqrt{2}}(|0\rangle - |1\rangle)$ in a logical qubit, and the originally encoded quantum information will be lost. Therefore, the repetition code is stable against bit-flip errors ($|0\rangle \rightarrow |1\rangle$ and $|1\rangle \rightarrow |0\rangle$), but is unstable against phase errors.

In order to create a quantum code which is resilient against errors, one needs to find a pair of two orthogonal states $|\tilde{0}\rangle$ and $|\tilde{1}\rangle$ where "$|\tilde{0}\rangle$ and $|\tilde{1}\rangle$" are separated, and "$|\tilde{0}\rangle + |\tilde{1}\rangle$ and $|\tilde{0}\rangle - |\tilde{1}\rangle$" are also separated. The simplest example of quantum codes is the nine qubit code, proposed by Shor, which encodes $|0\rangle$ and $|1\rangle$ into the following entangled states of nine qubits:

$$|\tilde{0}\rangle \ \equiv \ \frac{1}{2\sqrt{2}}(|000\rangle + |111\rangle) \otimes (|000\rangle + |111\rangle) \otimes (|000\rangle + |111\rangle) \tag{1.6}$$

$$|\tilde{1}\rangle \ \equiv \ \frac{1}{2\sqrt{2}}(|000\rangle - |111\rangle) \otimes (|000\rangle - |111\rangle) \otimes (|000\rangle - |111\rangle). \tag{1.7}$$

Codeword states $|\tilde{0}\rangle$ and $|\tilde{1}\rangle$ are stable against any types of single qubit errors. If an error happens to a qubit inside a group of (1,2,3) qubits, measurements on groups of (4,5,6) and (7,8,9) qubits allow us to reconstruct the original codeword state. Codeword states $|\tilde{0}\rangle \pm |\tilde{1}\rangle$ are also stable against any types of single qubit errors. If an error happens to a qubit inside a group of (1,2,3) qubits, measurements on (1,2,3) qubits allow us to recover the original codeword state. Therefore, the nine qubit code works as a quantum code which is stable against single qubit errors.

The above nine qubit code certainly works as a quantum error-correcting code. One can also generalize the construction of the nine qubit code to obtain a quantum code which is resilient against larger errors. Yet some questions still remain concerning physical realizations of quantum codes.

-How do we systematically construct pairs of orthogonal quantum states which are well separated?

-How do we construct a system Hamiltonian which can encode these codeword states as the energy ground states with a finite energy gap?

Stabilizer Hamiltonians: An answer to these questions was obtained by a beautiful theoretical framework, called the *stabilizer formalism*, which was invented by Gottesman [5], following constructions of the five qubit code [6, 7]. Instead of directly giving a pair of codeword states, the stabilizer formalism starts with giving a system Hamiltonian, called a *stabilizer Hamiltonian*. A stabilizer Hamiltonian is a certain class of spin Hamiltonians which are designed to be exactly solvable. Consider

the following Hamiltonian

$$H \;=\; -\sum_j S_j \tag{1.8}$$

where S_j are Pauli operators. Here, one designs interaction terms S_j such that they commute with each other

$$[S_j, S_{j'}] \;=\; 0. \tag{1.9}$$

Since one can simultaneously diagonalize S_j, the energy ground states satisfy

$$S_j|\psi\rangle \;=\; |\psi\rangle \qquad \text{for all} \;\; j \tag{1.10}$$

if one properly chooses signs of S_j. In the stabilizer formalism, the energy ground space of the above Hamiltonian is equivalent to the codeword space of a quantum code. For instance, the following choice of interaction terms leads to a ferromagnet:

$$S_1 \;=\; Z_1Z_2, \qquad S_2 \;=\; Z_2Z_3, \qquad \cdots \quad S_{n-1} \;=\; Z_{n-1}Z_n \tag{1.11}$$

while the following choice leads to the nine qubit code:

$$\begin{array}{lllllllllll}
S_1 & = & Z_1 & Z_2 & & & & & & & \\
S_2 & = & & Z_2 & Z_3 & & & & & & \\
S_3 & = & & & & Z_4 & Z_5 & & & & \\
S_4 & = & & & & & Z_5 & Z_6 & & & \\
S_5 & = & & & & & & & Z_7 & Z_8 & \\
S_6 & = & & & & & & & & Z_8 & Z_9 \\
S_7 & = & X_1 & X_2 & X_3 & X_4 & X_5 & X_6 & & & \\
S_8 & = & & & & X_4 & X_5 & X_6 & X_7 & X_8 & X_9
\end{array} \tag{1.12}$$

as one may see from direct calculations.

Logical operators: The essence of the stabilizer formalism is to design interaction terms S_j such that degenerate ground states are well separated from each other. Yet, finding the "distance" between ground states is a non-trivial task especially for strongly entangled quantum states as the ones in the nine qubit code. This difficulty can be overcome by studying a certain set of operators, called *logical operators*. Logical operators are Pauli operators which commute with the stabilizer Hamiltonian

$$[H, \ell] \;=\; 0 \tag{1.13}$$

but act non-trivially inside the codeword space (the ground space). For instance, a ferromagnet has the following pair of logical operators

$$\ell \;=\; Z_1, \qquad r \;=\; X_1X_2\cdots X_n \tag{1.14}$$

where ℓ and r act as if they are Pauli matrices on a logical qubit:

$$\ell \ : \ |\tilde{0}\rangle \ \rightarrow \ |\tilde{0}\rangle \qquad |\tilde{0}\rangle \ \rightarrow \ -|\tilde{1}\rangle \tag{1.15}$$

$$r \ : \ |\tilde{0}\rangle \ \rightarrow \ |\tilde{1}\rangle \qquad |\tilde{1}\rangle \ \rightarrow \ |\tilde{0}\rangle. \tag{1.16}$$

Similarly, the nine qubit code has the following pair of logical operators.

$$\ell \ = \ Z_1 Z_4 Z_7, \qquad r \ = \ X_1 X_2 X_3. \tag{1.17}$$

Since logical operators can transform a ground state into other ground states, the "distance" between ground states depend on sizes of logical operators. A ferromagnet has a small logical operator ℓ and a large logical operator r. As a result, the distance between $|\tilde{0}\rangle$ and $|\tilde{1}\rangle$ is large, but the distance between $|\tilde{0}\rangle + |\tilde{1}\rangle$ and $|\tilde{0}\rangle - |\tilde{1}\rangle$ is short. Therefore, it does not work as a quantum code. On the other hand, the nine qubit code has a pair of logical operators whose weights are three. Therefore, ground states are separated by the distance $d = 3$, and it works as a quantum code which is stable against any types of single qubit errors.

The goal of this thesis: We have briefly reviewed the stabilizer formalism, which is a theoretical framework to systematically construct quantum codes along with system Hamiltonians. Now, let us return to a question concerning physical properties arising in correlated spin systems. Recall that a physical realization of the repetition code is a ferromagnetic phase. Then, one may be naturally led to the following questions:

- What kinds of quantum phases may arise in stabilizer Hamiltonians?

- How do we classify quantum phases arising in stabilizer Hamiltonians?

These are exactly the questions we would like to address in this thesis.

Studying quantum phases arising in correlated spin systems, however, is a notoriously difficult problem which has been addressed in condensed matter physics community for more than a century. Indeed, calculations of ground state properties arising in systems with simple neighboring interactions could be a hard problem even for a quantum computer ! How do we circumvent this formidable challenge?

Fortunately, for stabilizer Hamiltonians, the situation is not so bad. There are a number of *coding theoretical techniques* available to study coding properties arising in stabilizer Hamiltonians. As seen in discussion on the repetition code and a ferromagnetic phase, physical properties arising in stabilizer Hamiltonians may have some coding theoretical origin such as the distance between ground states which is characterized by sizes of logical operators. Then, one may classify quantum phases arising in stabilizer Hamiltonians by classifying coding properties arising in stabilizer Hamiltonians.

The main message of this thesis is that classifications of quantum phases can be carried out by classifications of logical operators arising in stabilizer Hamiltonians.

In an informal language, the main result of the thesis can be summarized as follows:

-Different quantum phases arising in stabilizer Hamiltonians can be distinguished by geometric shapes of logical operators.

Therefore, classifications of logical operators arising in stabilizer Hamiltonians is fundamentally akin to classifications of quantum phases arising in stabilizer Hamiltonians (Fig 1-2).

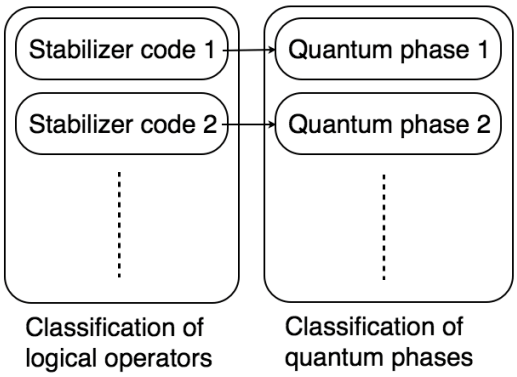

Figure 1-2: Quantum phases in stabilizer Hamiltonians.

1.2 Quantum phases in stabilizer Hamiltonians

In this section, we briefly summarize the main results of this thesis concerning quantum phases arising in stabilizer Hamiltonians in a more technical language.

Stabilizer Hamiltonians with continuous scale symmetries: In the first part of the thesis, we study quantum phases arising in a certain class of stabilizer Hamiltonians with physical realizability, called stabilizer codes with translation and continuous scale symmetries (STS models), which are constrained to the following two conditions:

- **Translation symmetries:** Stabilizer Hamiltonians remain invariant under translations on a D-dimensional lattice.
- **Continuous scale symmetries:** The number of logical qubits does not scale up with respect to the system size, and remains constant.

In other words, STS models are stabilizer Hamiltonians defined on a discrete lattice where the number of logical qubits (or degenerate ground states) is small. We note that, due to the presence of continuous scale symmetries, STS models correspond to *fixed points* of RG transformations, which is a notion often used in classifying quantum phases in condensed matter physics community.

In order to characterize and classify quantum phases, one needs to specify order parameters to distinguish different quantum phases. By recalling that quantum phases must be classified by some scale-invariant quantities or objects, one may notice that geometric shapes of logical operator can be used as "order parameters" for classifications of quantum phases arising in STS models since geometric shapes are scale-invariant. The main result concerning D-dimensional STS models is summarized as follows ($D = 1, 2, 3$):

- **Dimensional duality:** m-dimensional and $(D - m)$-dimensional logical operators form anti-commuting pairs where m are integers.

- **Quantum phases:** One can classify quantum phases arising in STS models completely by geometric shapes of logical operators.

- **Topological quantum phase transitions:** Quantum phase transitions between two different classes of STS models are driven by non-analytic changes of logical operators with different topological properties.

- **Topological deformations:** One can continuously deform geometric shapes of logical operators while keeping them equivalent. In other words, logical operators arising in STS models can be completely characterized by the notion of topology.

Therefore, we present a complete classification of quantum phases arising in STS models.

The above results on quantum phases arising in stabilizer Hamiltonians at fixed points give valuable insights on a number of interesting problems concerning many-body spin systems. As applications, we obtain the following physical results:

- **Topological order at finite temperature:** Stabilizer Hamiltonians at fixed points cannot have topological order that is stable at non-zero temperature.

- **Self-correcting quantum memory:** Stabilizer Hamiltonians at fixed points do not serve as a self-correcting quantum memory.

- **Universal theory:** Stabilizer Hamiltonians at fixed points are effectively described by topological field theory.

While our treatment is limited to models of stabilizer Hamiltonians with a small number of logical qubits, we think that similar conclusions hold for thermal stability of topological order and feasibility of self-correcting quantum memory even without continuous scale symmetries. This is essentially because the presence of a large number of ground states would lead to increasing entropic contributions at finite temperature, which would result in inducing thermal instability with a phase transition at $T = 0$ and suppressing the qubit memory time when the system size becomes large as discussed in [8].

Stabilizer Hamiltonians with discrete scale symmetries: Now, we turn to another problem concerning information storage capacity of discrete spin systems. Understanding the fundamental limit on information storage capacity of physical systems is a problem of fundamental and practical importance bridging physics and information science. There is a well-known bound on the amount of information that can be reliably stored inside the gapped energy ground space of discrete spin systems:

$$kd^{1/D} \leq O(n) \tag{1.18}$$

where k is the number of logical bits, d is the code distance of *classical* error-correcting codes, n is the total number of spins and D is the spatial dimension. Yet, previously found spin systems were far below this theoretical limit, and it remained open whether spin systems which saturate the theoretical limit may exist or not.

In the second part of the thesis, we present a positive solution to this problem by proposing a model of local stabilizer Hamiltonians which asymptotically saturate the bound. The model, called *fractal codes*, borrows an idea from fractal geometries arising in the Sierpinski triangle, and is shown to have the following coding properties

$$k \sim O(L^{D-1}), \qquad O(L^{D-\epsilon}) \leq d \leq O(L^D) \tag{1.19}$$

where L is the linear length of the system with $d = L^D$ and ϵ is an arbitrary small positive number.

Fractal codes have a large number of logical bits, and are beyond descriptions of STS models. Instead of continuous scale symmetries, fractal codes have discrete scale symmetries where ground state properties remain similar only under some specific scale transformations. As a result, fractal codes possess fractal dimensional logical operators. The presence of discrete scale symmetries also leads to a rare manifestation of limit cycle behaviors under RG transformations which implies that fractal codes may be beyond descriptions of topological field theory.

1.3 Organization of the thesis

The thesis is divided into three parts. (a) Chapter 2 presents a brief introduction to stabilizer codes and introduces a theoretical tool to address physical and coding properties of stabilizer codes. (b) Chapter 3-6 discuss a problem of searches and classifications of quantum phases at fixed points with applications to problems of feasibility of self-correcting quantum memory and thermal stability of topological order. (c) Chapter 7-8 discuss information storage capacity of discrete spin systems. The logical flow of the thesis is summarized in Fig. 1-3. Each chapter is organized as follows.

Chapter 2 - Stabilizer codes in a bi-partition

Before starting serious attempts to address problems mentioned above, we begin by developing a theoretical tool which is particularly useful for studying properties of entanglement arising in stabilizer Hamiltonians.

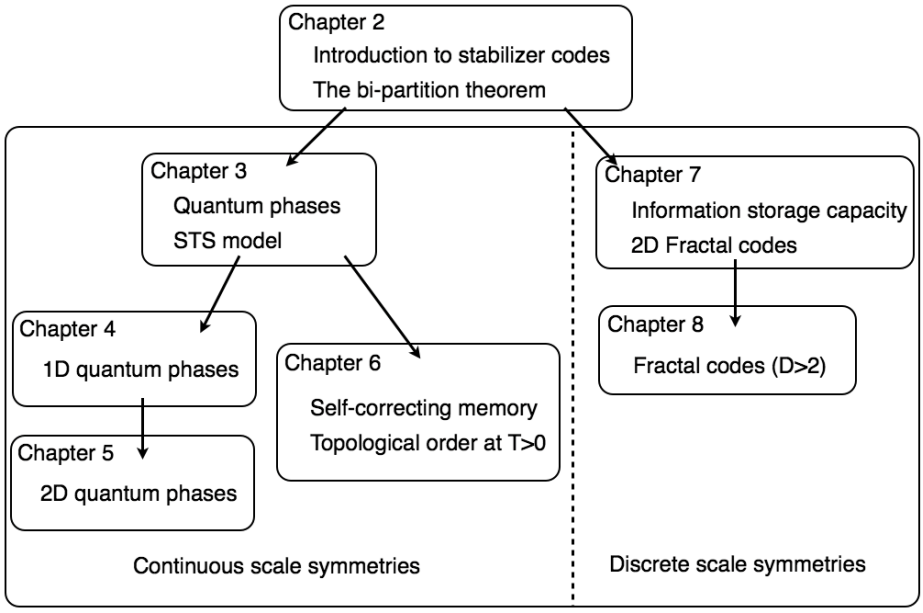

Figure 1-3: The organization of the thesis.

After a brief review of stabilizer codes, we derive a simple formula concerning a geometric duality of logical operators arising in stabilizer codes. This theoretical tool, called a *bi-partition theorem*, is found useful in addressing various problems in condensed matter physics and quantum information science. We demonstrate the usefulness of the bi-partition theorem by applying it to a problem of how the notion of topology arises in topologically ordered materials, some fundamental problems on coding properties of local stabilizer codes, and a problem of when stabilizer codes are useful for classical and quantum secret-sharing.

Chapter 3 - Classification of quantum phases and stabilizer Hamiltonians

Chapter 3 to Chapter 6 are devoted to a problem of finding and classifying fixed-point quantum phases arising in gapped spin systems.

We begin by arguing that quantum phases arising in gapped spin systems can be studied by a certain class of exactly solvable models, called *frustration-free Hamiltonians*, where ground states can be obtained by minimizing each term locally. Noticing that stabilizer Hamiltonians are the simplest class of frustration-free Hamiltonians, we introduce a model of stabilizer Hamiltonians with reasonable physical realizability. The model, called stabilizer codes with translation and continuous scale symmetries (STS models), is constrained to the following conditions; a) translation symmetries and b) continuous scale symmetries (small number of degenerate ground states).

Then, we briefly review a general idea of how to classify quantum phases by the presence of quantum phase transitions and address some challenges such as the path-dependence of the presence of phase transitions. To overcome this difficulty, we ask what kinds of objects can be used as order parameters to distin-

guish different quantum phases arising in STS models. Recalling the underlying philosophy of RG transformations, we point out that geometric shapes of logical operators can be used as order parameters of STS models since geometric shapes are scale-invariant objects.

Chapter 4 - Universal quantum phases in one-dimensional stabilizer Hamiltonians

We analyze quantum phases arising in one-dimensional STS models. We start with several specific examples of one-dimensional STS models and establish the connection between global entanglement and geometric shapes of logical operators. Then, we show that, in one-dimensional STS models, zero-dimensional and one-dimensional logical operators always form anti-commuting pairs. We point out that geometric shapes of logical operators can be used as order parameters since geometric shapes do not change under local unitary transformations.

After establishing the connection between logical operators and quantum phases, we show that the universal quantum phase in one-dimensional STS models is a ferromagnetic phase. In particular, we show the following two facts; a) When the number of logical operators are the same, two STS models belong to the same quantum phases, in a sense that there is a parameterized Hamiltonian connecting them without undergoing a quantum phase transition. 2) When the number of logical operators changes, two STS models belong to different quantum phases with the occurrence of quantum phase transitions regardless of the path connecting two models.

Chapter 5 - Two-dimensional STS model: topological phases and geometric shapes of logical operators

We continue our analysis on quantum phases arising in STS models for two-dimensional systems. We start with several specific examples of two-dimensional STS models and establish the connection between geometric shapes of logical operators and quantum phases including topological phases. We show that m-dimensional and $2-m$-dimensional logical operators form anti-commuting pairs where $m = 0, 1$. We also show that universal quantum phases in two-dimensional STS models are the Toric code and a ferromagnetic phase.

A technical difficulty arises in showing the existence of quantum phase transitions between two STS models with the same number of ground states, but with different geometric shapes of logical operators. We circumvent this difficulty by relating the presence of quantum phase transitions to the presence of non-analyticity associated with topological changes of geometric shapes of logical operators by borrowing an idea from theory of adiabatic continuation.

Chapter 6 - Feasibility of self-correcting quantum memory and thermal stability of topological order

Before starting an analysis on three-dimensional STS models, we turn to problems of feasibility of self-correcting quantum memory and thermal stability of

topological order. We begin by reviewing how self-correcting memory works and discussing why feasibility of self-correcting quantum memory is an important open problem in quantum information science community. Then we review the notion of topological order and its thermal stability, and formally define topological order both at zero temperature and finite temperature. Then, we ask whether there exists a topologically ordered system which is stable at finite temperature or not.

Given these two important open problems, our approach is as follows. We first argue that thermal stability of topological order and self-correcting properties are fundamentally akin to each other. Then, we address these two problems simultaneously by utilizing the solution of three-dimensional STS models. We show that m-dimensional and $3-m$-dimensional logical operators form anti-commuting pairs where $m = 0, 1$. As a result, one can show that three-dimensional STS models have only constant energy barriers between degenerate ground states, which implies that topological order arising in three-dimensional models are thermally fragile, and the system does not work as a self-correcting quantum memory. The assumption of continuous scale symmetries is justified by investigating the relation between the memory time and the number of ground states and local minima. Finally, we interpret our result on thermal instability of topological order in the context of the Schrödinger's cat.

Chapter 7 - Information storage capacity of discrete spin systems

Chapter 7-8 are devoted to a problem concerning information storage capacity of discrete spin systems.

We start with reviewing a theoretical limit, derived by Bravyi, Terhal and Poulin, on the amount of stored information, denoted by k, and the reliability of encoding, quantified by the distance d; $kd^{1/D} \leq O(n)$. Then, we give a construction of local stabilizer Hamiltonians, called *fractal codes*, which asymptotically saturate this theoretical limit. Fractal codes have a large number of ground states with fractal spin configurations which are similar to the Sierpinski triangle. We introduce a theoretical tool to lower bound the distance between codewords (ground states) and prove that fractal codes asymptotically saturate the theoretical limit.

Chapter 8 - Higher-dimensional fractal codes

We continue our discussion on information storage capacity of discrete spin systems for $D > 2$. Our extension utilizes higher-dimensional versions of the Sierpinski triangle. We introduce some theoretical tool to lower bound the distance, and show that fractal codes saturate the theoretical limit for arbitrary $D \geq 2$.

The technical goal of this thesis is to determine all the possible quantum phases arising in stabilizer Hamiltonians with translation symmetries:

$$H \;=\; -\sum_{\mathbf{r}} S_{\mathbf{r}} \qquad T_m(H) \;=\; H \tag{1.20}$$

where T_m represents a translation operator in the $\hat{m}$ direction on a lattice (which may be a unit translation or some finite translation). Fig. 1-4 summarizes our contributions toward this goal.

	Continuous scale symmetries		Discrete scale symmetries	
	classical	quantum	classical	quantum
1 dim	Chapter 4 Ferromagnet	N/A	N/A	N/A
2 dim	Chapter 5 Ferromagnet	Chapter 5 Toric code	Chapter 7 Fractal code	N/A
3 dim	Chapter 6 Ferromagnet	Chapter 6 Toric code	Chapter 8 Fractal code	Cubic code

Figure 1-4: Quantum phases in stabilizer Hamiltonians with translation symmetries. This thesis provides a characterization of quantum phases in shaded entries of the table.

Here we classified stabilizer Hamiltonians into two types in terms of scale symmetries. The first type of stabilizer Hamiltonians possesses the so-called *continuous scale symmetries*. Roughly speaking, systems with continuous scale symmetries are scale invariant, and their coding and physical properties remain the same under any scale transformations. Such systems are known to correspond to fixed points of RG transformations and are described by topological field theory as discussed in this thesis. The second type of stabilizer Hamiltonians possesses the so-called *discrete scale symmetries*. Unlike continuous scale symmetries, systems with discrete scale symmetries remain scale-invariant only under some discrete set of scale transformations. Such systems are known to correspond to limit cycles of RG transformations, and exhibits glassy behaviors with fractal spin configurations [9].

The STS model, stabilizer codes with translation and continuous scale symmetries, covers all the stabilizer Hamiltonians with continuous scale symmetries. Chapter 3-6 are devoted to the analysis on STS models. Fractal codes introduced in Chapter 7-8 are examples of stabilizer Hamiltonians with discrete scale symmetries. We note that a cubic code proposed by Haah [10] is an example of quantum codes with discrete scale symmetries which is beyond the scope of this thesis.

Comments: Some comments on the thesis follow. Mathematical rigor is a virtue, but so is physical intuition. Substantial parts of mathematical proofs in the original

papers are skipped in this thesis. Readers interested in mathematical proofs are urged to look at the original four papers with which this thesis is written [11, 12, 13, 14]. Bombin's work on two-dimensional stabilizer Hamiltonians is also helpful [15]. A more mathematical viewpoint on stabilizer Hamiltonians with translation symmetries is given in Haah's recent work [16]. This thesis is meant to be accessible to anyone familiar with the basics of quantum mechanics and written as self-consistently as possible. We hope that this thesis may also serve as a modern introduction to the stabilizer formalism for physicists.

Chapter 2

Stabilizer codes in a bi-partition

To analyze non-local correlations arising in many-body systems, one often considers a bi-partition of the entire system into two complementary regions A and $B = \bar{A}$. For instance, entanglement entropy, an information theoretical quantity which measures the amount of entanglement between A and B, provides valuable insights on properties of correlated many-body systems [17, 18, 19, 20, 21, 22, 23, 24]. The notion of entanglement entropy, however, is defined only for a single state $|\psi\rangle$, and is not directly applicable to systems with multiple ground states such as quantum codes. Indeed, many of interesting condensed matter systems, such as magnets and topologically ordered materials, have degenerate ground states which may have different values of entanglement entropies inside the energy ground space. Thus, the need is to create a theoretical tool to analyze entanglement arising in systems with degenerate ground states.

The most striking difference between a single state $|\psi\rangle$ and a system with degenerate ground states, such as a stabilizer code, is the existence of a *logical operator* ℓ. In the language of condensed matter physics, logical operators represent hidden "symmetries" of the system and may characterize non-local correlations of degenerate ground states since they commute with the Hamiltonian:

$$[H, \ell] \;=\; 0. \tag{2.1}$$

In the language of coding theory, logical operators represent non-trivial transformations between degenerate ground states and characterize quantum entanglement. Therefore, one naturally hopes to create a theoretical tool to analyze non-local properties of logical operators in a bi-partition.

In this chapter, we present a theoretical tool to analyze logical operators of stabilizer codes in a bi-partition. The theoretical tool, called a *bi-partition theorem*, reveals a geometric duality on logical operators and becomes a powerful tool to analyze properties of entanglement and non-local correlations appearing in various interesting problems of condensed matter physics and quantum information theory. To demonstrate the power of the bi-partition theorem, we apply the theorem to three problems; how the notion of "topology" arises in topologically ordered systems, some fundamental problem concerning coding properties of local stabilizer codes, and a

problem of when a stabilizer code is useful for classical and quantum secret-sharing. Extensions to other degenerate spin systems are also discussed briefly.

Comment: This chapter may serve as an introduction to stabilizer codes and the notion of logical operators. Several examples of stabilizer codes are discussed here. Some of main results of this thesis are also "hinted" in this chapter. Studies on entanglement properties arising in stabilizer codes are initiated in [25, 26]. A systematic study of stabilizer code in a bi-partition was also made from a different perspective [27].

2.1 Stabilizer code and logical operators

We start by giving a review of a stabilizer code which is a basic theoretical framework to discuss quantum error-correcting codes [5].

Stabilizer group: A stabilizer code can be characterized by an Abelian subgroup of Pauli operators. Consider an n qubit system and the Pauli operator group

$$\mathcal{P} \;=\; \langle iI, X_1, Z_2, \ldots, X_n, Z_n \rangle \tag{2.2}$$

which is generated by Pauli operators X_j and Z_j acting on single qubits labeled by $j = 1, \cdots, n$. A stabilizer code is defined with the *stabilizer group*

$$\mathcal{S} \;=\; \langle S_1, S_2, \cdots, S_{n-k} \rangle \;\subset\; \mathcal{P}, \tag{2.3}$$

which is a self-adjoint Abelian subgroup of the Pauli operator group $\mathcal{P}$ without containing iI or $-I$. S_j represent independent generators for $\mathcal{S}$, and elements in the stabilizer group $\mathcal{S}$ are called *stabilizers*. Qubits are encoded in a subspace $V_{\mathcal{S}}$ spanned by states $|\psi\rangle$ which satisfy

$$S_j|\psi\rangle \;=\; |\psi\rangle \qquad \text{for all} \;\; j \tag{2.4}$$

where $V_{\mathcal{S}}$ is called the *codeword space* of the stabilizer code. In total, k qubits can be encoded in $V_{\mathcal{S}}$, and encoded qubits are called *logical qubits*.

In the stabilizer formalism, there exists a system Hamiltonian which can support the encoded states as degenerate ground states with a finite energy gap (Fig. 2-1). If a Hamiltonian

$$H \;=\; -\sum_j S_j \tag{2.5}$$

satisfies $\langle \{S_j, \forall j\} \rangle = \mathcal{S}$, the ground state space of the Hamiltonian is the same as the codeword space $V_{\mathcal{S}}$ since the energy of the system can be minimized for states satisfying $S_j|\psi\rangle = |\psi\rangle$. In principle, *stabilizer codes with geometrically local stabilizer generators S_j are physically realizable.* There are 2^k degenerate ground states where k logical qubits can be encoded since each constrain in Eq. (2.4) picks up one state

out of two states.

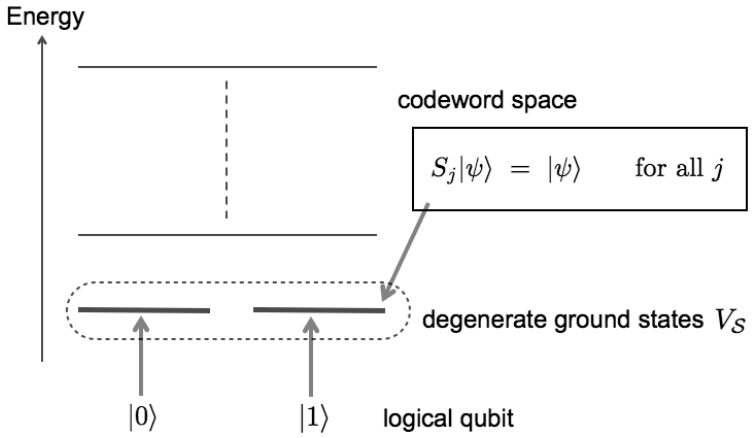

Figure 2-1: Physical realization of a stabilizer code via a stabilizer Hamiltonian. The codeword space is realized as the ground space of a gapped Hamiltonian where degenerate ground states are labelled as $|0\rangle$ and $|1\rangle$ which forms a logical qubit.

Logical operators: In analyzing coding and physical properties of stabilizer codes, *logical operators* become important. Logical operators are Pauli operators $\ell \in \mathcal{P}$ which satisfy

$$[\ell, S_j] = 0 \quad \text{for all} \quad j \qquad \text{and} \qquad \ell \notin \langle iI, \mathcal{S} \rangle. \tag{2.6}$$

Since logical operators commute with all the stabilizers, they transform a state inside $V_{\mathcal{S}}$ into another state inside $V_{\mathcal{S}}$. In other words, since logical operators commute with the Hamiltonian, they do not change the energy of the system, and they transform a ground state to another ground state inside the ground space $V_{\mathcal{S}}$.

Two logical operators ℓ and ℓ' are said to be *equivalent* if and only if ℓ and ℓ' act in a similar way inside the ground state space:

$$\begin{aligned} \ell \sim \ell' \qquad &\Leftrightarrow \qquad \ell|\psi\rangle = \ell'|\psi\rangle \quad \text{for all} \quad |\psi\rangle \in V_{\mathcal{S}} \\ &\Leftrightarrow \qquad \ell\ell' \in \langle \mathcal{S} \rangle \end{aligned} \tag{2.7}$$

where "$\sim$" represents the equivalence between logical operators ℓ and ℓ'. For instance, $\ell \sim \ell S_j$. Given a set of logical operators $\mathbf{L}$, all the logical operators inside $\mathbf{L}$ are said to be *independent* when

$$\langle \{\forall l \in \mathbf{L}\} \rangle \cap \mathcal{S} = \emptyset. \tag{2.8}$$

Here, "$\emptyset$" represents a null set.

The code distance is a measure of the reliability of encoding:

$$d = \min(w(U)) \qquad \text{where} \quad U \in \mathcal{C} \quad \text{and} \quad U \notin \langle iI, \mathcal{S} \rangle. \tag{2.9}$$

Here, $w(U)$ is the number of non-trivial Pauli operators in U. The code distance corresponds to a minimal number of single Pauli errors necessary to destroy a encoded qubit. Roughly speaking, a large code distance d for fixed n means that the code can encode qubits reliably. *When the code distance d is large, degenerate ground states are highly entangled* such that there is no local operator which connects a pair of degenerate ground states. As a result, the ground state properties of good stabilizer codes are known to be stable against any types of small local perturbations [28].

Canonical representation: Logical operators can be found in the centralizer group which consists of all the Pauli operators commuting with stabilizers:

$$\mathcal{C} \;=\; \Big\langle \Big\{ \; U \in \mathcal{P} : [U, S_j] = 0, \;\; \text{for all } j \; \Big\} \Big\rangle. \tag{2.10}$$

The centralizer group can be concisely represented in a *canonical form* [11]:

$$\mathcal{C} \;=\; \left\langle \begin{array}{ccccccc} \ell_1, & \cdots, & \ell_k, & S_1, & \cdots, & S_{n-k} \\ r_1, & \cdots, & r_k, & & & \end{array} \right\rangle \tag{2.11}$$

where each operator represents independent generators for $\mathcal{C}$. Pairs of generators ℓ_p and r_p anti-commute with each other while any other pair of generators commute with each other. For example, $\{\ell_p, r_p\} = 0$ while $[\ell_p, r_q] = 0$ for $p \neq q$. Pairs of anti-commuting generators ℓ_p and r_p ($p = 1, \cdots, k$) are independent logical operators in a stabilizer code. Thus, there are k logical qubits and $2k$ independent logical operators.

A set of logical operators with the following commutation relations is called a *canonical set of logical operators*:

$$\Pi(\mathcal{S}) \;=\; \left\{ \begin{array}{ccc} \ell_1, & \cdots, & \ell_k \\ r_1, & \cdots, & r_k \end{array} \right\}. \tag{2.12}$$

Here, the commutation relations are represented in a way similar to a canonical representation where only the operators in the same column anti-commute with each other. Note that the choice of a canonical set of logical operators is not unique. With a canonical set of logical operators, the subspace $V_{\mathcal{S}}$ can be decomposed as a direct product of k subsystems:

$$|\psi\rangle \;=\; \bigotimes_{p=1}^{k} \Big(\alpha_p |\tilde{0}\rangle_p + \beta_p |\tilde{1}\rangle_p \Big) \tag{2.13}$$

where ℓ_p and r_p act non-trivially only on $|\tilde{0}\rangle_p$ and $|\tilde{1}\rangle_p$. One can choose the basis $|\tilde{0}\rangle_p$ and $|\tilde{1}\rangle_p$ such that ℓ_p and r_p act like Pauli operators applied to a logical qubit represented by $|\tilde{0}\rangle_p$ and $|\tilde{1}\rangle_p$:

$$\ell_p |\tilde{0}\rangle_p \;=\; |\tilde{1}\rangle_p, \quad \ell_p |\tilde{1}\rangle_p \;=\; |\tilde{0}\rangle_p, \quad r_p |\tilde{0}\rangle_p \;=\; |\tilde{0}\rangle_p, \quad r_p |\tilde{1}\rangle_p \;=\; -|\tilde{1}\rangle_p \tag{2.14}$$

The number of independent generators for a group of Pauli operators $\mathcal{O} \in \mathcal{P}$ is

denoted as $G(\mathcal{O})$. Note that $G(\mathcal{O})$ does not count trivial generators such as iI. For example,

$$G(\mathcal{P}) \;=\; 2n, \quad G(\mathcal{S}) \;=\; n-k, \quad G(\mathcal{C}) \;=\; n+k. \tag{2.15}$$

Examples of stabilizer codes: Here, we present some examples of stabilizer codes to give some intuitions on definitions of logical operators and related groups of Pauli operators. The first example we consider is called a five qubit code [6, 7]. Consider a system of five qubits which is governed by the following Hamiltonian:

$$H \;=\; -\sum_{j=1}^{5} S^{(j)}, \qquad S^{(j)} \;=\; X^{(j)}Y^{(j+1)}Y^{(j+2)}X^{(j+3)} \tag{2.16}$$

with periodic boundary conditions. Note that $S^{(j)}$ commute with each other, and this Hamiltonian is a stabilizer Hamiltonian. The stabilizer group is

$$\mathcal{S} \;=\; \langle S^{(1)}, S^{(2)}, S^{(3)}, S^{(4)} \rangle \tag{2.17}$$

since $S^{(5)}$ is not independent from other stabilizers. This may be seen from the following equation:

$$S^{(1)} \;\times\; S^{(2)} \;\times\; S^{(3)} \;\times\; S^{(4)} \;\times\; S^{(5)} \;=\; I. \tag{2.18}$$

This stabilizer Hamiltonian has two degenerate ground states with $k = 1$ since $G(\mathcal{S}) = 4$, and logical operators are

$$\ell \;=\; X^{(1)}Z^{(2)}X^{(3)}, \qquad r \;=\; Z^{(1)}Y^{(2)}Z^{(3)} \tag{2.19}$$

where $\{\ell, r\} = 0$. Note that these are examples of logical operators, and there are many equivalent representations for logical operators. One may see that logical operators ℓ and r commute with all the stabilizers $S^{(j)}$ through direct computations. The centralize group can be represented in the following way:

$$\mathcal{C} \;=\; \left\langle \begin{array}{l} \ell, \quad S^{(1)}, \quad S^{(2)}, \quad S^{(3)}, \quad S^{(4)} \\ r, \end{array} \right\rangle \tag{2.20}$$

Note that logical operators ℓ and r have equivalent representations which can be obtained by applying stabilizers. It turns out that ℓ and r are representations with minimal weights, and the code distance is $d = 3$.

The stabilizer formalism can characterize not only quantum codes but also classical codes. The second example we consider is a prototypical classical error-correcting code, called the repetition code, which encodes 0 as the repetition of 0s and 1 as the repetition of 1s. The stabilizer group of the repetition code is given by

$$\mathcal{S} \;=\; \langle Z^{(1)}Z^{(2)}, Z^{(2)}Z^{(3)}, \cdots \rangle \tag{2.21}$$

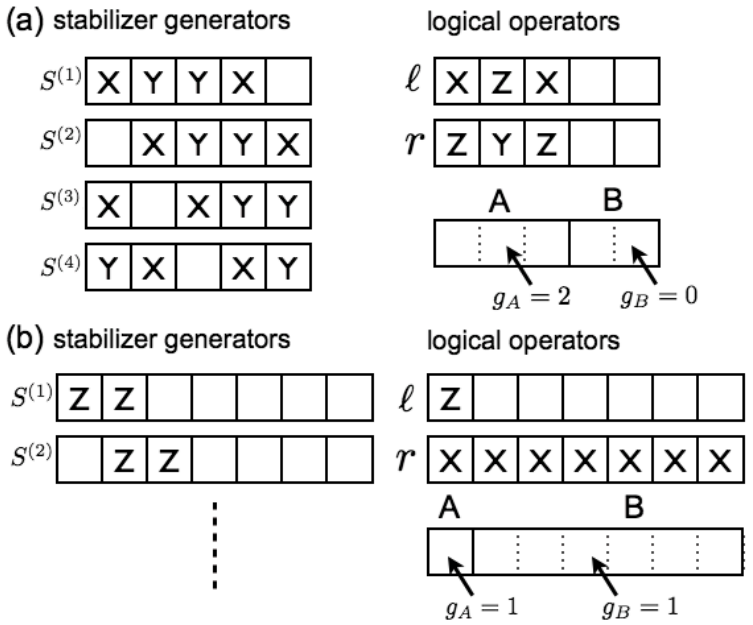

Figure 2-2: Examples of stabilizer codes. Stabilizer generators and logical operators are shown. (a) A five qubit code. (b) One-dimensional ferromagnet (the repetition code).

with $k = 1$, and logical operators are

$$\ell \;=\; Z^{(1)}, \qquad r \;=\; X^{(1)} \cdots X^{(n)}. \tag{2.22}$$

The repetition code is a good classical error-correcting code since the distance between $|0 \cdots\rangle$ and $|1 \cdots\rangle$ is $\tilde{d} = n$ where $\tilde{d}$ is the code distance as a classical error-correcting code. Yet, the code distance as a quantum error-correcting code is $d = 1$ since the weight of ℓ is one.

2.2 Bi-partition theorem

In this subsection, we consider a bi-partition of stabilizer codes, and derive a simple formula which captures a geometric duality of logical operators arising in stabilizer codes [11]:

Theorem 2.1 (Bi-partition theorem)**.** *For a stabilizer code with k logical qubits, let g_A and g_B be the numbers of independent logical operators which can be supported only by qubits inside A and B respectively with $B = \bar{A}$. Then the following formula holds:*

$$g_A + g_B \;=\; 2k. \tag{2.23}$$

The formula, called a *bi-partition theorem*, is the key to deriving many results

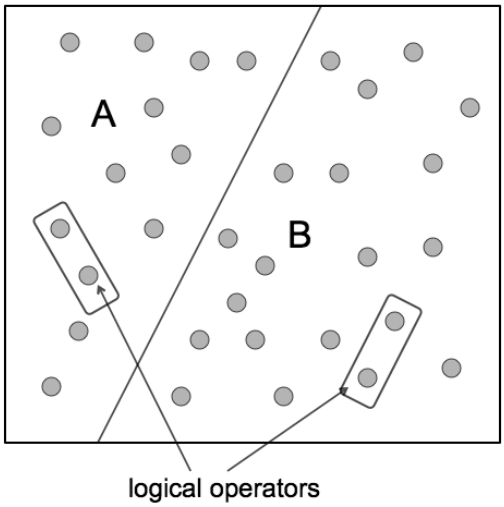

Figure 2-3: Geometric duality on stabilizer codes ($g_A + g_B = 2k$). The figure shows a bi-partition into two complementary regions A and B. Shaded dots represent qubits and rectangles represent logical operators.

presented in the thesis. The bi-partition theorem states that by naively counting the number of independent logical operators which can be defined inside each region and taking the sum of them, the sum is equal to $2k$.

We begin by demonstrating that the bi-partition theorem holds in a five qubit code and the repetition code. For a five qubit code, we denote the subset of qubits which consists of the first, second and third qubits as A (Fig. 2-2(a)). Then, we have $g_A = 2$, $g_B = 0$ and $g_A + g_B = 2$ since logical operators ℓ and r can be defined inside A while there is no logical operator defined inside B. Recall that logical operators have equivalent representations. The bi-partition theorem states that all the logical operators in a five qubit code must have non-trivial supports on at least three qubits since $g_B = 0$. This shows that $d = 3$ for a five qubit code. Next, for a repetition code, we denote the first qubit as A and a set of other qubits as B (Fig. 2-2(b)). Then, we have $g_A = 1$ since ℓ is defined inside A. Note that ℓ also has an equivalent representation supported inside B since $Z^{(2)} \sim \ell$. Thus we have $g_B = 1$ which is consistent with the bi-partition theorem $g_A + g_B = 2$. The theorem states that equivalent representations of r cannot be defined inside a region with $n - 1$ qubits, and must have supports on all the n qubits.

The bi-partition theorem clearly shows limitations on the possible geometric shapes of equivalent logical operators. In order to create a quantum code with large logical operators, we need to have a small g_A for large region A. However, the effort of decreasing g_A for large A results in increasing g_B for small B for $B = \bar{A}$ since we have $g_A + g_B = 2k$. Thus, our theorem shows a clear restriction on the *sizes of logical operators*, and indicates the *intrinsic duality on geometric shapes of localized logical operators* of stabilizer codes in a bi-partition.

For the proof of theorem, it is convenient to define projections of operators. The projection of a Pauli operator $U \in \mathcal{P}$ onto a subset of qubits A is denoted as $U|_A$. This keeps only the non-trivial Pauli operators which are inside A and truncates Pauli operators acting outside the subset A. The restriction of a group of Pauli operators $\mathcal{O}$ into some subset of qubits A is defined as

$$\mathcal{O}_A \;=\; \Big\langle \Big\{ U \in \mathcal{O} \;:\; U|_{\bar{A}} = I \Big\} \Big\rangle. \tag{2.24}$$

Here, $\bar{A}$ represents a complement of A. $\mathcal{O}_A$ contains all the operators in $\mathcal{O}$ which are defined inside A. In this thesis, we use the restrictions of the stabilizer group $\mathcal{S}$, the centralizer group $\mathcal{C}$ and the Pauli operator group $\mathcal{P}$, which are denoted as $\mathcal{S}_A$, $\mathcal{C}_A$ and $\mathcal{P}_A$ respectively.

Proof. An arbitrary logical operator ℓ defined inside A can be found in $\mathcal{C}_A$: $\ell \in \mathcal{C}_A$. Recall that an application of stabilizers to a logical operator keeps it equivalent to the original one. Then the following logical operator $\ell' = \ell U$ for $U \in \mathcal{S}_A$ is equivalent to ℓ and is defined inside A. Thus the number of independent logical operators supported inside A is given by

$$g_A \;=\; G(\mathcal{C}_A) - G(\mathcal{S}_A). \tag{2.25}$$

Similarly one has

$$g_B \;=\; G(\mathcal{C}_B) - G(\mathcal{S}_B). \tag{2.26}$$

Next we analyze the number of independent generators for $\mathcal{C}_A$ and $\mathcal{C}_B$, denoted by $G(\mathcal{C}_A)$ and $G(\mathcal{C}_B)$. Let v_A and v_B be the numbers of qubits inside A and B (i.e. the volumes of A and B) respectively. For a centralizer operator $\ell \in \mathcal{C}_A$, one has

$$[\ell, U|_A] \;=\; 0, \qquad \text{for all} \;\; U \;\in\; \mathcal{S}. \tag{2.27}$$

Recall that a choice of stabilizer generators is not unique. One can choose a set of $n-k$ independent stabilizer generators of the stabilizer group $\mathcal{S}$ as follows:

$$S_1, \cdots, S_a, S_{a+1}, \cdots, S_{n-k}, \qquad \text{where} \;\; \Big\langle \Big\{ S_1, \cdots, S_a \Big\} \Big\rangle \;=\; \mathcal{S}_B. \tag{2.28}$$

Then, the constraints in Eq. (2.27) can be written as

$$[\ell, S_j|_A] \;=\; 0, \qquad \text{for all} \quad j \;=\; a+1, \cdots, n-k \tag{2.29}$$

since $S_1, \cdots, S_a$ do not overlap with ℓ. Since there are $2v_A$ independent Pauli operators inside A, one has

$$G(\mathcal{C}_A) \;=\; 2v_A - (G(\mathcal{S}) - G(\mathcal{S}_B)) \tag{2.30}$$

by noticing $S_j|_A$ for $j = a+1, \cdots, n-k$ are independent. Similarly one has

$$G(\mathcal{C}_B) \;=\; 2v_B - (G(\mathcal{S}) - G(\mathcal{S}_A)). \tag{2.31}$$

Finally, since $v_A + v_B = n$, one has

$$g_A + g_B \;=\; 2(v_A + v_B) - 2G(\mathcal{S}) \;=\; 2k. \tag{2.32}$$

□

2.3 Application to topological order

Studies of topologically ordered materials have been frontiers of modern theoretical physics for three decades not only because of the fundamental importance in condensed matter physics, but also because of the practical importance in quantum information science. Despite a significant amount of work done in attempts to characterize physical properties of topologically ordered materials, our understanding on topological order is still elusive and incomplete. In particular, one of the big conceptual puzzles regarding topologically ordered materials is how the notion of "topology" arises in their physical properties. A standard argument says that, if a system is put on some geometric manifold $\mathcal{M}$ such as a torus, its physical properties depend on topological properties of $\mathcal{M}$ [29]. Yet, it is often difficult to see the notion of topology for a fixed $\mathcal{M}$ in an evident way.

Below, we demonstrate how the notion of topology emerges in topologically ordered systems by studying the Toric code with the bi-partition theorem.

The Toric code: The Toric code is the simplest known, exactly solvable, model which is described in the stabilizer formalism, supporting degenerate ground states, with topological order [30]. Consider an $L \times L$ square lattice on the torus. The Toric code is defined with qubits which live on edges of bonds (Fig.2-4 (a)). There are $n = 2(L \times L)$ qubits in total. For simplicity of discussion, we set periodic boundary conditions. The Hamiltonian is:

$$H \;=\; -\sum_{s,p}(\mathcal{A}_s + \mathcal{B}_p), \qquad \mathcal{A}_s \;=\; \prod_{i\in s} X_i, \qquad \mathcal{B}_p \;=\; \prod_{i\in p} Z_i \tag{2.33}$$

where s represent "stars" and p represent "plaquettes" (Fig. 2-4(a)). The Toric code has $2k = 4$ independent logical operators since $G(\mathcal{S}) = n - 2$. Each of independent logical operators ℓ_1, r_1, ℓ_2 and r_2 are shown in Fig. 2-4(b). These four logical operators obey the following commutation relations:

$$\left\{ \begin{array}{cc} \ell_1, & \ell_2 \\ r_1, & r_2 \end{array} \right\} \tag{2.34}$$

where commutation relations are defined in a way similar to the canonical representation.

In stabilizer codes, logical operators have equivalent representations. For instance, translations of ℓ_1, ℓ_2, r_1, r_2 are equivalent to themselves:

$$T_x(\ell_1) \sim \ell_1 \qquad T_x(\ell_2) \sim \ell_2 \qquad T_y(r_1) \sim r_1 \qquad T_y(r_2) \sim r_2. \tag{2.35}$$

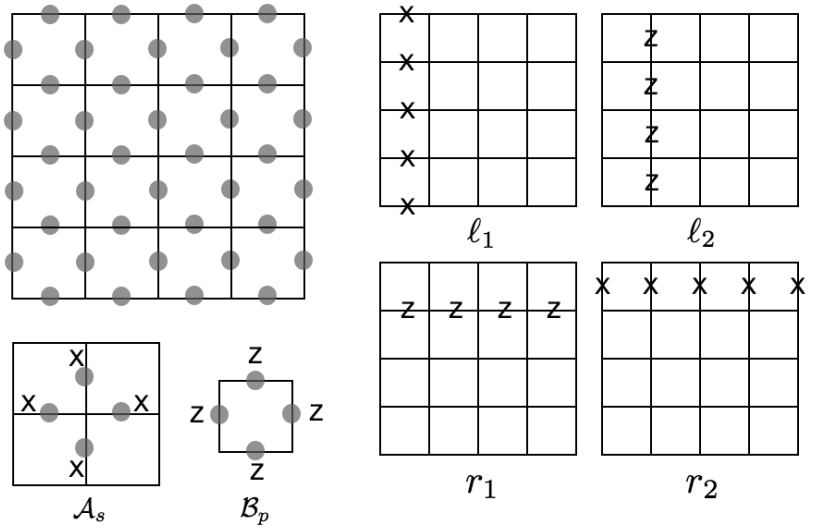

Figure 2-4: The Toric code and its logical operators.

Topological properties of logical operators: Now we analyze how the notion of topology arises in geometric shapes of logical operators. Let us define the following regions. $Q(x)$ is a region which circles the lattice in $\hat{x}$-direction (Fig.2-5(a)). $Q(y)$ is a region which circles the lattice in the $\hat{y}$-direction (Fig.2-5(b)). Finally, $R(1) = Q(x) \cup Q(y)$ is a region which is the union of $Q(x)$ and $Q(y)$ (Fig.2-5(c)).

Consider first a bi-partition into two subsets $Q(x)$ and $\overline{Q(x)}$ described in Fig.2-5(a). Logical operators r_1 and r_2 are defined inside $Q(x)$, and we have $g_{Q(x)} \geq 2$. r_1 and r_2 also have equivalent logical operators in $\overline{Q(x)}$ since translations of r_1 and r_2 in $\hat{y}$-direction are equivalent to original logical operators r_1 and r_2 respectively. Then, we have $g_{\overline{Q(x)}} \geq 2$. Now apply theorem 2.1 to this bi-partition. Since $g_{Q(x)} + g_{\overline{Q(x)}} = 4$ due to the theorem, we must have $g_{Q(x)} = g_{\overline{Q(x)}} = 2$. Let us interpret these equations and discuss the geometries of logical operators. Since $g_{\overline{Q(x)}} = 2$, r_1 and r_2 are all the independent logical operators which can be defined inside $Q(x)$. In other words, *logical operators ℓ_1 and ℓ_2 (and their equivalent representations) cannot both be defined inside $Q(x)$.*

It is more illuminating when we consider the equation $g_{\overline{Q(x)}} = 2$. Even when we expand the region $Q(x)$ to $\overline{Q(x)}$, logical operators ℓ_1 and ℓ_2 still cannot be defined inside $\overline{Q(x)}$ since r_1 and r_2 are all the independent logical operators which can be defined inside $\overline{Q(x)}$. Therefore, one can conclude that logical operators ℓ_1 and ℓ_2 (and their equivalent representations) can be defined *only inside regions which circle around the lattice in the $\hat{y}$ direction.* The similar discussion holds for logical operators ℓ_1 and ℓ_2 by considering a bi-partition into $Q(y)$ and $\overline{Q(y)}$ (Fig.2-5(b)). Logical operators

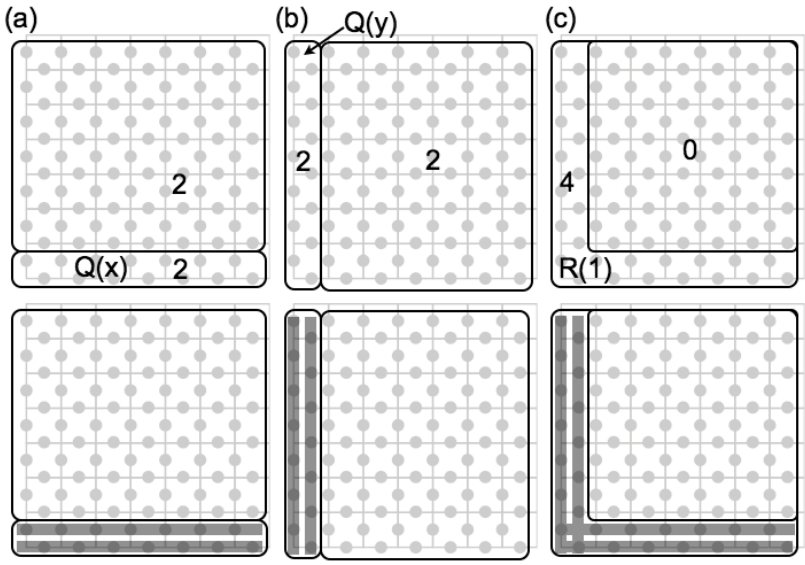

Figure 2-5: The bi-partition theorem for the Toric code.

ℓ_1 and ℓ_2 can be defined *only inside regions which circle around the lattice in the* $\hat{x}$ *direction*.

Next, let us consider a bi-partition into two subsets $R(1) = Q(x) \cup Q(y)$ and $\overline{R(1)}$ described in Fig.2-5(c). Since all the four independent logical operators can be defined inside $R(1)$, we have $g_{R(1)} = 4$. Then, there is no logical operator which can be defined inside $\overline{R(1)}$ since $g_{\overline{R(1)}} = 0$. One notices that $\overline{R(1)}$ has no winding either in x or y direction. Therefore, *there is no logical operator defined inside a region which does not circle around the lattice in any direction*.

These discussions clarify that the geometric shapes of logical operators have universal, *topological* properties, which are invariant under the application of stabilizers. Specifically, whether a region circles around the lattice in x and y directions can be quantified by the *winding numbers* of regions. The winding numbers of geometric shapes of logical operators are quantities which are invariant among all the equivalent logical operators, and thus may be viewed as topological invariants. As a result, we notice that ℓ_1, ℓ_2, r_1, r_2 are representations with minimal weights and the code distance of the Toric code is $d = L$.

Topological deformability of logical operators: A similar manifestation of the notion of topology can be seen in a two-dimensional ferromagnet. Notice that a two-dimensional ferromagnet has a pair of a zero-dimensional logical operator $\ell = Z^{(1,1)}$ and a two-dimensional logical operator $r = \prod_{i,j} X^{(i,j)}$. Due to the bi-partition theorem, we notice that r cannot be defined inside any region with $n - 1$ qubits. Thus, a logical operator r can be defined only inside a two-dimensional region and one cannot change topological properties of the geometric shape of r.

From these arguments, we notice that logical operators in the Toric code and a ferromagnet on a two-dimensional lattice are both "topological". In order to make

this observation more concrete, we introduce the notion of *deformability of logical operators*. To begin with, let us consider two regions A and $A' \subset A$ which can support the same number of independent logical operators with $g_A = g_{A'}$(Fig.2-6). Note that all the logical operators defined inside A can be transformed into equivalent logical operators defined inside A' by applying appropriate stabilizers. Therefore, *all the logical operators in A can be deformed into other equivalent logical operators defined inside a smaller subset A'.*

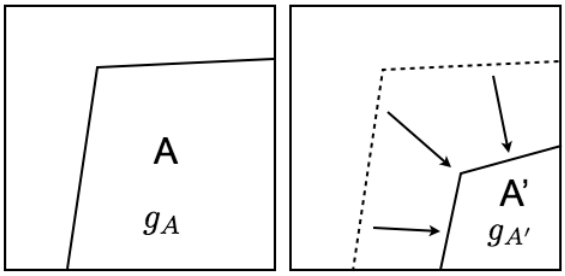

Figure 2-6: Deformation of a logical operator. When $g_A = g_{A'}$, a logical operator ℓ supported inside A can be shrunk into another equivalent logical operator ℓ' defined inside A' by applying some appropriate stabilizer.

Now, one can summarize topological properties of logical operators arising in the Toric code and a ferromagnet as follows:

Observation 2.2 (Topological deformation of logical operators)**.** *Consider a ferromagnet or the Toric code on a two-dimensional lattice. For a given logical operator ℓ defined inside some connected region R, one can always find an equivalent logical operator ℓ' inside another connected region R' as long as R and R' are topologically equivalent:*

$$g_R = g_{R'} \qquad for \quad R \simeq R'. \tag{2.36}$$

Therefore, one can continuously deform geometric shapes of logical operators freely as long as one does not change topological properties of logical operators. Examples are shown in Fig. 2-6. We call this continuous deformation of logical operators *topological deformation of logical operators.*

While our argument on topological deformation of logical operators is limited to the Toric code and a ferromagnet on a two-dimensional lattice, it turns out that this is a universal property for a fairly large class of physically realizable stabilizer codes. In particular, one can show that all the stabilizer codes with translation and continuous scale symmetries (STS models) have this topological property of logical operators for $D = 1, 2, 3$. This observation is a strong evidence that STS models can be effectively described by topological field theory.

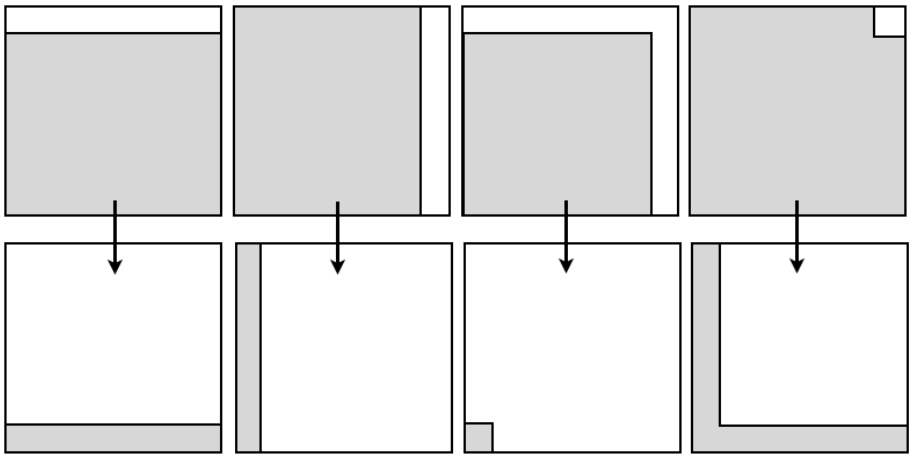

Figure 2-7: Topological deformation of logical operators. Recall that the entire lattice is a torus with periodic boundary conditions.

2.4 Application to coding theory

In this subsection, we discuss applications of the bi-partition theorem to the problem of analyzing coding properties of a local stabilizer code and the derivation of quantum singleton bound.

Local stabilizer code: Now that we have the restriction $g_A + g_B = 2k$ in hand, we discuss the problem of giving an upper bound on the code distance for a local stabilizer code. A local stabilizer code is a class of stabilizer codes whose stabilizer generators S_j are defined in geometrically local regions. A local stabilizer code is physically realizable in principle since the stabilizer Hamiltonian

$$H = -\sum_j S_j \tag{2.37}$$

involves only local terms S_j.

The central question concerning local stabilizer codes is to find upper bounds on the number of logical qubits k and the code distance (reliability of encoding) d for a fixed system size n. This problem has been first addressed by Bravyi and Terhal [31] via a beautiful construction of logical operators in which logical operators can be shorten to equivalent logical operators defined in smaller subsets. The *cleaning lemma*, at the heart of this method, can now be understood as resulting from an application of our formula. Let us suppose that there is no logical operators defined inside A at all. Then, one has $g_A = 0$ and $g_B = 2k$ from the bi-partition theorem. Since B can contain $2k$ logical operators, we notice that *all the logical operators in the system can be defined in* B by applying appropriate stabilizers. Therefore, by finding a region A such that $g_A = 0$, we can deform logical operators to its complement A.

As a corollary of this cleaning lemma, one can derive an upper bound on the sizes

of logical operators, the code distances and the amount of classical and quantum information stored easily. Consider a local stabilizer code constructed on a D-dimensional hypercubic lattice with $n = L^D$ where D is the spatial dimension of the system. Then the following bound is known to hold [31, 32]

$$k\tilde{d}^{\frac{1}{D}} \leq O(n) \qquad \text{Classical code} \tag{2.38}$$

$$kd^{\frac{2}{D-1}} \leq O(n) \quad \text{and} \quad d \leq O(L^{D-1}) \qquad \text{Quantum code} \tag{2.39}$$

where $\tilde{d}$ represents the code distance as a classical error-correcting code while d represents the code distance as a quantum error-correcting code.

Finding local stabilizer codes which saturate the above bounds is an important question in both classical and quantum coding theory. As for a classical error-correcting code, one may see that the repetition code is far below the bound since $k = 1$ and $\tilde{d} = n$. In Chapter 7, we give the first example of classical error-correcting codes which asymptotically saturate this bound, and provide a solution to this problem for classical error-correcting codes. As for a quantum error-correcting code, for $D = 2$, the Toric code is known to saturate this bound with $k = 2$ and $d \sim O(L)$. However, for $D = 3$, whether a local stabilizer code which saturates the bound or not remains open. For example, a three-dimensional generalization of the Toric code has $k = 3$ and $d \sim O(L)$, and is far below the bound. At the time of writing this thesis, this problem for quantum error-correcting codes has not been solved.

Quantum singleton bound: The bi-partition theorem also allows us to derive the quantum singleton bound, which is one of the earliest analytical bound on coding properties of stabilizer codes [33]. Let us define three subsets such that $V_A = d - 1$, $B = \bar{A}$ and $B' \subseteq B$ with $V_{B'} = d - 1$. Then, we have

$$g_A = g_{B'} = 0 \qquad g_B = 2k. \tag{2.40}$$

Since we have $g_B \leq 2(V_B - V_{B'})$, we obtain

$$k \leq n - 2(d - 1). \tag{2.41}$$

This is the quantum singleton bound.

2.5 Application to secret-sharing

Finally, we discuss the application of the bi-partition theorem to problems concerning classical and quantum secret-sharing schemes [34, 35]. Due to the bi-partition theorem, logical qubits arising in stabilizer codes can be classified into two types, called *local logical qubits* and *non-local logical qubits*. In this subsection, we show that only non-local logical qubits are useful for classical secret-sharing. However it is shown that none of logical qubits arising in a stabilizer code is useful for quantum secret-sharing.

Local and non-local logical qubits: We begin by classifying logical operators into four sets $M(A)$, $M(B)$, $M(A,B)$ and $M(\phi)$ by seeing whether they can be supported inside A and B or not. $M(A)$ represents a set of logical operators which can be supported inside A, but cannot be supported inside B. In other words, a logical operator inside $M(A)$ has an equivalent logical operator defined inside A, but does not has an equivalent logical operator defined inside B. $M(B)$ represents a set of logical operators which can be supported inside B, but cannot be supported inside A. $M(A,B)$ represents a set of logical operators which can be supported both inside A and B in a sense that a logical operator in $M(A,B)$ has equivalent logical operators supported inside A and B respectively. $M(\phi)$ represents a set of logical operators which cannot be supported either inside A or B. In other words, a logical operator in $M(\phi)$ does not have an equivalent logical operator either inside A or B. Note that all the non-trivial logical operators can be classified into these four sets without any overlap. Then we have the following theorem:

Theorem 2.3 (Local and non-local logical qubits)**.** *One can choose a canonical set of logical operators*

$$\Pi(\mathcal{S}) \;=\; \left\{ \begin{array}{ccc} \ell_1, & \cdots, & \ell_k \\ r_1, & \cdots, & r_k \end{array} \right\}. \tag{2.42}$$

where each pair of anti-commuting logical operators ℓ_j, r_j satisfy one of the followings:

(a) $\ell_j, r_j \;\in\; M(A)$.

(b) $\ell_j, r_j \;\in\; M(B)$.

(c) $\ell_j \;\in\; M(A,B)$ *and* $r_j \;\in\; M(\phi)$.

For the proof, see [11]. We represent possible commutation relations between logical operators as follows:

$$\begin{aligned} M(A) &\;\leftrightarrow\; M(A) \\ M(B) &\;\leftrightarrow\; M(B) \\ M(A,B) &\;\leftrightarrow\; M(\phi) \end{aligned}$$

where double-sided allows represent anti-commutations (see Fig. 2-8). From theorem 2.3, one notices that there are two types of logical qubits in a stabilizer code (Fig. 2-9). A first type of logical qubits, called *local logical qubits*, is characterized by a pair of anti-commuting logical operators ℓ and r where both of them are supported locally inside A or B. The second type of logical qubits, called *non-local logical qubits*, is characterized by a pair of anti-commuting logical operators ℓ and r where ℓ can be locally defined inside both A and B while r cannot be defined locally inside either A or B.

Classical and quantum secret-sharing with a stabilizer code: Now we discuss an application of theorem 2.3 to studies of secret-sharing. Secret-sharing is a scheme which allows sharing of information between two parties or multiple parties so that each party cannot access the encoded information individually. Shared information can be accessed only when all the parties agree and execute a protocol together. Such encoded information is shared by multiple parties as a secret among all the parties. Some entangled quantum system can be used as a resource for secret-charing of classical or quantum information. Below, we analyze how secret-charing schemes work with a stabilizer code.

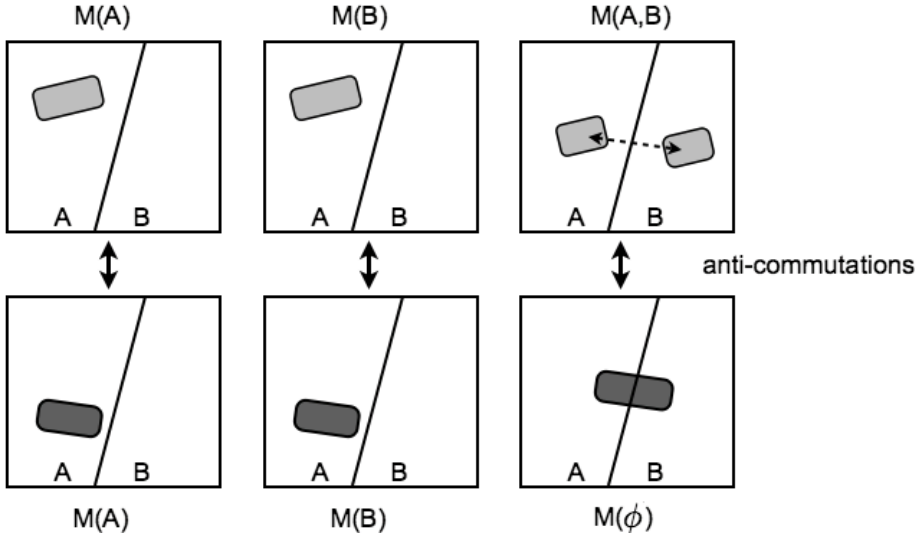

Figure 2-8: Possible pairs of anti-commuting logical operators. A double-sided dotted arrow shows that two logical operators are equivalent.

First, we discuss secret-sharing of classical information between two parties using a stabilizer code. Consider a situation where one party A possesses a subset of qubits A and the other party B possesses a complementary subset of qubits B. Consider a non-local logical qubit supported by ℓ and r where r can be supported inside both A and B while ℓ cannot be supported inside either A or B. A bit of information can be shared between A and B by assigning 0 and 1 to each of eigenstates of ℓ. This observation is summarized in the following corollary:

Corollary 2.4 (Classical secret-sharing)**.** *The necessary and sufficient condition for a stabilizer code to be useful for classical information sharing is the existence of a non-local logical qubit.*

Next, let us discuss secret-sharing of quantum information. To encode quantum information, a pair of anti-commuting logical operators ℓ and r is required. However, from theorem 2.3, we know that one of logical operators must be defined locally inside either A or B. This allows one of two parties to access the encoded logical qubit. This observation is summarized in the following corollary:

Corollary 2.5 (Quantum secret-sharing)**.** *One cannot share quantum information secretly between two parties inside the ground state space of stabilizer codes.*

In actual implementations of secret-sharing schemes, decoding complexity of shared information matters too. For instance, if a shared information cannot be read out easily for each party A and B, but can be easily read out when A and B agree to collaborate, a shared information is accessible only when A and B agree with each other. In such a circumstance, secret-sharing schemes work in practice, though discussion on decoding complexity is beyond the scope of this thesis.

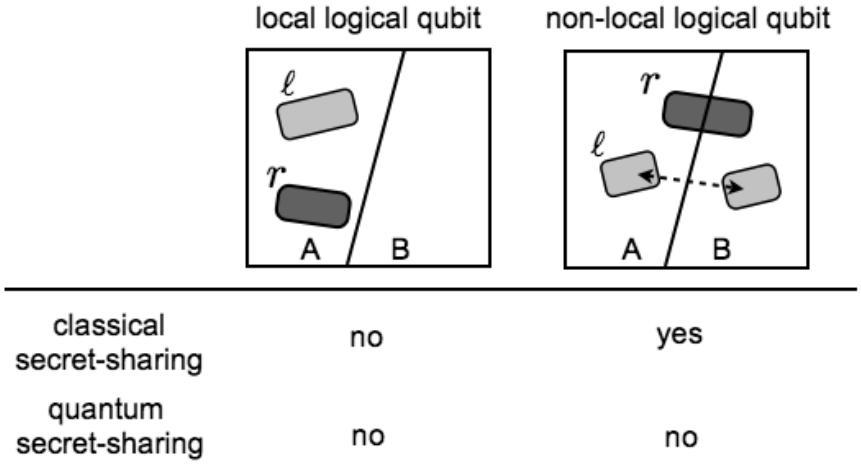

Figure 2-9: Local and non-local logical qubits.

2.6 Discussion

In this chapter, we have derived a formula "$g_A + g_B = 2k$" concerning a geometric duality on logical operators. This bi-partition theorem was found useful in addressing various problems in condensed matter physics and quantum information theory.

Below is the summary of important findings in this chapter.

(a) Stabilizer codes are physically realizable as the gapped ground space of stabilizer Hamiltonians $H = -\sum_j S_j$.

(b) Stabilizer codes with large code distances d imply the presence of strong entanglement in degenerate ground states.

(c) Logical operators may characterize hidden symmetries of the system since $[\ell, H] = 0$.

(d) For stabilizer codes, the bi-partition theorem $g_A + g_B = 2k$ holds for an arbitrary bi-partition.

(e) Geometric shapes of logical operators can be classified in terms of topology in many of stabilizer Hamiltonians.

Extensions of the bi-partition theorem: Here we briefly discuss possible extensions and future problems. Though we have limited our considerations to stabilizer codes, there are many quantum codes and spin systems which cannot be described through the stabilizer formalism. One novel class of quantum codes, called *subsystem codes* [36], replaces the commuting interaction terms of stabilizer codes with interaction terms which may anti-commute with each other. These subsystem codes are interesting, particularly because they may potentially provide several promising features, such as a lower fault-tolerance threshold [37, 38] compared with certain codes utilizing similar space and time resources. Physical properties arising from the quantum compass model have been studied numerically [39], and are interesting, for example, in the notable role they play in explaining the effects of the orbital degree of freedom of atomic electrons on the properties of transition-metal oxides [40].

After the publication of our original work, the bi-partition theorem has been extended to subsystem codes in [41, 42]. Recall that there are two types of logical operators, called bare logical operators and dressed logical operators in a subsystem code. For a subsystem code with k logical qubits in a bi-partition into A and B, the following formula is known to hold:

$$g_A + \hat{g}_B = 2k \tag{2.43}$$

where g_A is the number of independent bare logical operators inside A and $\hat{g}_B$ is the number of independent dressed logical operators inside B. For a stabilizer code, one has $g_B = \hat{g}_B$ which recovers the original bi-partition theorem. It may be an interesting future problem to extend the bi-partition theorems to various systems such as frustration-free systems and systems with rotational symmetries. Also, an extension of the theorem to multi-partitions may be an interesting future problem.

Chapter 3

Classification of quantum phases and stabilizer Hamiltonians

In condensed matter physics, studies on quantum phases in correlated spin systems have been central in addressing the underlying mechanisms behind many-body physics. Also there have been considerable interests in quantum phases in two-dimensional systems from quantum information science community, as topological phases of spin systems are useful in realizing quantum information theoretical ideas [30, 43, 1]. In this thesis, we ask two fundamental questions concerning quantum phases arising in correlated spin systems.

(a) What kinds of quantum phases are allowed to exist in correlated spin systems?

(b) How do we classify these quantum phases? What kinds of properties distinguish different quantum phases?

We approach this condensed matter theoretical question on searches and classifications of quantum phases by using quantum coding theory. The present chapter is devoted to discussion on why one can study quantum phases arising in gapped spin systems through quantum coding theory and how we approach this problem.

The main focus of this chapter is to introduce a certain model of stabilizer codes, called stabilizer codes with translation and continuous scale symmetries (STS models) which may cover a large class of physically realizable quantum codes and correspond to fixed point Hamiltonians under RG transformations. Our approach is to find geometric shapes of logical operators and use their topological properties as "order parameters" to classify quantum phases arising in the model.

Comment: We will discuss classifications of quantum phases arising in STS models in Chapter 4-6. Examples of stabilizer Hamiltonians without continuous scale symmetries, but with discrete scale symmetries, are discussed in Chapter 7-8. Such models are beyond descriptions of STS models and correspond to limit cycles of RG transformations.

3.1 Exactly solvable models and quantum phases

Finding exactly solvable models is a key to searching for possible quantum phases. The AKLT state, which is the ground state of an exactly solvable spin 1 Hamiltonian, provides useful clues about the ground state properties of quantum antiferromagnets [44, 45]. The Toric code, the simplest exactly solvable model with topological order, gives insights on how topological phases emerge in correlated spin systems [30, 1]. These Hamiltonians mentioned here are called *frustration-free* Hamiltonians since ground states can be obtained by minimizing each term locally. While these exactly solvable frustration-free models may not be physical, involving more than two spins at one time or higher order interactions, it is relatively easy to find their ground states compared with frustrated Hamiltonians which we encounter in realistic systems. A key idea is to realize that these frustration-free Hamiltonians may appear as low energy effective theories for real spin systems [46], and thus, may serve as a "bureau of quantum phases" with which one may approximately study the ground state properties of actual Hamiltonians.

So far, a lot of frustration-free spin Hamiltonians with various physical properties have been found [1, 2]. However, whether these models could exhaust all the possible quantum phases or not is far from obvious. A brute force approach might be to analyze all the possible frustration-free Hamiltonians and study their ground state properties. However, being frustration-free does not mean that Hamiltonians are exactly solvable since studying their ground state properties may be still challenging. Moreover, finding frustration-free Hamiltonians is difficult. For example, even when a Hamiltonian consists only of commuting projectors, to determine whether the Hamiltonian is frustration-free or not is known to be the hardest problem in the computational complexity class QMA (Quantum Marlin-Arthur), a quantum analog of NP [47, 48]. (So, it could be a difficult problem even for a quantum computer to solve !).

Stabilizer Hamiltonians: While analyses on arbitrary frustration-free Hamiltonians are indeed challenging, there exists a certain subclass of frustration-free Hamiltonians, called stabilizer Hamiltonians [5], which play a crucial role in quantum information science. Stabilizer Hamiltonians serve as a natural architecture to realize quantum error-correcting codes in correlated many-body spin systems as we have seen in Chapter 2. The basic idea of stabilizer codes is to encode a qubit in strongly entangled and correlated states so that no small error can break the encoded qubit. A remarkable feature of stabilizer codes is the existence of system Hamiltonians which supports encoded qubits in degenerate ground states with a finite energy gap.

Stabilizer Hamiltonians are certainly limited compared with arbitrary frustration-free Hamiltonians. Yet, many interesting spin systems can be described in the language of stabilizer codes [30, 25, 26, 49, 50]. Also, a good news is that there are a number of useful theoretical tools to analyze the ground state properties in stabilizer codes, which are originally developed in quantum coding theoretical contexts, but are potentially useful for studying non-local correlations arising in many-body systems [31, 11]. Thus, the analysis on quantum phases arising in stabilizer Hamil-

tonians and their classification will be the necessary first step in order to address quantum phases arising in arbitrary frustration-free Hamiltonians and search for all the possible two-dimensional quantum phases.

Several authors have initiated studies on physically realistic stabilizer Hamiltonians by analyzing coding properties of stabilizer codes supported by local terms [31, 32, 51]. However, physically realizable Hamiltonians must have some physical symmetries such as translation symmetries too if they are to be realized in some lattice of spins. Also, there is another important physical constraint which must be considered in analyzing quantum phases arising in stabilizer Hamiltonians. According to the underlying philosophy behind RG transformations, quantum phases must be characterized by non-local correlations which survive even at the thermodynamic limit (a limit where the system size becomes infinite) and are invariant under scale transformations. Since quantum phases must be classified in a scale invariant way, stabilizer Hamiltonians need to have scale invariance too if they are to be used as candidates for possible quantum phases at fixed points of RG transformations.

In this thesis, to search for possible quantum phases in correlated spin systems, we begin by proposing a model of stabilizer Hamiltonians which have both physical realizability and scale invariance. In particular, the model is built on the following physical constraints.

- **Locality of interactions:** A system of qubits, defined on a D-dimensional lattice, is governed by a stabilizer Hamiltonian which consists only of local interactions.

- **Translation symmetries:** The Hamiltonian is invariant under some finite translations of qubits.

- **Continuous scale symmetries:** The number of degenerate ground states of the Hamiltonian does not depend on the system size.

We call stabilizer Hamiltonians which satisfy the above three physical constraints *Stabilizer codes with Translation and Scale symmetries* (**STS models**).

3.2 The model: Stabilizer code with Translation and Scale symmetries

Below, a more precise definition of the STS model is introduced.

(1) Locality of interaction: Physically realistic systems must have only geometrically local interaction terms. To introduce the notion of locality to stabilizer codes, we consider a system of qubits defined on a D-dimensional square lattice (hypercubic lattice) which consists of $n = L_1 \times \cdots \times L_D$ qubits where L_m is the total number of qubits in the $\hat{m}$ direction for $m = 1, \cdots, D$. Therefore, qubits are distributed in the physical space with a *metric*.

Here, the entire system is separated into a collection of hypercubes which consists of $v = v_1 \times \cdots \times v_D$ qubits. (We assume that $n_m \equiv L_m/v_m$ are integer values so that hypercubes do not overlap with each other). We consider a block of $v = v_1 \times \cdots \times v_D$ qubits as the single unit block which constitutes the entire system. In particular, we consider these unit blocks as single *composite particles* with a larger Hilbert space $(\mathbb{C}^2)^{\otimes v}$ (Fig. 3-1). Thus, the entire system is viewed as a hypercubic lattice of $n_1 \times \cdots \times n_D$ composite particles.

Now, we assume that interaction terms of the stabilizer Hamiltonian are defined *locally*:

$$H = -\sum_j S_j \tag{3.1}$$

where S_j are supported inside some regions with $2 \times \cdots \times 2$ composite particles (Fig. 3-1). (Otherwise, we coarse-grain the system). In the analysis of STS models, instead of qubits, we consider composite particles as the smallest building blocks of the system.

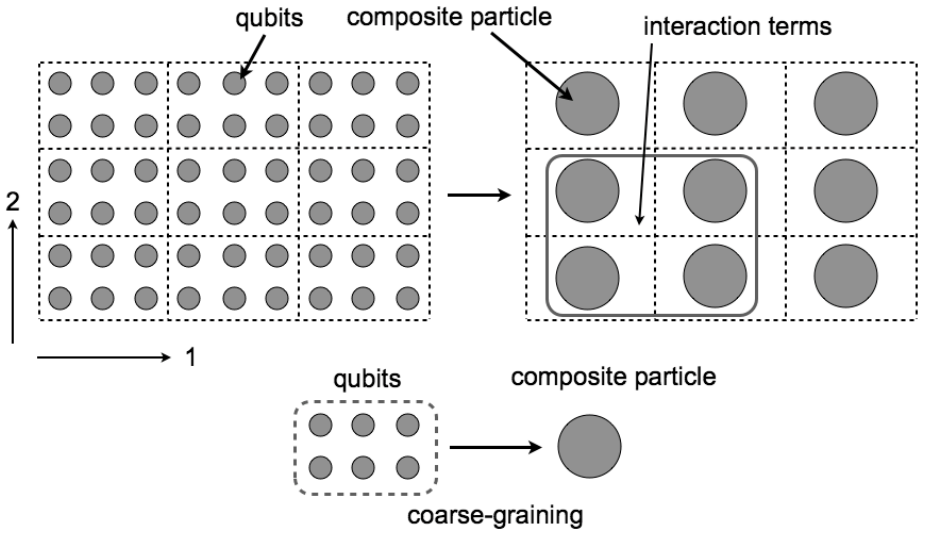

Figure 3-1: An illustration of the STS model. A two-dimensional example is shown where a unit block of 3×2 qubits is considered as a composite particle with a larger Hilbert space. Interaction terms S_j are defined locally inside a region of 2×2 composite particles. The Hamiltonian is invariant under unit translations of composite particles.

(2) Translation symmetries: Physically realistic systems often have not only local interactions, but also some physical symmetries. Here, we assume that the stabilizer Hamiltonian possesses *translation symmetries*:

$$T_m(H) = H \qquad (m = 1, \cdots, D) \tag{3.2}$$

where T_m represent *unit translations of composite particles* in the $\hat{m}$ direction (Fig. 3-1).

For simplicity of discussion and in order to accommodate translation symmetries, we set the periodic boundary conditions. Then, the entire system may be viewed as a D-dimensional torus: $\mathbf{T}^D = \mathbf{S}^1 \times \cdots \times \mathbf{S}^1$ where $\mathbf{S}^1$ is a circle. Thus, the entire system has a topologically non-trivial geometric shape *a priori*. Yet, we emphasize that most of long-range physical properties in the bulk are immune to boundary conditions.

(3) Scale symmetries: In this thesis, we are interested in coding properties at the limit where the system size goes to the infinity (in other words, at the *thermodynamic limit*). So far, we have considered the cases where the system size $\vec{n} \equiv (n_1, \cdots, n_D)$ is fixed. Here, we consider changes of the number of composite particles n_m while keeping interaction terms S_j the same.

It is commonly believed that there is a tradeoff between the number of logical qubits k and the code distance [31, 32, 41] where the code distance d decreases as the number of logical qubits k increases for a fixed n, as seen in Eq. (2.38) and Eq. (2.39) in Chapter 2. Then, it may be legitimate to limit our considerations to the cases where the number of logical qubits k remains small when the system size increases.

We assume that stabilizer codes have *continuous scale symmetries* by requiring that the number of logical qubits $k_{\vec{n}}$ is independent of the system size $\vec{n}$:

$$k_{\vec{n}} \;=\; k, \qquad \forall \vec{n}. \tag{3.3}$$

Here, we emphasize that, in a system with continuous scale symmetries, the number of logical qubits k remains constant under not only global scale transformations: $\vec{n} \to c\vec{n}$ where c is some positive integer, but also arbitrary changes of n_m.

One might think that continuous scale symmetries are too strong as physical constraints. However, through appropriate coarse-graining, a fairly large class of local stabilizer codes with translation symmetries can be considered as the STS model. In particular, let us consider the cases where the number of logical qubits $k_{\vec{n}}$ is small:

$$k_{\vec{n}} \;\leq\; k_0, \qquad \forall \vec{n} \tag{3.4}$$

where $k_{\vec{n}}$ does not grow with the system size $\vec{n}$. Then, there always exists some finite coarse-graining such that a coarse-grained system has continuous scale symmetries, as proven in [12]. As a result, by analyzing coding properties of stabilizer codes in the presence of continuous scale symmetries, one can easily deduce coding properties of stabilizer codes which satisfy Eq. (3.4). Therefore, *solutions of STS models are sufficient to discuss coding properties of translation symmetric stabilizer codes with a small number of logical qubits.*

Translation equivalence of logical operators: There is a certain property of logical operators which emerges naturally as a result of translation and continuous scale symmetries. For STS models, the following theorem holds [12] (Fig. 3-2).

Theorem 3.1 (**Translation equivalence**). *For each and every logical operator* ℓ

in an STS model, a unit translation of ℓ with respect to composite particles in any direction is always equivalent to the original logical operator ℓ:

$$T_m(\ell) \ \sim \ \ell, \qquad \forall \ell \ \in \ \boldsymbol{L}_{\vec{n}} \qquad (m \ = \ 1, \cdots, D) \tag{3.5}$$

where $\boldsymbol{L}_{\vec{n}}$ is a set of all the logical operators for an STS model defined with the system size $\vec{n}$.

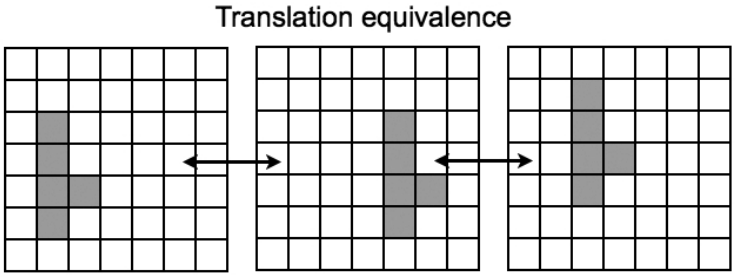

Figure 3-2: The translation equivalence of logical operators. Each square represents a composite particle. Shaded regions represent translated logical operators which are equivalent to each other.

We have already seen that the translation equivalence of logical operator holds in a ferromagnet and the two-dimensional Toric code. See Eq. (2.35) for example. It turns out that this is a universal property in STS models.

Here, we only give an intuition on why this theorem holds. Let us consider the case where the system size $\vec{n}$ is large. Then, since the number of logical qubits k does not depend on the system size, k is relatively small compared with the system size $\vec{n}$. Now, due to the translation symmetries of the system Hamiltonian, translations of a given logical operator ℓ are also logical operators. However, there are only $2k$ independent logical operators. Then, there must be a finite integer a_m such that $\ell \sim T_m^{a_m}(\ell)$ for all the logical operators ℓ. (Otherwise, there would be so many independent logical operators). It turns out that $a_m = 1$ for any ℓ and m. While we have used only the condition that the number of logical operators k is small, due to continuous scale symmetries (k is constant), one can prove the above theorem by showing $a_m = 1$ for any ℓ, m and $\vec{n}$.

Weak-breaking of translation symmetries: The translation equivalence of logical operators has some interesting relation to the notion of weak-breaking of translation symmetries in topologically ordered systems. Kitaev pointed out that, in topologically ordered systems, various symmetries such as translation symmetries may break "weakly" and proposed a unifying picture of all the known topologically ordered systems in terms of the levels of weak symmetry breaking [23]. How logical operators change under translations is intrinsically related to how ground states change under translations. In particular, the translation equivalence of logical operators states that weak breaking of translation symmetries do not occur in ground states of

STS models [12]. In other words, stabilizer Hamiltonians are properly coarse-grained to be fixed point Hamiltonians in the presence of continuous scale symmetries.

3.3 Classification of quantum phases

Having introduced a model of stabilizer Hamiltonians which are to be used as candidates of quantum phases, we turn to a problem of how we classify them.

Quantum phase transitions: Two frustration-free Hamiltonians may be classified through the presence or the absence of a quantum phase transition (QPT). In quantum many-body systems, two quantum phases with different physical properties are separated by a QPT, which is a sudden non-analytic change of the ground state properties as a result of parameter changes in the Hamiltonian bridging two quantum phases [52]. Two frustration-free Hamiltonians may be considered to belong to different quantum phases when a parameterized Hamiltonian connecting them undergoes a QPT [28, 53, 54].

As an example, we consider the Ising model in a transverse field in one dimension with periodic boundary conditions:

$$H(\epsilon) \ = -(1-\epsilon)\sum_j Z^{(j)}Z^{(j+1)} - \epsilon\sum_j X^{(j)} \tag{3.6}$$

where $Z^{(j)}$ acts on j-th qubit (spin 1/2 particle). The system consists of N qubits (spin 1/2 particles). At $\epsilon = 0$, the system Hamiltonian is

$$H(0) \ = -\sum_j Z^{(j)}Z^{(j+1)} \tag{3.7}$$

and the ground states are $|0\cdots 0\rangle$ and $|1\cdots 1\rangle$. At $\epsilon = 1$, the system Hamiltonian is

$$H(1) \ = -\sum_j X^{(j)} \tag{3.8}$$

and the ground state is $|+\cdots+\rangle$ where $|+\rangle = \frac{1}{\sqrt{2}}(|0\rangle + |1\rangle)$. It is well known that physical properties of ground states drastically change around $\epsilon = 1/2$. When $0 \le \epsilon < 1/2$, physical properties of a ground state are close to ones of $H(0)$. When $1/2 < \epsilon \le 1$, physical properties of a ground state are close to ones of $H(1)$. This drastic change of physical properties at $\epsilon = 1/2$ is called a QPT. Two Hamiltonians $H(0)$ and $H(1)$ are separated by a QPT at $\epsilon = 1/2$, and may represent different quantum phases (Fig. 3-3(a)).

The existence of a QPT can be detected by considering the energy gap between a ground state and excited states. Let us consider how the energy gap changes around the transition point in this model. Then, at the transition point $\epsilon = 1/2$, the energy gap $\Delta(\epsilon)$ between a ground state and excited states becomes zero at the thermodynamic limit: $\Delta(1/2) \to 0$ for $n \to \infty$. Thus, the vanishing energy gap serves

as an indicator of a QPT.

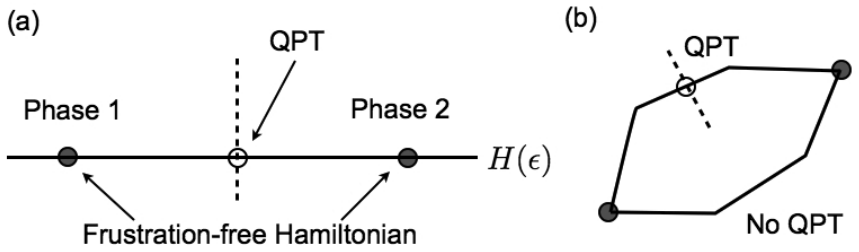

Figure 3-3: (a) Two quantum phases separated by a QPT. Black circles represent frustration-free Hamiltonians and a blank circle represents a QPT. Different quantum phases are represented by frustration-free Hamiltonians. (b) A path dependence of the presence of a QPT. Two frustration-free Hamiltonians are considered to belong to the same quantum phase when there exists a parametrized Hamiltonian which connects them without closing the energy gap.

Since a ground state of the original parameterized Hamiltonian $H(\epsilon)$ cannot be obtained by minimizing each term in the Hamiltonians except at $\epsilon = 0, 1$, $H(\epsilon)$ is said to be *frustrated*. In general, finding a ground state of a frustrated Hamiltonian is computationally difficult. However, Hamiltonians $H(0)$ and $H(1)$ are not frustrated, meaning that their ground states can be obtained by minimizing each term in the Hamiltonian independently. In this example, physical properties of frustration-free Hamiltonians $H(0)$ and $H(1)$ are easy to analyze. Then, physical properties of the original Hamiltonian $H(\epsilon)$ may be studied by adding perturbations to frustration-free Hamiltonians $H(0)$ and $H(1)$. Thus, $H(0)$ and $H(1)$ may serve as easily solvable reference models to characterize quantum phases (Fig. 3-3(a)).

Definition of frustration-free Hamiltonians: Since our goal is to study quantum phases arising in frustration-free Hamiltonians, we give their formal definition. When a Hamiltonian is said to be frustration-free, a ground state can be obtained by minimizing each local term in the Hamiltonian simultaneously. A useful feature of frustration-free Hamiltonians is that they can be represented as summations of projection operators. Consider a class of Hamiltonians which can be represented as summations of projectors:

$$H \;=\; -\sum_j \hat{P}_j \qquad \text{for all} \;\; j, \tag{3.9}$$

where $\hat{P}_j$ are projectors. Such Hamiltonians are called frustration-free when their ground states satisfy

$$\hat{P}_j|\psi\rangle \;=\; |\psi\rangle \qquad \text{for all} \;\; j. \tag{3.10}$$

A frustration-free Hamiltonian needs not to be a summation of projections. But, for any Hamiltonian whose ground states minimize each local term independently,

one can represent the Hamiltonian as a summation of commuting projectors. For example, one may obtain $H(0)$ and $H(1)$ appeared in the discussions on the Ising model in a transverse field by setting $\hat{P}_j = \frac{1}{2}(I + Z^{(j)}Z^{(j+1)})$ and $\hat{P}_j = \frac{1}{2}(I + X^{(j)})$ up to some constant correction.

In this thesis, we are particularly interested in a class of frustration-free Hamiltonians whose interaction terms commute with each other:

$$[P_j, P_{j'}] \ = \ 0 \tag{3.11}$$

since our primary focus is on quantum phases arising in gapped spin systems. Note that there are examples of frustration-free Hamiltonians whose projector terms do not commute with each other with a vanishing energy gap [55].

Path dependence of the presence of a QPT: One might be tempted to call two quantum phases different if they are separated by a QPT. However, there is a subtlety in this classification of quantum phases since the presence of a QPT may depend on how we change the Hamiltonian. The challenge in classifying quantum phases in correlated spin systems underlies behind the fact that the existence of a QPT depends on how Hamiltonians are varied from the one to the other. In particular, there are cases where two frustration-free Hamiltonians are connected through some parameterized Hamiltonian without a QPT, but are separated by a QPT for other parameterized Hamiltonian [17, 39, 56, 57, 58]. To show that two frustration-free Hamiltonians belong to different quantum phases, one needs to analyze all the possible paths of parameterized Hamiltonians connecting them and see if they are always separated by QPTs or not. Thus, the need is to find some order parameter to classify quantum phases in a way independent of choices of parameterized Hamiltonians.

Let us see an example:

$$H(\epsilon) \ = -(1-\epsilon)\sum_j Z^{(j)}Z^{(j+1)} - \epsilon\sum_j X^{(j)}X^{(j+1)}. \tag{3.12}$$

This model exhibit a QPT at $\epsilon = 1/2$ where the energy gap $\Delta(\epsilon)$ becomes zero. Then, one might hope to consider two quantum phases at $0 \leq \epsilon < 1/2$ and at $1/2 < \epsilon \leq 1$ different. However, there exists another parameterized Hamiltonian $H'(\epsilon)$ which connects $H(0)$ and $H(1)$ without closing an energy gap between ground states and excited states (Fig. 3-3(b)):

$$H'(\epsilon) \ = \ -\sum_j M(\epsilon)^{(j)}M(\epsilon)^{(j+1)}, \quad M(\epsilon)^{(j)} \ = \ (1-\epsilon)Z^{(j)} + \epsilon X^{(j)} \tag{3.13}$$

with $H'(0) = H(0)$ and $H'(1) = H(1)$. It is easy to see that the energy gap of the above Hamiltonian $H'(\epsilon)$ is independent of ϵ, and remain finite. Also, since $H(0)$ can be obtained by rotating the axis of each qubit in $H(1)$, we may consider two Hamiltonians to be in the same quantum phase.

Classification of quantum phases through frustration-free Hamiltonians:

As we have seen in the above examples, the existence of a QPT depends on paths of parameterized Hamiltonians which connect two frustration-free Hamiltonians.

A standard way to classify quantum phases is to consider two Hamiltonians belonging to the same quantum phase when they can be transformed each other without closing the energy gap through some path of a parameterized Hamiltonian [28, 53, 54]. Here, following this spirit, we shall state the criteria to classify quantum phases arising in frustration-free Hamiltonians as follows (Fig. 3-4).

- Two frustration-free Hamiltonians H_A and H_B belong to different quantum phases if and only if there is no parameterized Hamiltonian $H(\epsilon)$ which connects H_A and H_B without closing an energy gap or changing the number of ground states.

Here, by "parameterized Hamiltonians", we mean the following:

- Parameterized Hamiltonians $H(\epsilon)$ consist only of local terms which change continuously with some external parameter ϵ, and amplitudes (norms) of local terms do not depend on the system size.

By "without closing an energy gap", we mean that

- The energy gap between degenerate ground states and a first excited state is finite even at the thermodynamic limit.

Thus, two different quantum phases are always separated by a QPT regardless of choices of parameterized Hamiltonians $H(\epsilon)$.

Here, we make some comments on the validity of the above classification of quantum phases. While the vanishing energy gap may be a signature of QPTs, the original definition of a QPT is a non-analytic change of the ground state properties. In fact, there are examples of parameterized Hamiltonians whose ground state energy changes continuously while the energy gap vanishes [57]. Thus, the connection between the energy gap and the non-analyticity in ground states is not completely established. However, in this thesis, we often use the vanishing energy gap as a criteria for classifying quantum phases for simplicity of discussion for simplicity of discussion.

3.4 RG transformations, scale invariance and topology of logical operators

While classifications of quantum phases lie at the heart of studies on quantum many-body systems, this problem is typically difficult due to the issues described above. In this thesis, we make an attempt to overcome these difficulties concerning studies on quantum phases by combining theoretical tools developed in quantum information science and the notion of topology.

RG transformations: QPTs in parameterized Hamiltonians have been analyzed commonly through RG transformations which are certain scale transformations. Here,

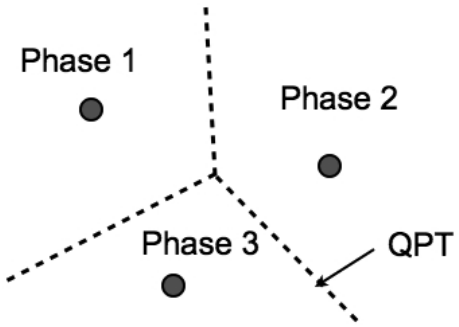

Figure 3-4: A classification of quantum phases. Black dots represent frustration-free Hamiltonians in corresponding quantum phases. Frustration-free Hamiltonians belonging to different quantum phases are always separated by a QPT regardless of the paths.

we review the basic idea of RG transformations and discuss the relation between RG transformations and frustration-free Hamiltonians in terms of scale invariance. Note that while we shall describe a general idea of RG transformations, we do not give any specific procedure of RG transformations since detailed reviews on various procedures of RG transformations are beyond the scope of this thesis.

RG transformation is a way to capture only the non-local correlations from many-body systems by analyzing how the system properties changes under scale transformations (Fig. 3-5). RG transformations usually consist of two elements, called coarse-graining and rescaling. Coarse-graining is a process to group several spins into a single particle with a larger Hilbert space. In this coarse-graining, a microscopic structure of original spins inside a larger spin (coarse-grained spin) is completely lost and one ends up with a system consisting only of larger spins. Rescaling is a process to replace a coarse-grained larger spin with a original small spin by eliminating some spin degrees of freedom inside each coarse-grained spin, which is interacting weakly with other coarse-grained spins. By repeating scale transformations consisting of coarse-graining and rescaling, only the non-local correlations extending all over the lattice may survive. In some types of RG transformations, after a rescaling process, one washes out short-range correlations.

When quantum phases are classified through RG transformations, the key idea is the use of Hamiltonians which are invariant under scale transformations, called *fixed point Hamiltonians*. By applying RG transformations to some parameterized Hamiltonian $H(\epsilon)$, one can systematically obtain Hamiltonians which are invariant under RG transformations. Since fixed point Hamiltonians are invariant under RG transformations, they do not have any length scale and can capture long-range physical properties which may survive even at the thermodynamic limit where the system size goes to the infinity. Then, fixed-point Hamiltonians help us to capture only the scale invariant properties of corresponding quantum phases.

Now, since fixed point Hamiltonians are obtained by washing out short-range correlations, it is known that fixed point Hamiltonians in gapped quantum phases can be often represented as frustration-free Hamiltonians where each term can be minimized

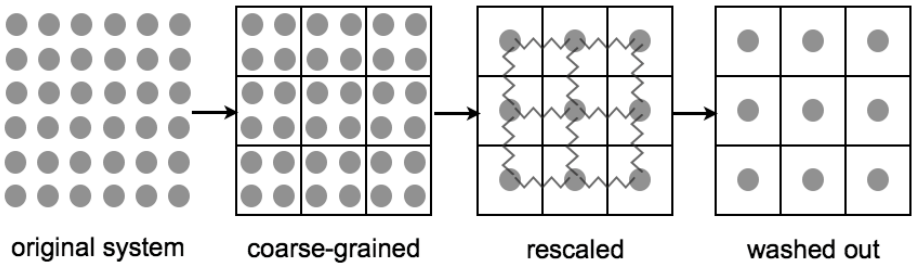

Figure 3-5: A typical procedure of RG transformations. An original system is first coarse-grained by grouping a finite number of spins into a single composite particle. Then a coarse-grained system is rescaled to have spins with fewer inner dimensions. Then, short-range entanglement is washed out. A Hamiltonian or a ground state is said to be at fixed points when there exists some RG transformation which leaves it invariant.

locally without considering neighboring terms. Then, one may take a slight liberty and say that a study of all the possible frustration-free Hamiltonians is almost equivalent to a study of all the possible fixed point Hamiltonians which may appear as a result of RG transformations. In fact, continuous scale symmetries in STS models result from the observation that fixed point Hamiltonians are free from any length scale.

Logical operator as an order parameter: Our goal is to analyze and classify quantum phases arising in STS models completely. In the analysis and classification of quantum phases arising in STS models, quantum phases must be distinguished by some quantities or objects which are scale invariant. Here, it is useful to realize the similarity between the notion of topology and the classification of quantum phases by observing that geometric shapes of objects are scale invariant. In topology, geometric shapes of objects are classified in terms of smoothness and non-analyticity. Two objects are considered to be the same when they can be transformed each other continuously, while they are considered to be different when they can be transformed each other through only non-analytic changes of geometric shapes. In a similar fashion, quantum phases are classified in terms of continuous changes of ground states induced by changes of parameterized Hamiltonians. Two frustration-free Hamiltonians are considered to belong to the same quantum phase when their ground states can be connected continuously. Two frustration-free Hamiltonians are considered to belong to different quantum phases when they can be connected through only parameterized Hamiltonians which undergo QPTs with non-analytic changes of ground states. Thus, the notion of topology and a classification of quantum phases are fundamentally akin to each other.

The notion of topology has been playing crucial roles in classifying physical properties of quantum many-body systems in various fields of physics [59, 60]. Quantum field theory, equipped with the notion of topology, has been proposed in high energy physics where physical properties of systems depend on topological characteristics of the geometric manifolds where the systems are defined [61]. As a physical realization

of such topological theories in low-dimensional many-body systems, quantum hall systems defined on a geometric manifold were studied and the notion of topological order has been introduced in order to discuss and characterize topology-dependent non-local correlations [29]. The notion of topology appears not only in real physical space, but also in the momentum space too where QPTs are triggered by topological changes in the spectrum [62]. Finally, when Hamiltonians have several parameters, the parameter space may have non-trivial topological structures which may result in interesting behaviors of geometric (Berry) phases [63].

With this intimate connection between topology and quantum phases, we wish to classify quantum phases arising in STS models by introducing the notion of topology into quantum coding theoretical tools developed in studies of stabilizer Hamiltonians. What plays a central role in analyses on the ground state properties in stabilizer Hamiltonians are *logical operators*, which are Pauli operators commuting with the system Hamiltonian, but act non-trivially inside the ground state space. A useful empirical knowledge commonly shared in quantum information science community is that ground states are highly entangled when logical operators are supported by a large number of spins for a fixed system size. In particular, it has been pointed out that geometric non-localities of logical operators may characterize global entanglement arising in ground states of stabilizer Hamiltonians, such as topological order [11, 31].

In this thesis, we classify quantum phases arising in STS models by introducing the notion of topology into geometric shapes of logical operators. In particular, we achieve the following two programs. First, we solve the STS model exactly by identifying all the possible geometric shapes of logical operators. We establish the connection between the scale invariant ground state properties, such as topological order, and geometric shapes of logical operators completely. Second, we show that STS models with different geometric shapes of logical operators are always separated by a QPT. We find that the existence of a QPT originates from changes of geometric shapes of topologically distinct logical operators. We show that topological structures of geometric shapes of logical operators can be used as order parameters to distinguish quantum phases arising in STS models.

3.5 Discussion

In this chapter, we outlined how to search for quantum phases in correlated spin systems through quantum coding theory and discussed how to classify them. Our approach was to introduce a model of stabilizer Hamiltonians with physical realizability and scale-invariance, and determine geometric shapes of logical operators.

Below, we summarize the main findings of this chapter.

(a) One may search for quantum phases by studying frustration-free Hamiltonians such as stabilizer Hamiltonians.

(b) We proposed stabilizer codes with translation and scale symmetries (STS models) as candidates of quantum phase at fixed points.

(c) Quantum phases are classified whether they are separated by QPTs or not.

(d) According to the philosophy of RG transformations, geometric shapes of logical operators may serve as order parameters as they are scale invariant.

(e) The translation equivalence of logical operators, $T_m(\ell) \sim \ell$, holds in the presence of translation and continuous scale symmetries.

Beyond continuous scale symmetries: We have limited our considerations to the cases where the number of logical qubits $k_{\vec{n}}$ does not scale up with respect to the system size $\vec{n}$. There is another class of stabilizer Hamiltonians which do not have continuous scale symmetries, but have *discrete scale symmetries* [9, 10, 13]:

$$k(c\vec{n}) \;=\; c^{\delta} k(\vec{n}) \tag{3.14}$$

only for some spacial set of integers c with some scaling dimension δ. Due to the absence of continuous scale symmetries, such models do not correspond to quantum phases at fixed point, but correspond to quantum phases at limit cycles of RG transformations. Examples of such stabilizer Hamiltonians with discrete scale symmetries are discussed in Chapter 7 and Chapter 8.

Chapter 4

Universal quantum phases in one-dimensional stabilizer Hamiltonians

Now, we start the analysis on quantum phases in STS models, which are stabilizer codes at fixed points of RG transformations with continuous scale symmetries. In this chapter, we discuss quantum phases arising in one-dimensional STS models.

Quantum phases arising in one-dimensional spin systems are relatively easy to analyze compared with higher-dimensional spin systems. There are several powerful numerical algorithms to analyze the ground state properties of parameterized Hamiltonians, such as the density matrix renormalization group (DMRG) approach [64]. Also, recent developments on the matrix product state (MPS) formalism solidified the usefulness of DMRG approaches and expanded its applicabilities [65, 66]. In fact, it has been rigorously proven that any gapped spin systems on one-dimensional lattices can be efficiently simulated [67].

However, a classification of quantum phases is much more challenging than an analysis on a single parameterized Hamiltonian through a numerical simulation. In particular, since the existence of a QPT depends on paths of parameterized Hamiltonians, one needs to analyze all the possible parameterized Hamiltonians connecting two STS models to see if they belong to different quantum phases or not. Thus, the need is to find order parameters to classify quantum phases in a path-independent way.

A key idea behind RG transformations in characterizing quantum phases is the use of fixed point Hamiltonians which capture only the scale invariant ground state properties of the corresponding quantum phases. Following the spirit of RG transformations, we wish to classify quantum phases through some quantity or object which is scale invariant. Here it is illuminating to notice that geometric shapes of logical operators do not change under scale transformations. Then geometric shapes of logical operators may be used as "order parameters" to distinguish different quantum phases.

In this chapter, we show that different quantum phases in one-dimensional STS models are completely characterized by geometric shapes of logical operators. In

particular, we show the followings:

- Two STS models belong to the same quantum phase if and only if geometric shapes of logical operators are the same.
- Logical operators in one-dimensional STS models are either one-dimensional or zero-dimensional.
- A ferromagnetic phase is the universal quantum phase arising in one-dimensional STS models

4.1 Role of logical operators: concrete examples

We start with three specific examples of one-dimensional STS models in order to discuss the role of logical operators in classifying quantum phases.

4.1.1 Classical ferromagnet as a quantum code

Recall that a classical ferromagnet, the simplest model of interacting spins, can be seen as a stabilizer code. Let us consider the following Hamiltonian (Fig. 4-1):

$$H \;=\; -\sum_{j} Z^{(j)} Z^{(j+1)} \tag{4.1}$$

where $Z^{(j)}$ represents the Pauli operator Z acts on a j-th qubit. The total number of qubits is n and the system has periodic boundary conditions.

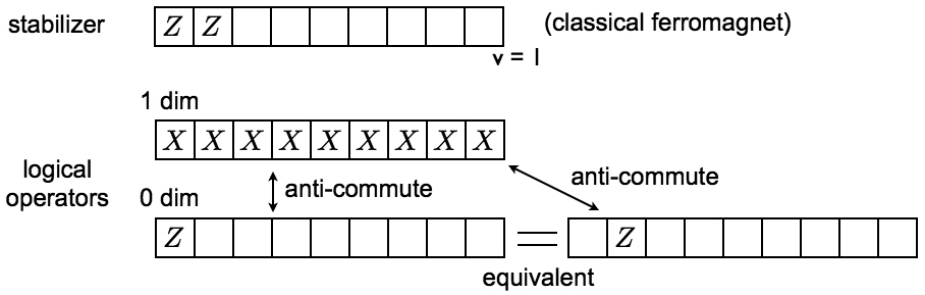

Figure 4-1: A classical ferromagnet.

The classical ferromagnet can be viewed as a stabilizer code with a translation symmetry since interaction terms $Z^{(j)}Z^{(j+1)}$ commute with each other. The stabilizer group is

$$\mathcal{S} \;=\; \langle Z^{(1)}Z^{(2)}, Z^{(2)}Z^{(3)}, \cdots, Z^{(n)}Z^{(1)} \rangle.$$

This stabilizer code is an STS model since it satisfies a scale symmetry. While there are n qubits and n stabilizers in this system, one stabilizer is redundant since

$$Z^{(1)}Z^{(2)} \times Z^{(2)}Z^{(3)} \times \cdots \times Z^{(n)}Z^{(1)} \;=\; I.$$

Thus, the stabilizer group has only $N-1$ independent generators, and $k=1$ for any n with $G(\mathcal{S}) = n-1$. Here, $G(\mathcal{S})$ is the number of independent generators for the stabilizer group $\mathcal{S}$.

Logical operators of a classical ferromagnet are

$$\ell \;=\; Z^{(1)}, \qquad r \;=\; X^{(1)}X^{(2)}\cdots X^{(n)}, \qquad \{\ell, r\} \;=\; 0. \tag{4.2}$$

One can see that both of logical operators satisfy the translation equivalence of logical operators since $T_1(r) = r$ and $\ell T_1(\ell) = Z^{(1)}Z^{(2)} \in \mathcal{S}$. According to geometric shapes of logical operators, we may call ℓ a *zero-dimensional logical operator* and r a *one-dimensional logical operator* (Fig. 4-1). Logical operators characterize transformations between degenerate ground states:

$$\begin{aligned} \ell|0\cdots0\rangle \;&=\; |0\cdots0\rangle, \quad \ell|1\cdots1\rangle \;=\; -|1\cdots1\rangle \\ r|0\cdots0\rangle \;&=\; |1\cdots1\rangle, \quad r|1\cdots1\rangle \;=\; |0\cdots0\rangle. \end{aligned}$$

Note that the translation equivalence of logical operators holds.

We naturally expect that a one-dimensional logical operator, non-locally defined all over the lattice, may characterize the existence of some global entanglement in ground states. Here, the ground state space is spanned by two orthogonal basis $|0\cdots0\rangle$ and $|1\cdots1\rangle$. Then, in principle, at zero temperature, a classical ferromagnet can support a GHZ state: $|\mathrm{GHZ}\rangle \;=\; \frac{1}{\sqrt{2}}(|0\cdots0\rangle + |1\cdots1\rangle)$. This GHZ state is "stabilized" by the one-dimensional logical operator r since $r|\mathrm{GHZ}\rangle = |\mathrm{GHZ}\rangle$. Now, we discuss entanglement in a GHZ state in a relation with the one-dimensional logical operator r. A GHZ state is a globally entangled state since it is a superposition of two globally separated ground states $|0\cdots0\rangle$ and $|1\cdots1\rangle = X^{(1)}\cdots X^{(n)}|0\cdots0\rangle$.

4.1.2 Cluster state: a model without logical operators

Next, let us discuss an example which does not have degenerate ground states or logical operators ($k=0$). The example we discuss is called a cluster state, possessing short-range entanglement between neighboring qubits. Its two-dimensional generalization is particularly useful as a resource to realize quantum information theoretical ideas such as measurement based quantum computation [49]. Though a cluster state has strong entanglement between neighboring qubits or composite particles, this short-range entanglement does not survive over the entire lattice, and is not a scale invariant property. In fact, such short-range entanglement can be removed by applying local unitary transformations on neighboring composite particles as we shall see below.

The Hamiltonian for a one-dimensional cluster state is the following (Fig. 4-2):

$$H \;=\; -\sum_j Z^{(j-1)}X^{(j)}Z^{(j+1)}. \tag{4.3}$$

This model is a stabilizer Hamiltonian since interaction terms $Z^{(j-1)}X^{(j)}Z^{(j+1)}$ commute with each other. The model does not have degenerate ground states since all the interaction terms $Z^{(j-1)}X^{(j)}Z^{(j+1)}$ are independent. The model has a unique ground state, called a cluster state, which satisfy the following conditions: $Z^{(j-1)}X^{(j)}Z^{(j+1)}|\psi\rangle = |\psi\rangle$.

A cluster state has short-range entanglement between neighboring qubits. To see this, we compute the entanglement entropy for a region A_1 which consists of only one qubit. Then, we have $E_{A_1} = 1$. Next, let us compute the entanglement entropy for a region A_j which consists of j consecutive qubits. Then, we have $E_{A_1} = 2$ for $1 \le j \le n-1$. This indicates the existence of short-range entanglement between neighboring qubits.

However, a cluster state does not have global entanglement. This can be seen from the fact that the Hamiltonian for a cluster state can be obtained by applying control-Z operations on the Hamiltonian for a product state $H = -\sum_j X^{(j)}$. Here, the control-Z operation acting on two qubits is defined as follows:

$$\mathrm{CZ} \;:\; |00\rangle \;\to\; |00\rangle, \quad |01\rangle \;\to\; |01\rangle, \quad |10\rangle \;\to\; |10\rangle, \quad |11\rangle \;\to\; -|11\rangle \tag{4.4}$$

where CZ represents the control-Z operation. The effect of the control-Z operation on two qubits can be represented in terms of Pauli operators in the following way:

$$\mathrm{CZ} \left\{ \begin{array}{cc} Z_1, & Z_2 \\ X_1, & X_2 \end{array} \right\} \mathrm{CZ}^{-1} \;=\; \left\{ \begin{array}{cc} Z_1, & Z_2 \\ X_1Z_2, & Z_1X_2 \end{array} \right\}$$

where the operation transforms X_1 into X_1Z_2 and X_2 into Z_1X_2. Here, Z_1 and X_1 act on the first qubit, and Z_2 and X_2 act on the second qubit. CZ^{-1} represents the inverse of CZ.

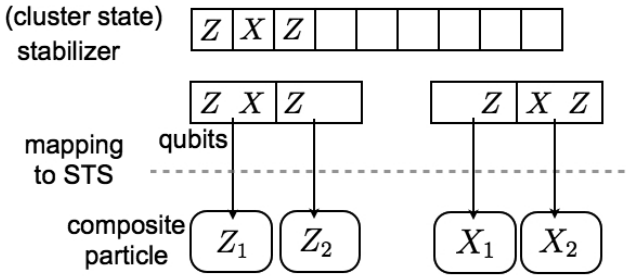

Figure 4-2: A cluster state. A mapping to an STS model is shown.

This model can discussed in the framework of an STS model by considering two consecutive qubits as a single composite particle ($v = 2$) when the total number of qubits n is even. Let $Z_p^{(j)}$ and $X_p^{(j)}$ be Pauli operators acting on a p-th qubit

$(p = 1, 2)$ inside a j-th composite particle $(j = 1, \cdots, n/2)$ particle with the following commutation relation:

$$\left\{ \begin{array}{cc} Z_1^{(j)}, & Z_2^{(j)} \\ X_1^{(j)}, & X_2^{(j)} \end{array} \right\}.$$

Then, after applying some appropriate unitary transformations on qubits inside each composite particle, one can represent the Hamiltonian for a cluster state in the following way:

$$H \;=\; -\sum_j Z_1^{(j)} Z_2^{(j+1)} - \sum_j X_1^{(j)} X_2^{(j+1)}. \tag{4.5}$$

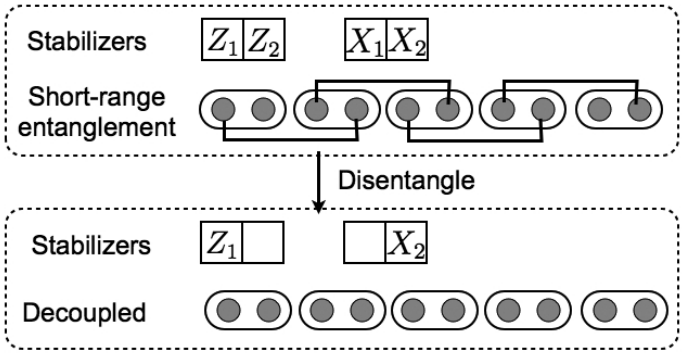

Figure 4-3: A disentangling operation in a cluster state described through composite particles. Short-range entanglement between composite particles can be removed by some local unitary transformations acting on neighboring composite particles.

Now, we describe the reduction from a cluster state to a product state by representing control-Z operations in terms of composite particles. In particular, through some observations, we notice that the following local unitary transformations $U^{(j)}$ acting on j-th and $j+1$-th composite particles can disentangle neighboring entanglement between composite particles in Eq. (4.5):

$$U^{(j)} \;\left\{ \begin{array}{cc} Z_1^{(j)} Z_2^{(j+1)}, & X_1^{(j)} X_2^{(j+1)} \\ X_1^{(j)}, & Z_2^{(j+1)} \end{array} \right\} \; (U^{(j)})^{-1} \;=\; \left\{ \begin{array}{cc} Z_1^{(j)}, & X_2^{(j+1)} \\ X_1^{(j)}, & Z_2^{(j+1)} \end{array} \right\}$$

where Pauli operators are transformed each other through $U^{(j)}$. Here, we note that $U^{(j)}$ commute with each other: $[U^{(j)}, U^{(j')}] = 0$. Then, by applying a unitary transformation $U \;=\; \prod_j U^{(j)}$, one can transform the original Hamiltonian in Eq. (4.5) to

$$UHU^{-1} \;=\; -\sum_j Z_1^{(j)} - \sum_j X_2^{(j)},$$

and short-range entanglement between neighboring composite particles can be washed

out (Fig. 4-3). Thus, the model can be reduced to a Hamiltonian which supports a "product state of composite particles".

These observations imply that short-range entanglement arising in a cluster state is not scale invariant. According to the basic principle of a classification of quantum phases through RG transformations, such short-range entanglement is not relevant for characterizations of quantum phases. At the end of this chapter, we shall confirm this expectation rigorously for quantum phases arising in STS models.

4.1.3 Extended five qubit code: reduction to a classical ferromagnet

We discuss our final example of one-dimensional STS models. We consider an example which can be obtained by generalizing the five qubit code to a one-dimensional spin chain. By introducing composite particles, one can discuss the model in the framework of STS models. We see that geometric shapes of logical operators are the same as those in a classical ferromagnet, and physical properties are similar. Then, we show that the model can be reduced to a "classical ferromagnet of composite particles" by disentangling short-range entanglement between neighboring composite particles.

As we have seen in Chapter 2, the five qubit code is constructed on five qubits, which is defined with the following stabilizer generator: $X^{(1)}Y^{(2)}Y^{(3)}X^{(4)}$ and its translations. Inspired by this five qubit code, we consider the following Hamiltonian defined with N qubits:

$$H \;=\; -\sum_{j=1}^{N} X^{(j)}Y^{(j+1)}Y^{(j+2)}X^{(j+3)}. \tag{4.6}$$

One can easily see that this extended five qubit code is also a stabilizer code since all the interaction terms $X^{(j)}Y^{(j+1)}Y^{(j+2)}X^{(j+3)}$ commute with each other. The code satisfies a scale symmetry since

$$\prod_{j} X^{(j)}Y^{(j+1)}Y^{(j+2)}X^{(j+3)} \;=\; I$$

and $k = 1$ for any N.

This model can be reduced to an STS model by considering three consecutive qubits as a single composite particle ($v = 3$). Let $Z_p^{(j)}$ and $X_p^{(j)}$ be Pauli operators acting on a p-th qubits ($p = 1, \cdots, 3$) inside a j-th composite particle ($j = 1, \cdots, n$) with the following commutation relations:

$$\left\{ \begin{array}{ccc} Z_1^{(j)}, & Z_2^{(j)}, & Z_3^{(j)} \\ X_1^{(j)}, & X_2^{(j)}, & X_3^{(j)} \end{array} \right\}.$$

Then, after applying some appropriate local unitary transformations on qubits inside

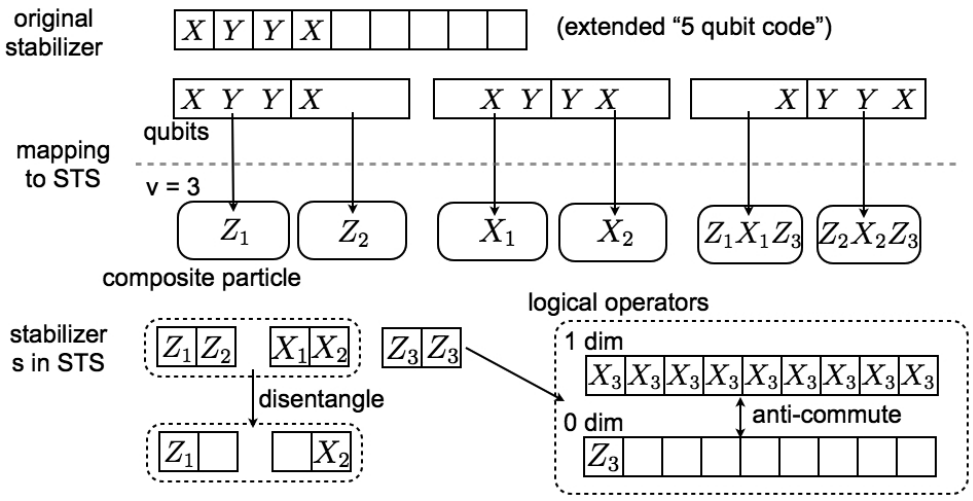

Figure 4-4: The extended five qubit code.

each composite particle, one can represent each of stabilizers in the following way:

$$Z_1^{(j)} Z_2^{(j+1)}, \qquad X_1^{(j)} X_2^{(j+1)}, \qquad Z_3^{(j)} Z_3^{(j+1)}.$$

With this notation through composite particles, one can easily write down logical operators:

$$\ell \;=\; Z_3^{(1)}, \qquad r \;=\; X_3^{(1)} X_3^{(2)} \cdots X_3^{(n)}, \qquad \{\ell, r\} \;=\; 0.$$

We notice that geometric shapes of logical operators are the same as those of a classical ferromagnet. Then, we expect that physical properties of the model are similar to those of a classical ferromagnet. In fact, one can discuss properties of entanglement in a way similar to a classical ferromagnet. The existence of a one-dimensional logical operator r implies the presence of a global entanglement. Here, we choose two degenerate ground states of the model in the following way:

$$\ell|\psi_0\rangle \;=\; |\psi_0\rangle, \qquad \ell|\psi_1\rangle \;=\; -|\psi_1\rangle, \qquad r|\psi_0\rangle \;=\; |\psi_1\rangle, \qquad r|\psi_1\rangle \;=\; |\psi_0\rangle.$$

Then, we notice that $|\psi\rangle$ has a *GHZ-like entanglement* since $|\psi\rangle = \frac{1}{\sqrt{2}}(|\psi_0\rangle + |\psi_1\rangle)$ and $|\psi\rangle$ is a superposition of two globally separated ground states.

As long as the scale invariant ground state properties are concerned, an extended five qubit code is similar to a classical ferromagnet. In fact, this model can be reduced to a classical ferromagnet by applying unitary transformations acting on neighboring composite particles in a way similar to the reduction of a cluster state:

$$U^{(j)} \;:\; Z_1^{(j)} Z_2^{(j+1)} \;\rightarrow Z_1^{(j)}, \qquad X_1^{(j)} X_2^{(j+1)} \;\rightarrow\; X_2^{(j+1)}.$$

Note that $[U^{(j)}, U^{(j')}] = 0$. Now, after this unitary transformations, only the third qubits in each composite particle are correlated through stabilizers $Z_3^{(j)} Z_3^{(j+1)}$ while

the first and second qubits in each composite particle are decoupled due to the existence of $Z_1^{(j)}$ and $X_2^{(j+1)}$. Thus, the extended five-qubit code is equivalent to a classical ferromagnet, when decoupled qubits are removed. Later, we shall show that this model and a classical ferromagnet belong to the same quantum phase.

4.2 Local unitary transformations and disentangling operations

We have seen that an extended five qubit code can be reduced to a classical ferromagnet by applying disentangling operations on neighboring composite particles. Here, it is worth noting that these disentangling operations are closely related to a "disentangler" which is a key element in a novel RG algorithm based on the tensor product state formalism [68, 54].

In the previous chapter, we have coarse-grained the system of qubits by introducing composite particles where microscopic properties of each qubit inside a newly defined composite particle are completely lost. In a coarse-grained lattice, one may consider two STS models as the same when they can be transformed each other through unitary transformations acting on qubits inside each composite particle. For example, Hamiltonians $H = -\sum_j Z^{(j)}Z^{(j+1)}$ and $H = -\sum_j X^{(j)}X^{(j+1)}$ may be considered to be the same, as discussed in Chapter 3.

However, coarse-graining is not sufficient to characterize the scale invariant ground state properties since there still remain some short-range correlations which cannot be washed out by coarse-graining, as we have seen in analyses on a cluster state and an extended five qubit code. Such short-range entanglement must be also removed in classifying quantum phases, according to the basic philosophy of the classification of quantum phases through RG transformations.

Recently, a remarkable idea of removing short-range correlations has been proposed in a search for efficient RG algorithms based on the tensor product state formalism. The key idea is the use of a disentangling operation, called a disentangler, through local unitary transformations to remove these short-range entanglement between neighboring particles [68]. It has been demonstrated that RG transformations which combine coarse-graining and disentangling operations work in a remarkably efficient way in analyzing quantum phases arising in two-dimensional strongly correlated spin systems.

A disentangling operation used in the analysis on a cluster state is essentially similar to a disentangler used in this RG algorithm (See Fig. 3-5 in Chapter 3 too). In particular, a central idea behind these disentangling operation is that short-range entanglement is irrelevant to characterizations of quantum phases. This observation will be rigorously confirmed for quantum phases arising in STS model at the end of this chapter.

Based on observations obtained in the analyses on a cluster state and an extended five qubit code, we wish to consider two STS models as the same when they can be transformed each other by local unitary transformations. By local unitary transfor-

mations, we include the following two elements:

- **Unitary operations on composite particles:** Unitary transformations acting on qubits inside each composite particle.

- **Disentangling operations:** Unitary transformations acting on neighboring composite particles.

Here, we note that this is consistent with our original approach to distinguish quantum phases through geometric shapes of logical operators since geometric shapes of logical operators are invariant under local unitary transformations.

4.3 Logical operators in one-dimensional STS models

We have seen that geometric shapes of logical operators are central in analyzing the scale invariant ground state properties of STS models through several examples. In this subsection, the analysis is extended to arbitrary one-dimensional STS models. We obtain a canonical set of logical operators (all the independent logical operators) of arbitrary STS models, and see that logical operators are either zero-dimensional or one-dimensional, as in a classical ferromagnet. We discuss how the ground state properties, such as global entanglement, in STS models can be studied by geometric shapes of logical operators, and show that any one-dimensional STS models can be reduced to multiple copies of a classical ferromagnet, or a product state, by disentangling neighboring entanglement between composite particles through local unitary transformations.

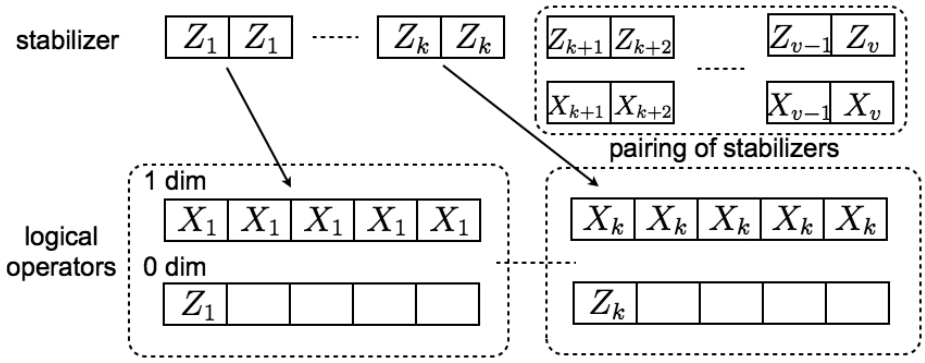

Figure 4-5: Stabilizers and logical operators in arbitrary STS models.

Let us consider an STS model defined with composite particles which consist of v qubits. For simplicity of discussion, we neglect stabilizers acting on single composite particles since decoupled qubits are to be removed. Then, stabilizers in one-

dimensional STS models can be represented in the following way (Fig. 4-5):

Ferromagnetic part:	$Z_1^{(j)} Z_1^{(j+1)},\ \cdots,\ Z_k^{(j)} Z_k^{(j+1)}$
Short-range entanglement:	$Z_{k+1}^{(j)} Z_{k+2}^{(j+1)},\ X_{k+1}^{(j)} X_{k+2}^{(j+1)},\ \cdots,\ Z_{v-1}^{(j)} Z_v^{(j+1)},\ X_{v-1}^{(j)} X_v^{(j+1)}$

where $v-k$ is an even integer. Here, stabilizers $Z_1^{(j)} Z_1^{(j+1)}, \cdots, Z_k^{(j)} Z_k^{(j+1)}$ create ferromagnet-like correlations, while $Z_{k+1}^{(j)} Z_{k+2}^{(j+1)}, X_{k+1}^{(j)} X_{k+2}^{(j+1)}, \cdots, Z_{v-1}^{(j)} Z_v^{(j+1)}, X_{v-1}^{(j)} X_v^{(j+1)}$ create short-range entanglement between neighboring composite particles as in a cluster state. Then, logical operators are

$$\Pi(\mathcal{S}_n) \ = \ \left\{ \begin{array}{cccc} \ell_1, & \cdots, & \ell_k \\ r_1, & \cdots, & r_k \end{array} \right\} \tag{4.7}$$

where

$$\ell_p \ = \ Z_p^{(1)}, \qquad r_j \ = \ X_p^{(1)} X_p^{(2)} \cdots X_p^{(N)}, \qquad \text{for} \ \ p \ = \ 1, \cdots, k. \tag{4.8}$$

Thus, geometric shapes of logical operators in one-dimensional STS models are either zero-dimensional or one-dimensional. Zero-dimensional logical operators and one-dimensional logical operators always form anti-commuting pairs (Fig. 4-6).

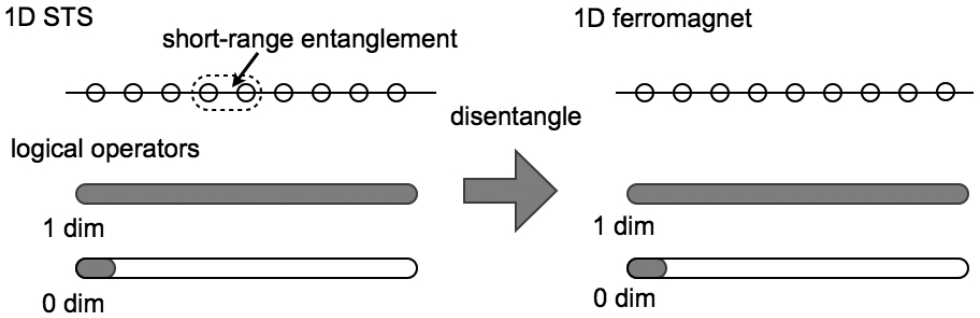

Figure 4-6: Reduction of one-dimensional STS models to classical ferromagnets by disentangling short-range entanglement between neighboring composite particles. Geometric shapes of logical operators characterize scale invariant properties of STS models.

We notice that geometric shapes of logical operator are the same as those in a classical ferromagnet. Then, we expect that the scale invariant ground state properties in one-dimensional STS models can be discussed in a way similar to discussions on a classical ferromagnet. This expectation turns out to be true. In fact, due to the existence of one-dimensional logical operators, ground states of STS models can have GHZ-like entanglement, as in a classical ferromagnet.

Even more, one can show that all the one-dimensional STS models can be reduced to classical ferromagnets by applying disentangling operations between neighboring composite particles. Let us focus on a pair of stabilizers $Z_{k+1}^{(j)} Z_{k+2}^{(j+1)}$ and $X_{k+1}^{(j)} X_{k+2}^{(j+1)}$. Then, these two stabilizers can be transformed into $Z_{k+1}^{(j)}$ and $X_{k+2}^{(j+1)}$ by removing

short-range entanglement between neighboring composite particles, as in the discussion of a cluster state. One can repeat the similar arguments for all the other pairs of stabilizers. Thus, one-dimensional STS models with k logical qubits can be reduced to the following STS model with $v = k$ through local unitary transformations:

$$H = -\sum_{j=1}^{n}\sum_{p=1}^{k} Z_p^{(j)} Z_p^{(j+1)}. \tag{4.9}$$

This model consists of "multiple copies" of a classical ferromagnet embedded in a non-interacting way. The p-th classical ferromagnet connects p-th qubits inside each composite particle with $Z_p^{(j)} Z_p^{(j+1)}$, and different classical ferromagnets embedded in the model are decoupled from each other. Therefore, when two STS models have logical operators with the same geometric shapes, they have similar global entanglement in ground states and can be reduced to an STS model in the above form.

Here, we mention the importance of geometric shapes of logical operators as indicators of global entanglement in ground states. Since geometric shapes of logical operators are invariant under local unitary transformations, they can capture the scale invariant ground state properties such as global entanglement as seen in a GHZ state (Fig 4-6). We shall soon see that geometric shapes of logical operators distinguish quantum phases in one-dimensional STS models completely, serving as order parameters.

4.4 Quantum phases and local unitary transformations

We have seen that the ground state properties, such as global entanglement, in STS models are similar when geometric shapes of their logical operators are the same. Here, our hope is to use geometric shapes of logical operators as order parameters to distinguish quantum phases. However, it is not clear if different geometric shapes of logical operators lead to different quantum phases separated by a QPT. It is also not clear if the same geometric shapes of logical operator imply that two STS models belong to the same quantum phase or not.

In this subsection and the next, we show that two STS models belong to different quantum phases if and only if geometric shapes of logical operators are different. Let us begin by showing that two STS models belong to the same quantum phase when they have the same geometric shapes of logical operators in this subsection.

Same quantum phase: Consider two STS models H_A and H_B with the same number of logical qubits k, or the same number of anti-commuting pairs of logical operators. For simplicity of discussion, let us assume that the number of qubits inside each composite particle is v for both H_A and H_B ($v \geq k$). We also assume that both H_A and H_B have the same system size. We denote the projection operators onto the ground state spaces of H_A and H_B as $\hat{P}_A$ and $\hat{P}_B$. From the discussion in the previous

subsection, there always exist a local unitary transformation U which transform $\hat{P}_A$ into $\hat{P}_B$:

$$U\hat{P}_A U^{-1} \;=\; \hat{P}_B. \tag{4.10}$$

Then, one can show that there exists a parameterized Hamiltonian which connects H_A and H_B without closing the energy gap.

Here, we give a sketch of a proof for the existence of such a parameterized Hamiltonian $H(\epsilon)$. From the discussion in the previous subsection, unitary transformations U which connects $\hat{P}_A$ and $\hat{P}_B$ can be decomposed into two parts:

$$U \;=\; U_{composite} \times U_{disentangle} \qquad \text{where} \quad [U_{composite}, U_{disentangle}] \;=\; 0. \tag{4.11}$$

The first part $U_{composite}$ represents unitary transformations acting on qubits inside each composite particle, while the second part $U_{disentangle}$ represents disentangling operations acting on neighboring composite particles. Let us begin with the case where $U_{disentangle} = I$. Then, by gradually inducing unitary transformations on each composite particle, one can transform H_A into UH_AU^{-1} without closing the energy gap or changing the number of ground states. Now, since the projection into the ground state space of UH_AU^{-1} is the same as $\hat{P}_B$, one can change $UH_AU^{\dagger}$ to H_B without closing the energy gap. Thus, H_A and H_B belong to the same quantum phase. Next, let us consider the case where $U_{composite} = I$. Let us recall a transformation from a product state Hamiltonian $H_A = -\sum_j X^{(j)}$ to a cluster state Hamiltonian $H_B = -\sum_j Z^{(j-1)}X^{(j)}Z^{(j+1)}$. Since the control-$Z$ operation acting on j-th and $j+1$-th qubits can be written as

$$\mathrm{CZ} \;=\; \exp\left[i\frac{\pi}{4}(Z^{(j)} - I)(Z^{(j+1)} - I)\right], \tag{4.12}$$

by gradually inducing the control-Z operation such that

$$\mathrm{CZ}(\epsilon) = \exp\left[i\frac{\epsilon\pi}{4}(Z^{(j)} - I)(Z^{(j+1)} - I)\right] \tag{4.13}$$

from $\epsilon = 0$ to $\epsilon = 1$, one can transform a product state Hamiltonian to a cluster state Hamiltonian without changing the energy gap by setting $H(\epsilon) = \mathrm{CZ}(\epsilon)H_A(\mathrm{CZ}(\epsilon))^{-1}$. By generalizing this idea, one can show that H_A and H_B can be transformed each other without closing the energy gap when the number of logical operators is the same. It is straightforward to extend these discussions to the cases where $U_{composite} \neq I$ and $U_{disentangle} \neq I$. Also, when the numbers of qubits inside each composite particles are different for H_A and H_B (say, v_A and v_B with $v_A \neq v_B$), we coarse-grain by grouping v qubits into a composite particle where v is the least common multiple of v_A and v_B. Then, one can repeat the similar argument and show that H_A and H_B belong to the same quantum phase. This completes the sketch of the proof.

Based on discussion in this subsection, we have the phase diagram of one-dimensional STS models as in Fig. 4-7. Note that we have not shown the existence of QPTs between different classes of STS models, which will be discussed in the next subsection.

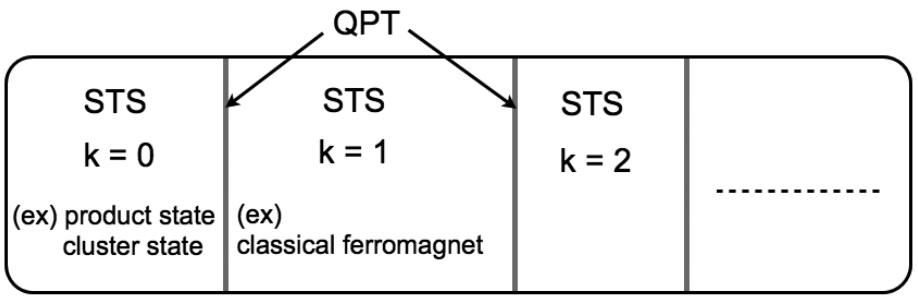

Figure 4-7: A "phase diagram" of one-dimensional STS models. Different quantum phases can be characterized by geometric shapes of logical operators (the number of logical operators). Different quantum phases are separated by QPTs.

4.5 Presence of quantum phases transitions

Next, let us show that quantum phases represented by two STS models are different when geometric shapes of logical operators are different.

One may easily see that energy gap must become gapless somewhere between two STS models when the numbers of ground states are different. When connecting two STS models through a parameterized Hamiltonian, the energy gap must close at some point as excited states need to be ground states in the course of a parameter change. Thus, two STS models with different k belong to different quantum phases which must be separated by a QPT.

One can also show the presence of non-analyticity in ground state properties by the emergence of global entanglement. As an example, let us consider the following Ising model in a transverse field:

$$\begin{aligned} H(\epsilon) &= -(1-\epsilon)H_A - \epsilon H_B \\ H_A &= H(0) = -\sum_j Z^{(j)}Z^{(j+1)}, \qquad H_B = H(1) = -\sum_j X^{(j)}. \end{aligned}$$

From the duality of the parameterized Hamiltonian, one notices that, if a system undergoes a phase transition, it must be at $\epsilon_c = 1/2$. Here, it is convenient to notice the following symmetry operator of the parameterized Hamiltonian

$$[\ell, H(\epsilon)] = 0 \qquad \ell = \prod_j X^{(j)}. \tag{4.14}$$

Note that ℓ is a logical operators of H_A, but is also a symmetry operator for $H(\epsilon)$ for arbitrary ϵ.

In order to show the presence of a QPT, we introduce the notion of *stoquastic Hamiltonians* [69].

Definition 4.1. *A non-trivial Hamiltonian H is said to be stoquastic when there*

exists a set of orthogonal states $|\psi_j\rangle$ *such that*

$$\langle\psi_i|H|\psi_j\rangle \;\leq\; 0 \qquad \textit{for} \quad (i \;\neq\; j). \tag{4.15}$$

In other words, off-diagonal elements in stoquastic Hamiltonians are zero or negative. For a more rigorous definition, see [48]. For a stoquastic Hamiltonian, one may use the Perron-Frobenius theorem which states that the energy ground state must be written as

$$|\psi_{gs}\rangle \;=\; \sum_j c_j|\psi_j\rangle \qquad c_j \;\geq\; 0. \tag{4.16}$$

One may easily see that the Ising model in a transverse field is stoquastic since a set of computational basis states satisfy the condition above. Then, as a result of the Perron-Frobenius theorem, the ground state $|\psi(\epsilon)\rangle$ for $0 < \epsilon \leq 1$ satisfies

$$\ell|\psi(\epsilon)\rangle \;=\; |\psi(\epsilon)\rangle. \tag{4.17}$$

In other words, the ground state $|\psi(\epsilon)\rangle$ is always in the $\ell = 1$ sector except at $\epsilon = 0$. Therefore, the ground state changes as follows

$$|\psi(1)\rangle \;=\; |++\cdots\rangle \;\rightarrow\; |\psi(0)\rangle \;=\; \frac{1}{\sqrt{2}}(|00\cdots\rangle + |11\cdots\rangle) \tag{4.18}$$

as ϵ goes to zero. In other words, while there are two ground states for $\epsilon = 0$, the ground state $|\psi(1)\rangle$ is adiabatically connected only to $|\psi(0)\rangle = \frac{1}{\sqrt{2}}(|00\cdots\rangle + |11\cdots\rangle)$. Since $|\psi(0)\rangle$ is a globally entangled state, there must be a QPT, involving non-analyticity in the ground state properties, somewhere during the transition. Due to the duality of the parameterized Hamiltonian, such a transition can occur only at $\epsilon = 1/2$.

A similar argument holds for the cases when H_A and H_B do not commute with each other since $H(\epsilon) = -(1-\epsilon)H_A - \epsilon H_B$ is stoquastic. While we have shown the existence of QPTs for a specific path of a parameterized Hamiltonian, this argument can be made more general by the use of Lieb-Robinson bound [70] for other paths of parameterized Hamiltonians.

Here, we would like to make some comments on phase transitions between two STS models H_A and H_B which commute with each other, but have different numbers of logical operators. In such cases, phase transitions may occur exactly at $\epsilon = 0$ or $\epsilon = 1$, instead of some intermediate point between $\epsilon = 0$ and $\epsilon = 1$. Let us look at an example. Consider the Ising model in a parallel field:

$$\begin{aligned} H(\epsilon) \;&=\; -(1-\epsilon)\sum_j Z^{(j)}Z^{(j+1)} - \epsilon\sum_j Z^{(j)} \\ H_A \;=\; H(0) \;&=\; -\sum_j Z^{(j)}Z^{(j+1)}, \qquad H_B \;=\; H(1) \;=\; -\sum_j Z^{(j)}. \end{aligned}$$

Since H_A and H_B belong to different quantum phases with different numbers of logical operators, we expect that the model undergoes some phase transition. This parameterized Hamiltonian is exactly solvable for any ϵ since all the terms in $H(\epsilon)$ commute with each other for any ϵ. Though this model connects H_A and H_B from $\epsilon = 0$ to $\epsilon = 1$, the phase transition occurs at $\epsilon = 0$. To see this more clearly, let us extend our analysis to the cases where $\epsilon < 0$ too. At $\epsilon = 0$, the model has degenerate ground states $|0\cdots 0\rangle$ and $|1\cdots 1\rangle$. At $\epsilon > 0$, the model has a single ground state $|0\cdots 0\rangle$. At $\epsilon < 0$, the model has a single ground state $|1\cdots 1\rangle$. Since the ground state properties change drastically at $\epsilon = 0$, the model undergoes a phase transition at $\epsilon = 0$. In this model H_A and H_B may not be "separated" by a phase transition since H_A lies exactly at the transition point. However, we consider that H_A and H_B belong to different quantum phases since the ground state degeneracy is lifted for $\epsilon \neq 0$. Such a phase transition is known to be first-order.

4.6 Summary and applications

We summarize the main result of this chapter (Fig. 4-7).

- Quantum phases in one-dimensional STS models can be characterized by geometric shapes of logical operators. Quantum phases represented by two STS models are different if and only if the numbers of logical operators, or the numbers of logical qubits k, are different.

Now, let us look at some examples. Within the framework of STS models, one can classify frustration-free Hamiltonians appeared in Chapter 3 in the following way:

$$H_A \;=\; -\sum_j Z^{(j)}Z^{(j+1)} \;\sim\; H'_A \;=\; -\sum_j X^{(j)}X^{(j+1)} \;\not\sim\; H_B \;=\; -\sum_j X^{(j)} \quad (4.19)$$

where H_A and $H_{A'}$ belong to the same quantum phase while H_B belong to a different quantum phase. This classification is consistent with the fact that the Ising model in a transverse field,

$$H(\epsilon) \;= -(1-\epsilon)\sum_j Z^{(j)}Z^{(j+1)} - \epsilon\sum_j X^{(j)}, \quad (4.20)$$

undergoes a QPT. Also, $H_A = -\sum_j Z^{(j)}Z^{(j+1)}$ and $H'_A = -\sum_j X^{(j)}X^{(j+1)}$ belong to the same quantum phase since they can be transformed each other through single qubit rotations without closing the energy gap. In combining the models discussed in Chapter 4.1, we have the following classification:

$$\begin{aligned} H_A \;&=\; -\sum_j Z^{(j)}Z^{(j+1)} \;\sim\; H''_A \;=\; -\sum_j X^{(j)}Y^{(j+1)}Y^{(j+2)}X^{(j+3)} \\ \not\sim\; H_B \;&=\; -\sum_j X^{(j)} \;\sim\; H'_B \;=\; -\sum_j Z^{(j-1)}X^{(j)}Z^{(j+1)}. \end{aligned} \quad (4.21)$$

While our discussions show only the existence of QPTs between STS models, analyses on QPTs in specific parameterized Hamiltonians are also important problems. However, detailed theoretical analyses on each parameterized Hamiltonian are beyond the scope of this thesis. We note that QPTs occurring in some parameterized Hamiltonians connecting the above STS models are studied in previous works [57, 58].

4.7 Discussion

We summarize the main findings in this chapter.

(a) Two quantum phases are considered to be equivalent when they are connected by local unitary transformations which consist of coarse-graining and disentangling.

(b) Quantum phases in one-dimensional STS models can be completely classified by the number of ground states.

(c) The universal quantum phase is a ferromagnetic phase.

(d) The presence of QPTs and non-analyticity in ground state properties can be shown by the emergence of global entanglement with the help of the Perron-Frobenius theorem.

One-dimensional quantum phases: Classifications of one-dimensional quantum phases have been addressed for systems described by the MPS formalism [71]. Recently, an extension of our work for systems supported by commuting frustration-free Hamiltonians was obtained [72]. While it is beyond the scope of this thesis, there have been considerable interests on classifications of quantum phases which do not break time reversal or parity symmetry [73]. These quantum phases are often called symmetry protected topological phases.

Non-commuting frustration-free Hamiltonians: In this chapter, we have limited our considerations to frustration-free Hamiltonians whose projector terms commute with each other. A novel class of spin systems has been recently proposed where the Hamiltonian is frustration-free, but projectors do not commute with each other [55]. As a result, its energy gap becomes gapless and the ground states properties are similar to the ones at quantum criticality. Studying and classifying critical spin chains arising in non-commuting frustration-free Hamiltonians may be an interesting future problem in order to deepen our understandings on quantum criticality.

Chapter 5

Two-dimensional STS model: topological phases and geometric shapes of logical operators

We have seen that, in one-dimensional STS models, different quantum phases are completely characterized by geometric shapes of logical operators. However, the only possible geometric shapes are anti-commuting pairs of zero-dimensional and one-dimensional logical operators, and thus, quantum phases are classified by only the number of logical operators without actually considering geometric shapes of logical operators. This resulted in the fact that a universal quantum phase in one-dimensional STS models is a ferromagnetic phase.

Unlike one-dimensional systems, two-dimensional systems have rich varieties of quantum phases, which may be seen from rich varieties of possible geometric shapes of logical operators in two dimensions. Here, we wish to search for possible quantum phases in two-dimensional STS models by finding logical operators and classify different quantum phases through geometric shapes of logical operators.

A useful insight in analyzing quantum phases in two-dimensional STS models is to realize the resemblance between a mathematical notion of topology and a classification of quantum phases. In classifying geometric shapes of objects by using the notion of topology, two objects are considered to be the same when they can be transformed each other through continuous deformation, while they are considered to be different when they can be transformed each other through only non-analytic changes of geometric shapes. In a similar fashion, when quantum phases are classified, two frustration-free Hamiltonians are considered to belong to the same quantum phase when their ground states can be connected continuously, while two Hamiltonians are considered to be different when they can be connected only through parameterized Hamiltonians which undergo QPTs.

In this chapter, we find that m-dimensional and $(2-m)$-dimensional logical operators form anti-commuting pairs in two-dimensional STS models where $m = 0, 1$. We also show that parameterized Hamiltonians connecting two STS models with different geometric shapes of logical operators are always separated by a QPT by proving that the energy gap must close at some point. We conclude that universal quantum phases

arising in STS models are the Toric code or a ferromagnetic phase.

5.1 Role of logical operators: concrete examples

In this subsection, we analyze geometric shapes of logical operators in three specific examples of two-dimensional STS models.

5.1.1 Two-dimensional classical ferromagnet

Recall that a two-dimensional classical ferromagnet is described by the following Hamiltonian:

$$H \;=\; -\sum_{i,j} Z^{(i,j)} Z^{(i,j+1)} - \sum_{i,j} Z^{(i,j)} Z^{(i+1,j)} \tag{5.1}$$

where $Z^{(i,j)}$ represents the Pauli operator Z acts on a qubit labeled by a vector (i,j). The total number of qubits is $n = L_1 \times L_2$, and the system has periodic boundary conditions. This stabilizer code is an STS model, satisfying continuous scale symmetries since $k = 1$ for any L_1 and L_2. Logical operators are

$$\ell \;=\; Z^{(1,1)} \;=\; \begin{bmatrix} I, & I, & \cdots, & I \\ \vdots & \vdots & \vdots & \vdots \\ I, & I, & \cdots, & I \\ Z, & I, & \cdots, & I \end{bmatrix}, \qquad r \;=\; \prod_{i,j} X^{(i,j)} \;=\; \begin{bmatrix} X, & X, & \cdots, & X \\ X, & X, & \cdots, & X \\ \vdots & \vdots & \vdots & \vdots \\ X, & X, & \cdots, & X \end{bmatrix}.$$

One can see that both of logical operators satisfy the translation equivalence of logical operators since

$$T_1(\ell) \;\sim\; T_2(\ell) \;\sim\; \ell, \qquad T_1(r) \;=\; T_2(r) \;=\; r. \tag{5.2}$$

According to geometric shapes of logical operators, we may call ℓ a *zero-dimensional logical operator* and r a *two-dimensional logical operator*. As in a one-dimensional classical ferromagnet, a two-dimensional classical ferromagnet can support a GHZ state at zero temperature: $|\mathrm{GHZ}\rangle = \frac{1}{\sqrt{2}}(|0\cdots 0\rangle + |1\cdots 1\rangle)$. A GHZ state is stabilized by a two-dimensional logical operator r since $r|\mathrm{GHZ}\rangle = |\mathrm{GHZ}\rangle$.

5.1.2 The Toric code as an STS model

Next, let us discuss the Toric code which is a stabilizer code with topological order. The Hamiltonian of the Toric code is shown in Fig. 5-1.

The Toric code can be reduced to an STS model by grouping two qubits into a composite particle ($v = 2$) as shown in Fig. 5-1. By applying some appropriate unitary transformations on qubits inside each composite particle, interaction terms

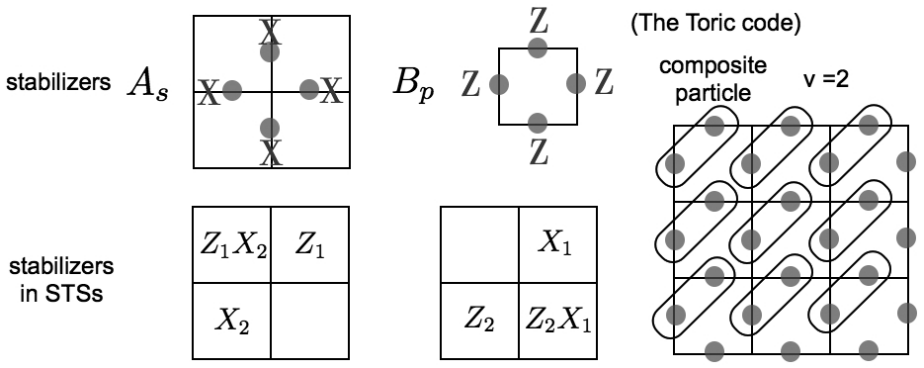

Figure 5-1: Reduction of the Toric code to an STS model.

$\mathcal{A}_s$ and $\mathcal{B}_p$ can be represented in the following way (Fig. 5-1):

$$\mathcal{A}^{(i,j)} = Z_1^{(i,j)} X_2^{(i,j)} Z_1^{(i+1,j)} X_2^{(i,j+1)} = \begin{bmatrix} X_2, & I \\ Z_1X_2, & Z_1 \end{bmatrix}^{(i,j)} \tag{5.3}$$

$$\mathcal{B}^{(i,j)} = X_1^{(i+1,j)} Z_2^{(i,j+1)} Z_2^{(i+1,j+1)} X_1^{(i+1,j+1)} = \begin{bmatrix} Z_2, & X_1Z_2 \\ I, & X_1 \end{bmatrix}^{(i,j)}. \tag{5.4}$$

Here, $Z_1^{(i,j)}$ represents a Pauli operator Z_1 acting on a composite particle labeled by (i,j). Z_1, Z_2, X_1 and X_2 are single Pauli operators acting on a single composite particle. 2×2 matrices represent stabilizers graphically. One can see that this model satisfies continuous scale symmetries by noticing $\prod_{i,j} \mathcal{A}^{(i,j)} = I$ and $\prod_{i,j} \mathcal{B}^{(i,j)} = I$.

Now, two pairs of anti-commuting logical operators in the Toric code can be described in the following way:

$$\ell_1 = \prod_j Z_1^{(1,j)} = \begin{bmatrix} Z_1, & I, & \cdots, & I \\ \vdots & \vdots & \vdots & \vdots \\ Z_1, & I, & \cdots, & I \\ Z_1, & I, & \cdots, & I \end{bmatrix} \qquad \ell_2 = \prod_j Z_2^{(1,j)} = \begin{bmatrix} Z_2, & I, & \cdots, & I \\ \vdots & \vdots & \vdots & \vdots \\ Z_2, & I, & \cdots, & I \\ Z_2, & I, & \cdots, & I \end{bmatrix}$$

$$r_1 = \prod_i X_1^{(i,1)} = \begin{bmatrix} I, & I, & \cdots, & I \\ \vdots & \vdots & \vdots & \vdots \\ I, & I, & \cdots, & I \\ X_1, & X_1, & \cdots, & X_1 \end{bmatrix} \quad r_2 = \prod_i X_2^{(i,1)} = \begin{bmatrix} I, & I, & \cdots, & I \\ \vdots & \vdots & \vdots & \vdots \\ I, & I, & \cdots, & I \\ X_2, & X_2, & \cdots, & X_2 \end{bmatrix}.$$

Here, $n_1 \times n_2$ matrices represent logical operators graphically where n_1 and n_2 are the numbers of composite particles in the $\hat{1}$ and $\hat{2}$ directions. According to geometric shapes of these logical operators, we may call them *one-dimensional logical operators*.

One can easily see that the translation equivalence of logical operators holds from

the following equations:

$$\prod_j \mathcal{A}^{(1,j)} = \ell_1 T_1(\ell), \quad \prod_i \mathcal{A}^{(i,1)} = r_2 T_2(r_2),$$
$$\prod_j \mathcal{B}^{(1,j)} = \ell_2 T_1(\ell_2), \quad \prod_i \mathcal{B}^{(i,1)} = r_1 T_2(r_1).$$

5.1.3 Another model with topological order

Here, we discuss another model with topological order. We consider a system of $L_1 \times L_2$ qubits governed by the following Hamiltonian:

$$H = -\sum_{i,j} S^{(i,j)} \tag{5.5}$$

where

$$\begin{aligned} S^{(i,j)} &= X^{(i-1,j)} X^{(i,j)} X^{(i+1,j)} Z^{(i,j-1)} Z^{(i,j+1)} \\ &= \begin{bmatrix} & Z & \\ X & X & X \\ & Z & \end{bmatrix}^{(i,j)} . \end{aligned} \tag{5.6}$$

Here, blank entries represent identity operators I. One can see that interaction terms $S^{(i,j)}$ commute with each other. In a strict sense, this system is not an STS model since the number of logical qubits change according to L_1 and L_2. In particular, with some calculations, we have

$$\begin{aligned} k &= 1 \quad \text{for} \quad L_1 \neq 0 \pmod 3, \quad L_2 \neq 0 \pmod 2 \\ k &= 2 \quad \text{for} \quad L_1 = 0 \pmod 3, \quad L_2 \neq 0 \pmod 2 \\ k &= 2 \quad \text{for} \quad L_1 \neq 0 \pmod 3, \quad L_2 = 0 \pmod 2 \\ k &= 4 \quad \text{for} \quad L_1 = 0 \pmod 3, \quad L_2 = 0 \pmod 2. \end{aligned}$$

However, the model can be treated as an STS model when we view 3×2 qubits as a composite particle. Let us define $n_1 = L_1/3$ and $n_2 = L_2/2$ by choosing L_1 to be a multiple of 3 and L_2 to be a multiple of 2. Then, the system possesses continuous scale symmetries since $k = 4$ for any n_1 and n_2.

Now, let us represent stabilizers in this model in terms of composite particles. By applying appropriate unitary transformations on qubits inside each composite particle, we can represent stabilizers in the following way:

$$S_1^{(i,j)} = \begin{bmatrix} Z_1, & I \\ Z_1X_2, & X_2 \end{bmatrix}^{(i,j)}, \; S_2^{(i,j)} = \begin{bmatrix} X_1, & X_1Z_2 \\ I, & Z_2 \end{bmatrix}^{(i,j)}, \; S_3^{(i,j)} = \begin{bmatrix} Z_3, & I \\ Z_3X_4, & X_4 \end{bmatrix}^{(i,j)}$$
$$S_4^{(i,j)} = \begin{bmatrix} X_3, & X_3Z_4 \\ I, & Z_4 \end{bmatrix}^{(i,j)}, \; S_5^{(i,j)} = \begin{bmatrix} X_5, & I \\ X_6, & I \end{bmatrix}^{(i,j)}, \; S_6^{(i,j)} = \begin{bmatrix} Z_5, & I \\ Z_6, & I \end{bmatrix}^{(i,j)}$$

Then, logical operators can be easily found by looking at stabilizers $S_1^{(i,j)}$, $S_2^{(i,j)}$, $S_3^{(i,j)}$ and $S_4^{(i,j)}$ since they have forms similar to $\mathcal{A}^{(i,j)}$ and $\mathcal{B}^{(i,j)}$ in the Toric code. Logical operators are

$$\Pi(\mathcal{S}_{n_1,n_2}) \;=\; \left\langle \begin{array}{cccc} \ell_1, & \ell_2, & \ell_3, & \ell_4 \\ r_1, & r_2, & r_3, & r_4 \end{array} \right\rangle \tag{5.7}$$

where

$$\begin{array}{llll} \ell_1 = \prod_i X_1^{(i,1)}, & \ell_2 = \prod_i X_2^{(i,1)}, & \ell_3 = \prod_i X_3^{(i,1)}, & \ell_4 = \prod_i X_4^{(i,1)} \\ r_1 = \prod_j Z_1^{(1,j)}, & r_2 = \prod_j Z_2^{(1,j)}, & r_3 = \prod_j Z_3^{(1,j)}, & r_4 = \prod_j Z_4^{(1,j)}. \end{array} \tag{5.8}$$

Thus, the model has four pairs of anti-commuting one-dimensional logical operators.

Now, since topological properties of ground states are similar to those of ground states in the Toric code, we naturally expect that this model and the Toric code may belong to the same quantum phase. In fact, the model can be reduced to two copies of the Toric code by applying local unitary transformations. From the forms of stabilizers $S_1^{(i,j)}, \cdots, S_6^{(i,j)}$, one may expect that stabilizers $S_1^{(i,j)}, \cdots, S_4^{(i,j)}$ are responsible for the existence of topological order. In particular, it can be seen that 5th and 6th qubits inside each composite particle are decoupled from other qubits, and are not relevant to topological order. In fact, one can remove $S_5^{(i,j)}$ and $S_6^{(i,j)}$ by applying disentangling operations between neighboring composite particles in a way similar to the reduction of a cluster state to a product state used in the discussion of one-dimensional STS models. $S_1^{(i,j)}, \cdots, S_4^{(i,j)}$ look the same as interaction terms $\mathcal{A}^{(i,j)}$ and $\mathcal{B}^{(i,j)}$ in the Toric code. Also, it can be seen that 1st and 2nd qubits are decoupled from 3rd and 4th qubits. Thus, one may see that *two copies of the Toric code are embedded in this model in a non-interacting way.*

Here, we briefly mention other two-dimensional stabilizer Hamiltonians with topological order. A notable model is the topological color code, which is particularly useful for quantum information processing tasks with high threshold values [74]. One can show that the topological color code can be also considered as an STS model after an appropriate coarse-graining, and can be reduced to the Toric code.

5.2 Logical operators in two-dimensional STS models and topological order

We have analyzed possible geometric shapes of logical operators in two-dimensional STS models through several examples, and found that logical operators form anti-commuting pairs in the following way:

Classical Ferromagnet ($k = 1$)	0-dim $-$ 2-dim
The Toric code ($k = 2$)	1-dim $-$ 1-dim

We have also seen that one-dimensional logical operators may be responsible for the existence of topological order.

Here, we present possible geometric shapes of logical operators. In two-dimensional STS models, possible geometric shapes are "anti-commuting pairs of zero-dimensional and two-dimensional logical operators" and "anti-commuting pairs of one-dimensional logical operators" (Fig. 5-2). In particular, there exist a canonical set of logical operators

$$\Pi(\mathcal{S}_{n_1,n_2}) \;=\; \left\{ \begin{array}{cccc} \ell_1, & \cdots, & \ell_k \\ r_1, & \cdots, & r_k \end{array} \right\} \tag{5.9}$$

which satisfy the following conditions after some appropriate local unitary transformations on qubits inside each composite particle:

- **Zero-dimensional and two-dimensional logical operators:** For $p = 1, \cdots, k_0$ ($k_0 \leq k$), ℓ_p are logical operators defined inside a region of $2v \times 1$ composite particles, and r_p are logical operators defined all over the lattice in a periodic way:

$$r_p \;=\; \prod_{i,j} X_p^{(i,j)} \;=\; \begin{bmatrix} X_p, & X_p, & \cdots, & X_p \\ \vdots & \vdots & \vdots & \vdots \\ X_p, & X_p, & \cdots, & X_p \\ X_p, & X_p, & \cdots, & X_p \end{bmatrix}.$$

- **One-dimensional logical operators:** For $p = k_0 + 1, \cdots, k$, ℓ_p are logical operators defined inside a region with $n_1 \times 1$ composite particles and r_p are logical operators defined inside a region with $1 \times n_2$ composite particles:

$$\ell_p = \prod_j Z_p^{(1,j)} = \begin{bmatrix} Z_p, & I, & \cdots, & I \\ \vdots & \vdots & \vdots & \vdots \\ Z_p, & I, & \cdots, & I \\ Z_p, & I, & \cdots, & I \end{bmatrix} \quad r_p = \prod_i X_p^{(i,1)} = \begin{bmatrix} I, & I, & \cdots, & I \\ \vdots & \vdots & \vdots & \vdots \\ I, & I, & \cdots, & I \\ X_p, & X_p, & \cdots, & X_p \end{bmatrix}.$$

Logical operators are graphically shown in Fig. 5-2. Here, we have assigned dimensions to logical operators according to their geometric shapes. Note that zero-dimensional logical operators are "not completely zero-dimensional" since they are defined inside a region with $2v \times 1$ composite particles. For ease of graphical representations, we draw logical operators ℓ_p ($p = 1, \cdots, k_0$) by assuming that they can be actually supported by a single composite particle in Fig. 5-2.

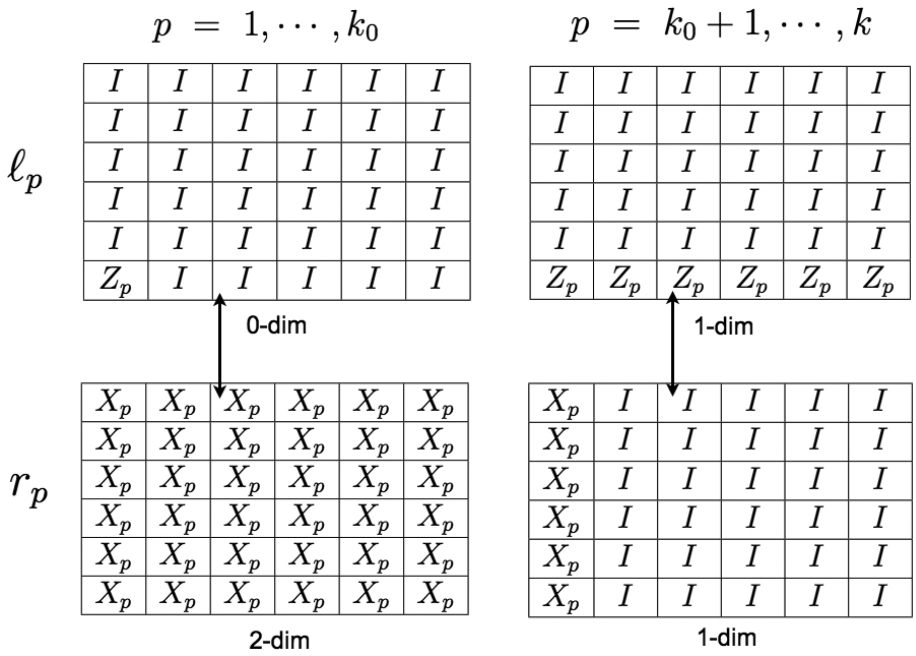

Figure 5-2: A canonical set of logical operators in a two-dimensional STS model. Two-sided arrows represent anti-commutations. Note that zero-dimensional logical operators ℓ_p ($p = 1, \cdots, k_0$) are represented inside a single composite particle instead of a region with $2v \times 1$ composite particles for ease of graphical representations. Dimensions are assigned to logical operators according to their geometric shapes.

5.3 Quantum phases in two-dimensional STS models

Finally, let us classify quantum phases arising in two-dimensional STS models. Here, we show that geometric shapes of logical operators can be used as "order parameters" to distinguish quantum phases, including topological phases, by proving that any parameterized Hamiltonians connecting two STS models with different geometric shapes of logical operators are always separated by QPTs. We also show that the existence of a QPT originates from the non-analyticity of transforming logical operators with topologically distinct shapes each other since there is no continuous deformation (diffeomorphism) between them at the thermodynamic limit.

The vanishing energy gap and topological QPT: Let us begin by clarifying the problem we address. Consider two STS models H_A and H_B. When the number of logical operators in H_A and H_B are different, there must always be a QPT between H_A and H_B as discussed in the previous chapter. Therefore, we consider the cases where H_A and H_B have the same number of logical operators, but different geometric shapes of logical operators. In particular, for simplicity of discussion, we consider the case where H_A has two pairs of anti-commuting zero-dimensional and two-dimensional logical operators ($k_0 = 2$, $k_1 = 0$ and $k = 2$) while H_B has two pairs of anti-commuting

one-dimensional logical operators ($k_0 = 0$, $k_1 = 2$ and $k = 2$). One may think that H_A is two copies of ferromagnets and H_B as the Toric code for simplicity. One can generalize this discussion to the cases with arbitrary numbers of logical operators easily.

Our goal is to show that H_A and H_B belong to different quantum phases. For this purpose, we use the contradiction; suppose that there exists a parameterized Hamiltonian $H(\epsilon)$ which connects H_A and H_B without closing the energy gap or changing the number of ground states:

$$H(0) \;=\; H_A, \qquad H(1) \;=\; H_B, \qquad \Delta(\epsilon) \;\geq\; c \quad \text{for all } \epsilon \tag{5.10}$$

where $\Delta(\epsilon)$ is the energy gap and c is some constant which does not depend on the system size. More precisely, we assume that four ground states of $H(\epsilon)$ are separated from excited states by $\Delta(\epsilon)$. We assume that $H(\epsilon)$ connects H_A and H_B without any sudden changes in interaction terms, and there is no source of non-analyticity *a priori*. Our discussion can be easily generalized to the cases where ground state degeneracy is broken, yet the lowest four ground states are separated from excited states.

The most striking difference between H_A and H_B is the presence and the absence of topological order which can be seen by different geometric shapes of their logical operators. This drastic change of geometric shapes may underlie a non-analytic change of the ground state properties and a vanishing energy gap. Then, one might hope to show the existence of a QPT by looking at how geometric shapes of logical operators change with a parameter change. However, unlike H_A and H_B, one cannot define logical operators inside the Pauli group for $H(\epsilon)$ at $0 < \epsilon < 1$ since the Hamiltonian $H(\epsilon)$ is frustrated in general.

Despite $H(\epsilon)$ is frustrated and not a stabilizer Hamiltonian in general, it is possible to define operators which act like logical operators. Let us denote projection operators onto the ground state space of $H(\epsilon)$ as $\hat{P}(\epsilon)$. Since the number of degenerate ground states does not change with ϵ, one can find some unitary transformation which satisfy the following condition:

$$\hat{P}(\epsilon) \;=\; U(\epsilon)\hat{P}_A U(\epsilon)^{-1}, \qquad \hat{P}_A \;\equiv\; \hat{P}(0), \quad \hat{P}_B \;\equiv\; \hat{P}(1) \tag{5.11}$$

where $\hat{P}_A$ and $\hat{P}_B$ represent projections onto the ground state spaces of H_A and H_B respectively. Here, we note that such a unitary transformation is not uniquely determined and has many degrees of freedom. The unitary transformation $U(\epsilon)$ may characterize the evolution of ground states with respect to ϵ. Let us pick up some ground state $|\psi(0)\rangle$ of H_A at $\epsilon = 0$. Then, the following state $|\psi(\epsilon)\rangle = U(\epsilon)|\psi(0)\rangle$ is a ground state of $H(\epsilon)$. Here, we denote an anti-commuting pair of zero-dimensional and two-dimensional logical operators in H_A as ℓ_A and r_A. Then, the following operators act like logical operators inside the ground state space of $H(\epsilon)$, transforming degenerate ground states among them:

$$\ell(\epsilon) \;=\; U(\epsilon)\ell_A U(\epsilon)^{-1}, \qquad r(\epsilon) \;=\; U(\epsilon) r_A U(\epsilon)^{-1} \tag{5.12}$$

since they act non-trivially inside the ground state space:

$$\{\ell(\epsilon), r(\epsilon)\} \;=\; 0, \qquad \ell(\epsilon)^2 \;=\; r(\epsilon)^2 \;=\; I. \tag{5.13}$$

Note that $\ell(0) = \ell$ and $r(0) = r$. We call $\ell(\epsilon)$ and $r(\epsilon)$ *analytically continued logical operators* [67]. Note that $\ell(\epsilon)$ and $r(\epsilon)$ may not commute with the parameterized Hamiltonian $H(\epsilon)$.

Intuitive approach based on topology in logical operators: Now, let us discuss how analytically continued logical operators $\ell(\epsilon)$ change with respect to ϵ. Here, we first give an intuitive explanation why the assumption of no QPT leads to a contradiction. Then, we add some mathematical rigor to our intuition.

At the beginning of the discussion, we have assumed that there is no QPT between $\epsilon = 0$ and $\epsilon = 1$. Then, we naturally hope that the geometric shapes of $\ell(\epsilon)$ change smoothly with respect to ϵ. A unitary transformation $U(\epsilon)$ must not have any non-analyticity with respect to ϵ even at the thermodynamic limit since a ground state $|\psi(\epsilon)\rangle$ must change continuously with ϵ. Then, $\ell(\epsilon)$ also changes continuously with respect to ϵ without non-analyticity. At $\epsilon = 0$, a zero-dimensional logical operator $\ell(0) \equiv \ell_A$ is defined inside some localized region (Fig. 5-3). For ϵ sufficiently close to zero, $\ell(0)$ and $\ell(\epsilon)$ are similar, and $\ell(\epsilon)$ may be approximated as:

$$\ell(\epsilon) \approx \ell(0) + \epsilon\ell(0)' \tag{5.14}$$

where $\ell(0)'$ represents the derivative of $\ell(\epsilon)$ with respect to ϵ at $\epsilon = 0$. Then, the geometric shape of $\ell(\epsilon)$ should be similar to the one of $\ell(0)$ (Fig. 5-3). The assumption that $\ell(0)'$ is local can be justified by the fact that $H(\epsilon)$ consists only of local terms which change continuously.

Next, let us analyze geometric shapes of $\ell(\epsilon)$ at $\epsilon = 1$. At $\epsilon = 1$, the analytically continued logical operators $\ell(1)$ and $r(1)$ act non-trivially inside the ground state space of H_B. Let us recall that H_B has pairs of one-dimensional logical operators, and is free from zero-dimensional logical operators. Here, we define a region R which is the largest zero-dimensional region with $(n_1 - 1) \times (n_2 - 1)$ composite particles. Then, we have $g_R = 0$ due to the bi-partition theorem since $g_{\bar{R}} = 4$. In other words, one cannot induce non-trivial transformation on ground states through actions on composite particles inside R. Therefore, $\ell(\epsilon = 1)$ cannot be defined inside localized regions.

Then, geometric shapes of $\ell(\epsilon)$ changes from a zero-dimensional object ℓ_A to a one-dimensional object $\ell(1)$ as we vary ϵ from $\epsilon = 0$ to $\epsilon = 1$. However, it is impossible to change geometric shapes of a zero-dimensional object to a one-dimensional object continuously at the thermodynamic limit since a continuous deformation between them is topologically prohibited. This contradicts with our original assumption that there is no QPT in $H(\epsilon)$. Thus, there must be a QPT between H_A and H_B, and we may conclude that H_A and H_B belong to different quantum phases. Though we have assumed that $\ell(1)$ happens to be a one-dimensional logical operator ℓ_B in H_B, the observation that $\ell(1)$ cannot be defined locally is sufficient to reach the same

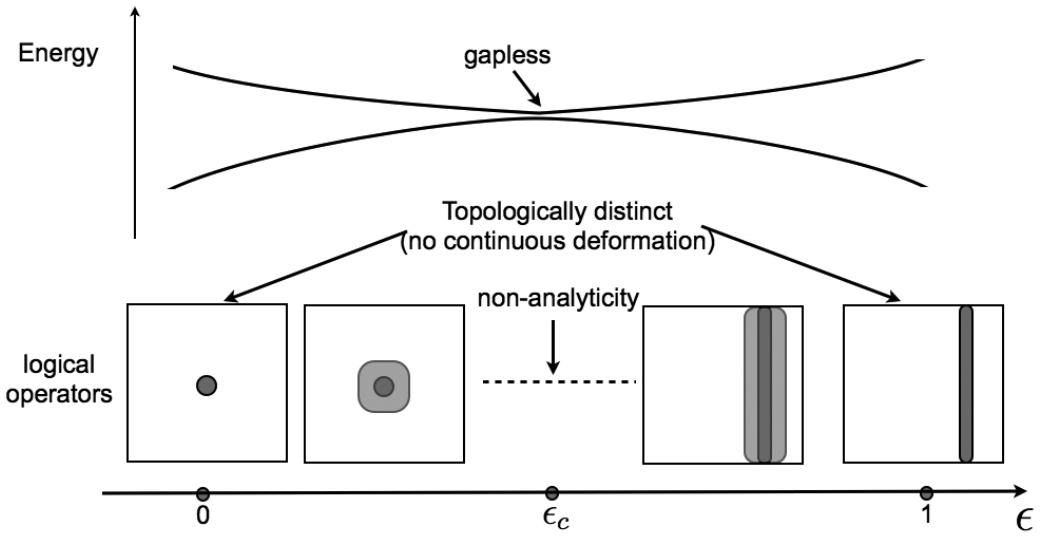

Figure 5-3: Geometric shapes of an analytically continued logical operator, the vanishing energy gap, and the existence of a QPT. Lightly shaded regions represent the "shapes" of analytically continued logical operators.

conclusion.

5.4 Adiabatic continuation and quantum phase transitions

While the above analysis implies that the topological distinction between geometric shapes of logical operators in H_A and H_B lead to the existence of a QPT, the discussion may lack in a mathematical rigor. In particular, we have assumed that geometric shapes of $\ell(0)$ and $\ell(\epsilon)$ for small ϵ are close. However, it is not clear if this assumption is correct or not. Also, while we have used the expression "geometric shape" naively to describe geometric properties of analytically continued logical operators $\ell(\epsilon)$, we have not stated clearly the definition of geometric shapes of analytically continued logical operators.

Below, we shall clear these ambiguities by borrowing theoretical techniques developed in studies of adiabatic continuation [53, 70, 75, 28]. Adiabatic continuation is an idea of studying the ground state properties of Hamiltonians belonging to the same quantum phase by finding a gapped parameterized Hamiltonian connecting them. Here, for simplicity of discussion, we begin with the cases where there is always a single ground state in parameterized Hamiltonians. If two Hamiltonians H and H' are in the same quantum phase, one can always find gapped parameterized Hamiltonian $H(\epsilon)$ connecting them due to the definition of quantum phases. Then, according to the adiabatic theorem [76, 77], by varying the parameterized Hamiltonian $H(\epsilon)$ sufficiently slowly, one can transfer a ground state of H (denoted as $|\psi\rangle$) to a ground state of H' (denoted as $|\psi'\rangle$). A key idea is to realize that a unitary operator U required to

transform $|\psi\rangle$ to $|\psi'\rangle$ ($|\psi'\rangle = U|\psi\rangle$) can be extracted from the parameterized Hamiltonians $H(\epsilon)$. In particular, theoretical techniques on adiabatic continuation provide systematic formulas to obtain such a unitary transformation U from a gapped parameterized Hamiltonian $H(\epsilon)$. While we have started our discussions with the cases where there is only a single ground state, adiabatic continuation also works when there is the ground state degeneracy and the number of degenerate ground states does not change. Even more, it works when the ground state degeneracy is slightly broken.

Now, we interpret our previous analyses on the parameterized Hamiltonians in Eq. (5.10) through adiabatic continuation. Let us recall that we have supposed that there exists a gapped parameterized Hamiltonian $H(\epsilon)$ which connect H_A and H_B, and the number of ground stated does not change as we vary ϵ. Then, one can represent the unitary transformation $U(\epsilon)$ defined in Eq. (5.11) through the parameterized Hamiltonian $H(\epsilon)$. Now, we discuss properties of analytically continued logical operator $\ell(\epsilon) = U(\epsilon)\ell_A U(\epsilon)^{-1}$. A remarkable discovery from recent developments on studies of adiabatic continuation is the fact that one can approximate analytically continued logical operators $\ell(\epsilon)$ with some operator $\tilde{\ell}(\epsilon)$ whose geometric shape is close to the one of ℓ_A as long as a parameterized Hamiltonian $H(\epsilon)$ remains gapped at the thermodynamic limit [53, 28]. In particular, there exists an approximation $\tilde{\ell}(\epsilon)$ defined inside some localized region with $\xi(\epsilon) \times \xi(\epsilon)$ composite particles:

$$\ell(\epsilon) \ \sim \ \tilde{\ell}(\epsilon) \tag{5.15}$$

where $\xi(\epsilon)$ depends on the energy gap $\Delta(\epsilon)$, but remains finite even at the thermodynamic limit. Here, by approximation, we mean that $\ell(\epsilon)$ and $\tilde{\ell}(\epsilon)$ act in a similar way inside the ground state space. In particular, if $\ell(\epsilon)$ transforms two degenerate ground states $|\psi(\epsilon)\rangle$ and $|\psi'(\epsilon)\rangle$ of $H(\epsilon)$ in the following way:

$$\ell(\epsilon)|\psi(\epsilon)\rangle \ = \ |\psi(\epsilon)'\rangle, \qquad \langle\psi'(\epsilon)|\tilde{\ell}(\epsilon)|\psi(\epsilon)\rangle \ \sim \ O(1). \tag{5.16}$$

Here, the inner product is some constant which does not depend on the system size.

Since $\tilde{\ell}(\epsilon)$ approximates $\ell(\epsilon)$, one may consider a localized region with $\xi(\epsilon) \times \xi(\epsilon)$ composite particles as the geometric shape of $\ell(\epsilon)$. Now, at $\epsilon = 1$, we have an approximation $\tilde{\ell}(1)$ which is defined inside some finite region with $\xi(1) \times \xi(1)$ composite particles. Then, we have

$$\langle\psi'(1)|\tilde{\ell}(1)|\psi(1)\rangle \ \sim \ O(1) \tag{5.17}$$

for two orthogonal ground states $|\psi(1)\rangle$ and $|\psi'(1)\rangle$ of $H(1) \equiv H_B$. However, from the indistinguishability condition, there is no local physical observable which can transform ground states each other in H_B. Thus, $\xi(1)$ must be an infinite number at the thermodynamic limit, which leads to a contradiction. Therefore, there must be a QPT between H_A and H_B since the energy gap vanishes or the number of degenerate ground states changes at some point.

QPTs and topology in logical operators: We have seen that non-analytic

changes of geometric shapes of logical operators lead to the existence of the vanishing energy gap. This observation may be better understood by the notion of topology. Topology is a study of classifying objects in terms of smoothness and non-analyticity. If two objects can be transformed each other through continuous deformations (diffeomorphism), they are considered to be the same. Roughly speaking, diffeomorphism is a one-to-one mapping between two geometric manifolds where both the map itself and its inverse are differentiable. The notion of topology has been particularly useful in characterizing physical properties which may survive even at the thermodynamic limit, mainly in the context of field theory where physical properties are to be discussed at the continuum limit.

In a strict sense, the notion of topology cannot be introduced in discussions of quantum phases arising in lattice systems since spins on lattices are discretely distributed and geometric shapes of logical operators are not smoothly determined. However, by considering a system of qubits at the thermodynamic limit, one can smoothen geometric shapes of logical operators effectively. Then, the fact that there is no continuous unitary transformation $U(\epsilon)$ transforming $\ell(0)$ into $\ell(1)$ is a direct consequence of the fact that there is no diffeomorphism which map a topologically trivial object (a zero-dimensional point) to a topologically non-trivial object (a one-dimensional loop winding around the torus). In other words, one cannot cut the winding of a one-dimensional logical operator without introducing some non-analyticity.

5.5 Summary and application

We have shown that H_A and H_B belong to different quantum phases when geometric shapes of logical operators are different. Though discussions have been limited to the cases where H_A has two pairs of anti-commuting logical operators and H_B has two pairs of anti-commuting logical operators, our analysis can be readily generalized to arbitrary two-dimensional STS models.

Let us consider the case when H_A and H_B have various numbers of pairs of anti-commuting logical operators. In particular, let us denote the numbers of logical qubits as $k^{(A)}$ and $k^{(B)}$, and the numbers of zero-dimensional logical operators $k_0^{(A)}$ and $k_0^{(B)}$ with $k_1^{(A)} = k^{(A)} - k_0^{(A)}$ and $k_1^{(B)} = k^{(B)} - k_0^{(B)}$:

	(1 dim)-(1 dim)	(0 dim)-(2 dim)
H_A	$k_1^{(A)}$	$k_0^{(A)}$
H_B	$k_1^{(B)}$	$k_0^{(B)}$

Then, two STS models belong to different quantum phases when $k_1^{(A)} \neq k_1^{(B)}$ or $k_0^{(A)} \neq k_0^{(B)}$. Finally, consider the cases where two STS models have the same geometric shapes of logical operators: $k_0^{(A)} = k_0^{(B)}$ and $k_1^{(A)} = k_1^{(B)}$. Then one can prove that two STS models are in the same quantum phase by explicitly giving local unitary transformations connecting them. We note that k_1 must be even as a result of some constraints arising in the form of stabilizer generators. See [12] for the details.

Here, we summarize the main result of this chapter (Fig. 5-4).

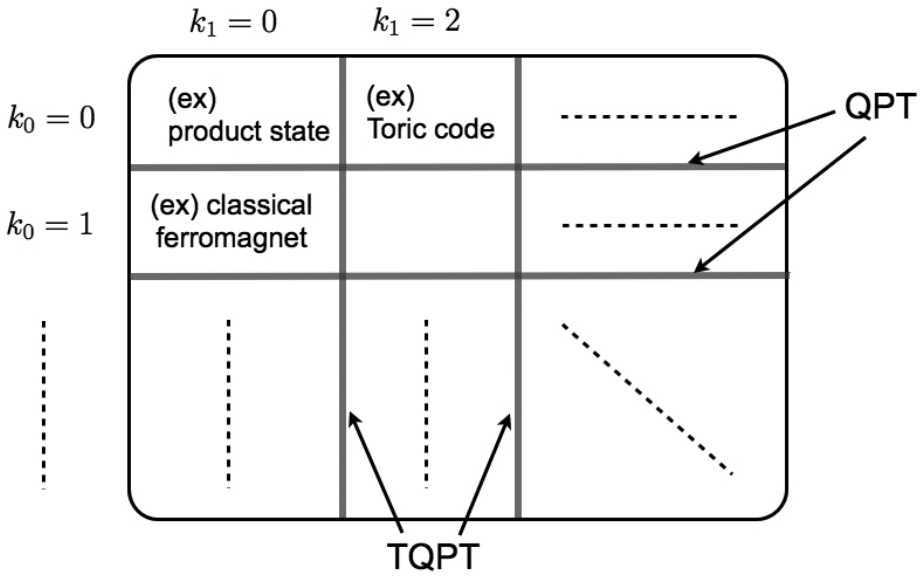

Figure 5-4: A "phase diagram" of two-dimensional STS models.

- Different quantum phases in two-dimensional STS models can be classified by geometric shapes of logical operators. There must be a QPT when there is a topologically prohibited change in geometric shapes of logical operators between two STS models. Geometric shapes of logical operators can be used as order parameters to distinguish quantum phases arising in two-dimensional STS models.

Note that a QPT with a change of the numbers of one-dimensional logical operators involves the emergence or the loss of topological order. Such QPTs are called topological QPT (TQPT). In Fig. 5-4, a QPT which crosses the boundary in the lateral direction is a topological QPT, while a QPT which crosses the boundary in the vertical direction is a non-topological QPT.

Now, let us look at some examples. As a result of our analysis on geometric shapes of logical operators, one can classify quantum phases arising in STS models in the following way:

$$H_A = \sum_{i,j} \begin{bmatrix} Z & X \\ X & Z \end{bmatrix}^{(i,j)} \qquad (k_0 = 0,\ k_1 = 2)$$

$$\not\sim H_B = -\sum_{i,j} X^{(i,j)} \sim H'_B = \sum_{i,j} \begin{bmatrix} & Z & \\ Z & X & Z \\ & Z & \end{bmatrix}^{(i,j)} \qquad (k_0 = 0,\ k_1 = 0)$$

$$\not\sim H_C = -\sum_{i,j} Z^{(i,j)} Z^{(i,j+1)} - \sum_{i,j} Z^{(i,j)} Z^{(i+1,j)} \qquad (k_0 = 1,\ k_1 = 0)$$

$$\not\sim H_D = -\sum_{i,j} \begin{bmatrix} & Z & \\ X & X & X \\ & Z & \end{bmatrix}^{(i,j)} \sim H'_D = -\sum_{i,j} \begin{bmatrix} & Z & \\ X & & X \\ & Z & \end{bmatrix}^{(i,j)} \qquad (k_0 = 0,\ k_1 = 4).$$

Here, H_A is the Toric code, H_B is a Hamiltonian supporting a single product state, H'_B is a Hamiltonian supporting a two-dimensional cluster state, H_C is a classical ferromagnet and H_D and H'_D are Hamiltonians discussed in Chapter 5.1. H_A and H'_A have two pairs of anti-commuting one-dimensional logical operators, H_B and H'_B have no logical operators, H_C has a pair of zero-dimensional and two-dimensional logical operators and H_D and H'_D have four pairs of anti-commuting one-dimensional logical operators.

5.6 Discussion

We have studied possible quantum phases in one-dimensional and two-dimensional STS models and classified them by geometric shapes of logical operators. We summarize the main findings in this chapter as follows:

(a) In two-dimensional STS models, m-dimensional and $2-m$-dimensional logical operators form anti-commuting pairs.

(b) Universal quantum phases in two-dimensional STS models are the Toric code and ferromagnet.

(c) Topological phase transitions are induced by non-analytical changes of geometric shapes of logical operators.

(d) The existence of non-analyticity can be shown with the help of the theory of adiabatic continuation and the Lieb-Robinson bound.

Two-dimensional quantum phases: A similar result for two-dimensional stabilizer Hamiltonians was obtained by a different approach [15] after the publication of our work. Searches and classifications of quantum phases in arbitrary commuting frustration-free Hamiltonians may be an interesting future problem. See [54] for an approach based on TPS formalism.

Topological deformation of logical operators: In Chapter 2, we have demonstrated that geometric shapes of logical operators arising in a ferromagnet and the Toric code can be continuously deformed while keeping them equivalent. One can show that this continuous deformability of logical operators also holds for arbitrary STS models for $D = 1, 2, 3$. We think that this is a strong evidence that STS models can be effectively described by topological field theory, which is a field theory with invariance under diffeomorphism.

Chapter 6

Feasibility of self-correcting quantum memory and thermal stability of topological order

Feasibility of self-correcting quantum memory is an important open problem in quantum information science concerning reliable storage of qubits. Thermal stability of topological order at finite temperature is a problem of fundamental importance in condensed matter physics concerning whether topological order is stable at non-zero temperature or not. While these two problems may look very different from each other, they are fundamentally akin to each other [43, 78, 31, 79, 80, 81, 82]. In particular, by searching for self-correcting quantum memory, one can search for topological ordered spin systems which are stable at finite temperature.

This surprising correspondence enables us to address a condensed matter theoretical question, thermal stability of topological order, by analyzing a quantum information theoretical question, feasibility of self-correcting quantum memory. In this chapter, we address these two problems, feasibility of self-correcting quantum memory and thermal stability of topological order, simultaneously by using the solution of three-dimensional STS models. Through the analysis on geometric shapes of logical operators, we argue that three-dimensional stabilizer Hamiltonians at fixed points do not work as a self-correcting quantum memory, and thus, topological order is not stable in three dimensions.

Comment: While our discussion is limited to the cases where k is small in the presence of continuous scale symmetries, this limitation may be justified in addressing the above two problems. As discussed in this chapter, a large number of ground states would lead to entropic contributions at finite temperature which would suppress the qubit storage time and induces thermal instability of topological order at finite temperature. See discussions in [10, 83, 8] for relevant works.

Since discussions on three-dimensional quantum phases are similar to the ones on two-dimensional quantum phases, we skip them in this thesis. Instead, we only list geometric shapes of logical operators arising in three-dimensional STS models.

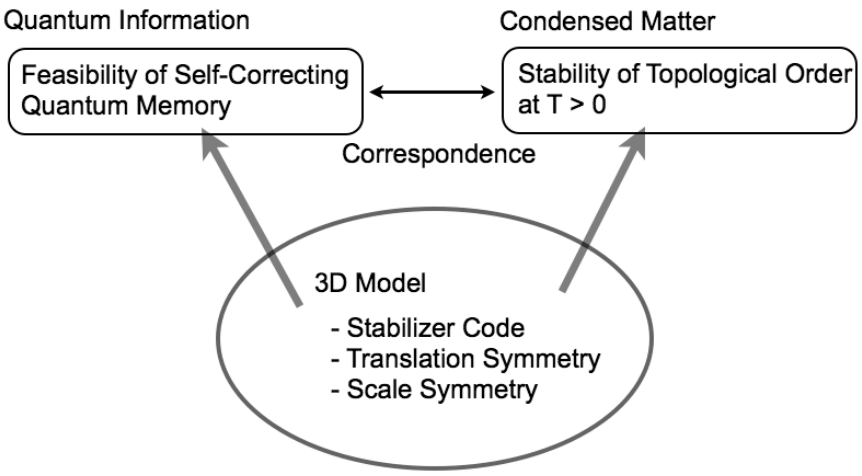

Figure 6-1: The correspondence between feasibility of self-correcting quantum memory and thermal stability of topological order.

6.1 Feasibility of self-correcting quantum memory

Quantum entanglement decays easily. This underlying difficulty in quantum information science gave birth to the beautiful art of protecting qubits from decoherence; *quantum coding theory*. The central idea of quantum error-correcting codes is to encode a qubit in many-body entangled states, and perform error-corrections so that encoded qubits are not lost. After discoveries of first examples of quantum codes [84, 7, 6, 85, 30] which culminated in stabilizer codes [5], a large number of quantum codes have been found. Now, quantum coding theory constitutes one of the most important building blocks for realizing fault-tolerant quantum computation [4].

Yet, performing active-error corrections is often technologically difficult and not efficient. In theory, sufficiently frequent and accurate error-corrections guarantee that a qubit encoded in a quantum error-correcting code is reliably stored [43]. However, the frequency and accuracy thresholds seem beyond the reach of current technologies. Indeed, there have been no convincing experimental demonstrations of error-corrections performed. In addition, one needs to keep performing error-corrections during the time we wish to store a qubit. Therefore one may hope to have a quantum memory device that would work without any active error-corrections.

Self-correcting quantum memory is an ideal memory device which corrects errors by itself [43, 37, 78, 31, 79, 86]. Due to the large energy barrier separating degenerate ground states, natural thermal dissipation processes restore the system into the original encoded states by correcting errors automatically without any active error-correction. If such a memory device could exist, it will be a perfect quantum information storage device which may be used commercially in the future. Also, the reliable storage of qubits seems to be the starting point for building scalable quantum computers.

Below, we review how self-correcting quantum memory works in theory by connecting its memory time to the energy barrier. We also briefly review previous works

and define self-correcting quantum memory more precisely.

6.1.1 Classical self-correcting memory:

In order to gain some insights on how a self-correcting quantum memory works, we start by analyzing an example of self-correcting *classical* memory. Consider two-dimensional Ising model:

$$H = -\sum_{i,j} Z_{i,j}Z_{i+1,j} - \sum_{i,j} Z_{i,j}Z_{i,j+1} \tag{6.1}$$

which consists of $L \times L$ qubits with periodic boundary conditions. The model works as a classical code since one can encode a classical bit in the ground space by labeling $|0\cdots0\rangle$ as 0 and $|1\cdots1\rangle$ as 1. Now, let us see why this model works as self-correcting classical memory. Assume that the system is originally $|0\cdots0\rangle$. Then, in order for errors to change a ground state $|0\cdots0\rangle$ into another ground state $|1\cdots1\rangle$, errors must flip all the spins from $|0\rangle$ to $|1\rangle$. However, during these spin flips, the excitation energy becomes at least $O(L)$ because there is a domain wall separating the regions with $|0\rangle$s and $|1\rangle$s (Fig. 6-2). In other words, ground states $|0\cdots0\rangle$ and $|1\cdots1\rangle$ are separated by a *large energy barrier*. Then, before errors accumulate, natural thermal dissipation processes restore the system into the original encoded state[1]. Therefore, the system corrects errors by itself.

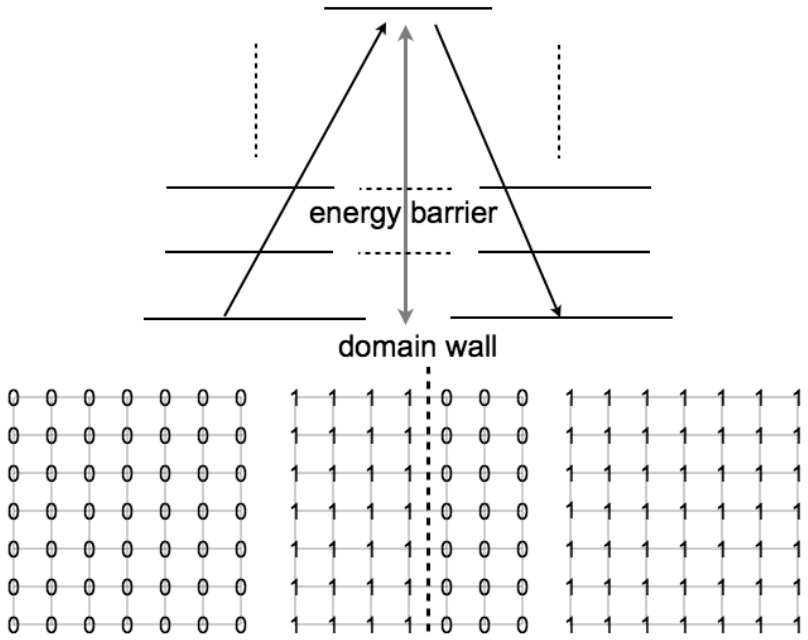

Figure 6-2: How a self-correcting *classical* memory works in two-dimensional Ising model.

[1]Precisely speaking, the system does not return to the original state, but return to a state which is sufficiently close to the original state with a probability approaching to unity at the thermodynamic limit. Therefore, one can reliably read out the encoded bit from such a state.

One may estimate the bit storage time of two-dimensional Ising model by a simple hopping argument. Suppose the system is initially in $|0\cdots 0\rangle$. We denote a set of states which are close to $|0\cdots 0\rangle$ as $\rho(0)$ and a set of states which are close to $|1\cdots 1\rangle$ as $\rho(1)$. If the initial state $|0\cdots 0\rangle$ changes to some other state in $\rho(1)$ as a result of thermal fluctuations, the initially encoded bit is destroyed. Since the energy barrier separating $|0\cdots 0\rangle$ and $|1\cdots 1\rangle$ is Δ, a hopping probability for a state $|0\cdots 0\rangle$ to jump to some state in $\rho(1)$ per unit time is given by

$$P_{hop} \ \sim \ \exp(\frac{T}{\Delta E}) \tag{6.2}$$

by assuming all the physical constants to be unity. A bit storage time τ_{bit} is estimated as

$$\tau_{bit} \ \sim \ \exp(\Delta E/T). \tag{6.3}$$

This law is often called the Arrhenius law. According to the Arrhenius law, the bit storage time of a two-dimensional ferromagnet can be estimated as $\tau \sim \mathrm{EXP}(L)$ since the energy barrier is $\Delta E \sim O(L)$. Therefore, the bit storage time of two-dimensional Ising model goes to infinity at the thermodynamic limit:

$$\tau_{bit} \ \rightarrow \ \infty \qquad \text{for} \quad L \ \rightarrow \ \infty. \tag{6.4}$$

This is a reliable classical memory device which works without any active error-corrections.

One-dimensional Ising model, however, does not work as a self-correcting classical memory since there is only a constant energy barrier between two ground states of one-dimensional Ising model. In particular, the bit storage time can be estimated as

$$\tau_{bit} \ \sim \ O(1) \tag{6.5}$$

which is upper bounded by some constant even at the thermodynamic limit. Therefore it does not work as a self-correcting classical memory.

It is illuminating to associate the energy barrier and geometric shapes of logical operators. In order to transform one ground state to another ground state, one needs to apply a logical operators to the initial ground state. If a logical operator is one-dimensional, one can apply it only by finite energy. The intermediate state can be obtained by applying a subpart of a logical operator. Since the edge of one-dimensional logical operators is zero-dimensional, such states have finite excitation energy. Yet, if a logical operator is two-dimensional, the edge of two-dimensional logical operators is one-dimensional, and the energy of the intermediate state becomes as high as $O(L)$.

Invalidity at large k: However, there is a caveat in using the Arrhenius law to estimate the bit or qubit storage time. Suppose a system has more than two ground states. For example, in a stabilizer code, the number of ground states is 2^k. Assume that we are initially in one of the ground states $|\psi(0)\rangle$. We denote all the other

ground states as $|\psi(j)\rangle$ where $j = 1, \cdots, 2^k - 1$ and denote their neighbors as $\rho(j)$. Then, a state $|\psi(0)\rangle$ may hop into $\rho(j)$ as a result of thermal fluctuations. So, in the worst case, a qubit storage time may be suppressed as follows:

$$\tau_{qubit} \sim \frac{1}{2^k P_{hop}} = 2^{-k} \exp(\Delta E/T). \tag{6.6}$$

Also, a special consideration is needed for the cases where a system has a large number of local minima. Therefore, in order for a system to work as a self-correcting quantum memory, one needs to have small k and large ΔE.

The number of ground states and local minima is closely related to the thermal stability of the system. In general, when there are a large number of ground states or local minima, at finite temperature, entropic contributions dominates over the energetic contributions. So, a system tends to be thermally unstable. This observation hints a possible relation between self-correcting properties and thermal stability. This observation on the invalidity of the Arrhenius law solidifies the usefulness of STS models which are stabilizer codes with small k.

6.1.2 Quantum self-correcting memory

Now, we move to discussion on self-correcting quantum memory. Recall that, in order for a system to work as a self-correcting quantum memory, the energy barrier both between $|0\rangle$ and $|1\rangle$ and between $|0\rangle + |1\rangle$ and $|0\rangle - |1\rangle$ must be large. Therefore, the qubit storage time can be estimated in a similar way:

$$\tau_{qubit} \sim \exp(\Delta E/T) \tag{6.7}$$

where ΔE is the minimum of energy barriers between all the possible pairs of ground states.

Two and three-dimensional Toric code: It is known that many of good local stabilizer codes with macroscopic code distances do not have self-correcting properties since they have string-like logical operators which lead to $O(1)$ energy barrier. As an example, let us consider two-dimensional Toric code:

$$H_{Toric} = -\sum_s \mathcal{A}_s - \sum_p \mathcal{B}_p \tag{6.8}$$

where qubits live on edges of $L \times L$ square lattice. Recall that two-dimensional Toric code has pairs of one-dimensional logical operators. One can create anyonic excitation by applying subparts of one-dimensional logical operators and these anyons can propagate the system without costing much energy. As a result, the energy barrier separating two ground stats is $O(1)$ which implies

$$\tau_{qubit} \sim O(1). \tag{6.9}$$

A similar discussion holds for three-dimensional Toric code too. Three-dimensional Toric code is known to have a pair of one-dimensional and two-dimensional logical operators. We denote a one-dimensional logical operator ℓ and two-dimensional logical operator r. By applying subparts of one-dimensional logical operator ℓ, one can create quasiparticle excitations which propagate the system without costing much energy. This implies that, the energy barrier between $|\psi(r=0)\rangle$ and $|\psi(r=1)\rangle$ is $O(1)$, which indicates that

$$\tau_{qubit} \sim O(1). \tag{6.10}$$

On the other hand, excitations associated with two-dimensional logical operators cost a lot of energy as in two-dimensional Ising model. In particular, the energy barrier between $|\psi(\ell=0)\rangle$ and $|\psi(\ell=1)\rangle$ is $O(L)$, which indicates that

$$\tau_{bit} \sim \exp(L). \tag{6.11}$$

Therefore, three-dimensional Toric code is a self-correcting classical memory while it does not work as self-correcting quantum memory.

Four-dimensional Toric code: It has been also pointed out that four-dimensional Toric code may have exponentially long storage time $\tau \sim \mathrm{EXP}(L)$ below the critical temperature since the model has a large energy barrier which scales as $O(L)$. This remarkable insight has been further investigated in [87], and later, rigorously verified in [80]. One can associate the self-correcting property of four-dimensional Toric code with geometric shapes of logical operators, as the model has pairs of two-dimensional logical operators which lead to $O(L)$ energy barrier. Yet, since one cannot embed four-dimensional Toric code in a three-dimensional space, one hopes to have three-dimensional self-correcting quantum memory whose qubit storage time grows as the system size increases.

As two-dimensional and three-dimensional Toric codes have $O(1)$ qubit storage time, they are not reliable quantum memories. Yet, it is worth noting that two-dimensional Toric code works as a reliable quantum memory device if one perform sufficiently frequent and accurate error-corrections. In particular, it has been shown [43] that the qubit storage time can be exponentially long: $\tau \sim \mathrm{EXP}(L)$ in the presence of active error-corrections; however, it seems very difficult to reach such accuracy and frequency which are necessary for reliably storing qubits.

6.1.3 Previous works

As we have seen, the Toric code does not work as self-correcting quantum memory in two and three dimensions. Here we briefly review some proposals of self-correcting quantum memory and point out problems in these models.

First, an interesting model of the mixture of two-dimensional Toric code and three-dimensional Bosonic gas, called the Toric-Boson model, was proposed [88] where Bosonic gas induces confining potential between anyonic excitations. The model

opened new capacities of quantum codes constructed in the so called mixed-dimensional configurations, which are also of particular interest in ultracold atom physics community. However, the model itself has two serious drawbacks as a candidate of self-correcting quantum memory. First, its storage time is only polynomial in L: $\tau \sim \mathrm{POLY}(L)$ since an effective energy barrier is: $\Delta E \sim \mathrm{LOG}(L)$. Why is this problematic? It is known that it takes at least $O(d)$ gate operations, which cannot be implemented simultaneously, to read out the encoded qubit, where d is the code distance of the system. Then, since the code distance d scales polynomially with respect to L in the model, polynomially long storage time is not sufficient for a model to work as efficient quantum memory device [79]. Second, the model needs to have a very strong coupling between the Toric code and Bosonic gas whose strength scales polynomially in L. Therefore, as the system size becomes large, it becomes difficult to physically realize the Toric-Boson model as the model has a problem in the scalability.

Later, another interesting proposal of three-dimensional spin glass models [10, 83, 8] has been made whose relaxation dynamics is very slow due to the existence of a large number of energy local minima. In particular, the model is known to have logarithmically large energy barrier: $\Delta E \sim \mathrm{LOG}(L)$. With this feature of the model, one might expect that the model has a polynomially long storage time: $\tau \sim \mathrm{POLY}(L)$ due to the Arrhenius law. However, this expectation holds only for a small system sizes, and the Arrhenius law does not generally hold for this model since the model has a large number of logical qubits $k \sim O(L)$ as well as a large number of local minima. As a result, for large L, the storage time does not scale up, and is upper bounded by some constant. Indeed, the system is known to undergo a phase transition at $T = 0$, which may imply a potential thermal instability of the system properties.

With these observations in mind, we formally describe the definition of a self-correcting quantum memory and define the problem we are going to address.

Definition 6.1. *A self-correcting quantum memory is a system whose memory time τ_{qubit} goes to infinity at the thermodynamic limit:*

$$\tau_{qubit} \ \rightarrow \ \infty \qquad \textit{for} \quad L \ \rightarrow \ \infty. \tag{6.12}$$

And, we are interested in whether a self-correcting quantum memory is feasible for D ≤ 3 or not.

6.2 Thermal stability of topological order

Feasibility of self-correcting quantum memory is closely related to another important problem in condensed matter physics; thermal stability of topological order.

Studies of topologically ordered systems [1, 24, 29, 30, 46, 89, 90, 91, 92] have been frontiers of researches in condensed matter physics community, as systems with topological order are beyond the description of the Landau's symmetry-breaking paradigm which was once considered as "theory of everything" for studies of many-body systems. Topologically ordered systems are also of practical importance in quantum

information science since many-body entanglement arising in ground states and quasi-particle excitations of topologically ordered systems is a primary resource for realizing various quantum information processing tasks [1, 30].

The notion of topological order was originally introduced in order to characterize the stability of ground states of many-body quantum systems against local perturbations [29]. Loosely speaking, a system is said to have topological order when its ground state properties do not change significantly under any types of small, but finite local perturbations. This stability of ground states against local perturbations is also valuable for quantum information processing since topologically ordered spin systems can be used as good quantum codes with macroscopic code distances [32].

However, the situation changes completely when one considers the effect of thermal fluctuations on topologically ordered systems. In fact, it is known that topological order in a two-dimensional Toric code is not stable at any finite temperature which may be quantitatively seen from the fact that topological order parameters such as topological entanglement entropy vanish at any non-zero temperature at the thermodynamic limit [93, 94]. A similar result is obtained in a recent numerical work on topological entanglement entropy in a spin liquid model at finite temperature [95]. It seems that topological order in a two-dimensional system is not stable at finite temperature according to general studies on the ground state properties of two-dimensional frustration-free Hamiltonians [31, 32].

The goal of this subsection is to properly define the notion of topological order both at $T = 0$ and $T > 0$. Here we define topological order in terms of the stability against local perturbations.

6.2.1 Stability against local perturbations

Let us first begin by describing the phenomenological definition of topological order which is commonly used in physics community. A system is said to have topological order when its ground state properties do not change significantly under any types of small perturbations [29].

Definition 6.2 (Stability against perturbations)**.** *Consider a degenerate spin system defined on some closed geometric manifold governed by a Hamiltonian H. The system is said to be topologically ordered at $T = 0$ if and only if the system satisfies the following conditions:*

- *There exists some finite positive number δ such that, for any perturbations V:*

$$H' \;=\; H + V, \qquad V \;=\; \sum_j V_j \tag{6.13}$$

  where V_j are locally defined and $|V_j| \leq \delta$, the ground state degeneracy is not broken at the thermodynamic limit (Fig. 6-3).

- *The perturbed ground space G can be approximated by the original ground space*

G_0 through some local unitary transformation:

$$UG_0U^\dagger \approx G \tag{6.14}$$

which can be represented as

$$U = \int_0^1 \exp(-i\hat{h}t)dt \tag{6.15}$$

where $\hat{h}$ is some hermitian operator which is a summation of local terms with finite amplitudes.

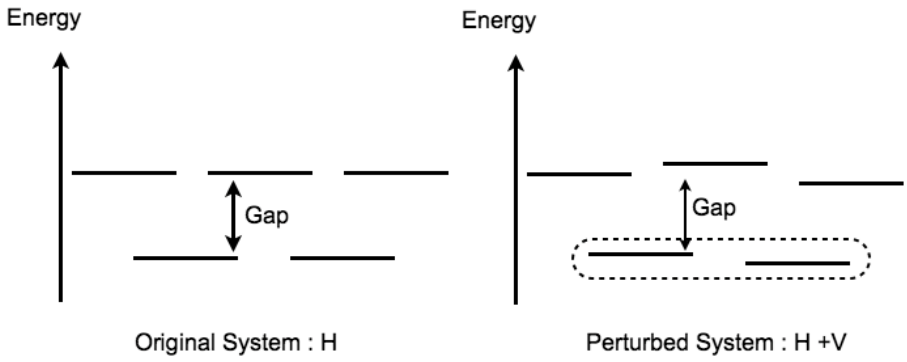

Figure 6-3: The stability of the ground state properties against local perturbations.

This stability against local perturbations is the underlying reason why topologically ordered materials are useful for fault-tolerant quantum computation. Suppose we want to create some Hamiltonian H. In reality we can only approximate H by some real Hamiltonian H' and there always exists some mismatch $\delta H = H - H'$. If the target Hamiltonian H is topologically ordered, the read Hamiltonian can be written as $H' = H - \delta H$ and δH can be considered as a perturbation. Then, at the thermodynamic limit, the effect of the mismatch becomes negligible.

It has been recently proven that a stabilizer code with large code distance d is stable against local perturbations under some assumptions [28]. This is essentially due to the fact that local perturbations V cannot connect two ground states in a topologically ordered system, and only the $O(d)$th perturbative constitution can connect degenerate ground states. However, such an effect is exponentially suppressed with respect to the system size. Therefore, if a system is a good quantum code, we automatically know that it is topologically ordered.

It is worth noting that a classical ferromagnet (Ising model) is not topologically ordered while it works as self-correcting classical memory. First of all, the ground state degeneracy of a classical ferromagnet is broken if a local magnetic field term Z_j is added as a perturbation:

$$V = -\epsilon \sum_j Z_j. \tag{6.16}$$

While the original Hamiltonian has $|0\cdots0\rangle$ and $|1\cdots1\rangle$ as ground states, the perturbed Hamiltonian has $|0\cdots0\rangle$ as a single ground state for positive ϵ. Second, the ground state property significantly changes as a result of perturbations. While a classical ferromagnet has $\frac{1}{\sqrt{2}}(|0\cdots0\rangle + |1\cdots1\rangle)$ as a ground state, the perturbed ground state is $|0\cdots0\rangle$, and there is no local unitary transformation which transforms $\frac{1}{\sqrt{2}}(|0\cdots0\rangle + |1\cdots1\rangle)$ into $|0\cdots0\rangle$ [70]. As a straightforward extension of this discussion, one may notice that STS models with zero-dimensional logical operators are not topologically ordered, and topological order may exist only in two or higher-dimensional systems due to the dimensional duality of logical operators.

While these systems with stability against local perturbations are called topologically ordered systems, there are some systems which are beyond the description of topological theory, without invariance under diffeomorphism [10, 96].

6.2.2 Thermal instability of topological order

The notion of topological order characterizes quantum phases of matter which are stable against any types of local perturbations. Yet, it has been pointed out that topological order is not stable against thermal fluctuations. Here, we define the notion of topological order at $T > 0$.

The smoking-gun evidence of thermal instability of topological order is obtained by analyzing the behaviors of topological entanglement entropy at finite temperature [93, 97]. Topological entanglement entropy S_{topo} is an entanglement measure which is particularly suited for detecting topological order [24, 46]. It has been shown that topological entanglement entropy counts the degree of freedoms for possible anyonic excitations arising in topologically ordered materials and has non-zero values when the system is topologically ordered.

In [93], topological entanglement entropy of the two-dimensional Toric code at finite temperature was calculated. The result shows that S_{topo} goes to zero at any finite temperature at the thermodynamic limit. This indicated that the two-dimensional Toric code undergoes a phase transition at $T = 0$, and is not stable against thermal fluctuations.

With this observations in mind, one can draw a phase diagram of two-dimensional Toric code as in Fig 6-4. Here, the system is stable against any types of local perturbation, denoted by V. Yet, the system is unstable against thermal fluctuation at any finite temperature. Therefore, one has topological order only at zero-temperature, and the system undergoes phase transitions at $T = 0$.

A naturally arising question is whether one can have topological order even at finite temperature or not.

Definition 6.3. *When a system has topological order at finite temperature, a system is stable against both thermal fluctuations and local perturbations simultaneously, as shown in Fig. 6-4.*

Our definition of topological order at $T > 0$ is phenomenological and may lack a mathematical rigor. For more precise approaches, see [78, 81, 82].

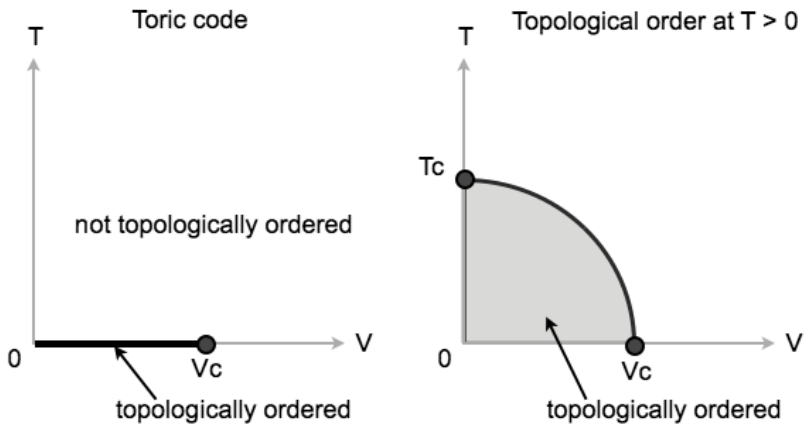

Figure 6-4: The stability of the ground state properties against local perturbations.

6.3 Correspondence between self-correcting memory and thermal stability

In this subsection, we establish the connection between self-correcting quantum memory and the thermal stability of topological order:

$$\begin{array}{rcl} \text{Quantum code} & \leftrightarrow & \text{Topological order at } T = 0 \\ \text{Self-correcting quantum memory} & \leftrightarrow & \text{Topological order at } T > 0 \end{array}$$

In this subsection, we describe the definition of topological order in spin systems on a lattice, and argue that quantum codes have topological order at zero temperature. Note that our discussion closely follows pioneering works [28, 98].

6.3.1 Classical equivalence

In this subsection, we establish the connection between self-correcting classical memory and thermal stability of ferromagnetic order at finite temperature:

$$\begin{array}{rcl} \text{Classical code} & \leftrightarrow & \text{Ferromagnetic order at } T = 0 \\ \text{Self-correcting classical memory} & \leftrightarrow & \text{Ferromagnetic order at } T > 0 \end{array}$$

Two-dimensional ferromagnet: We have seen that two-dimensional Ising model works as self-correcting classical memory since the energy barrier separating two degenerate ground states is $O(L)$. This self-correcting property of two-dimensional Ising model is closely related to the thermal stability of ferromagnetic order as seen from the following thermodynamic argument.

Consider two-dimensional Ising model:

$$H(\epsilon) \;=\; -\sum_{i,j} Z_{i,j}Z_{i+1,j} - \sum_{i,j} Z_{i,j}Z_{i,j+1} - \epsilon \sum_{i,j} Z_{i,j} \tag{6.17}$$

with an initial bias (symmetry-breaking field); $-\epsilon \sum_{i,j} Z_{i,j}$ for $\epsilon \geq 0$. As a result of an initial bias, the system is not degenerate anymore, and the ground state is $|0 \cdots 0\rangle$. The thermal stability of ferromagnetic order can be analyzed through the expectation value of the total magnetization m:

$$m \;=\; \frac{1}{N} \sum_{i,j} Z_{i,j} \tag{6.18}$$

at finite temperature, which can be computed as follows:

$$\langle m \rangle \;=\; \lim_{\epsilon \to 0} \frac{1}{\beta} \frac{\partial \log Z}{\partial \epsilon} \tag{6.19}$$

where the partition function is: $Z(\beta, \epsilon) = \mathrm{Tr} e^{-\beta H(\epsilon)}$. Here, we evaluate the expectation value of m at the limit where $\epsilon \to 0$ after we take the limit where N goes to infinity. (Otherwise, there is no use of introducing an initial bias). Then, we have:

$$\left\langle \frac{1}{N} \sum_{i,j} Z_{i,j} \right\rangle_{\epsilon \to 0} \;=\; 1 \qquad (T \;=\; 0) \tag{6.20}$$

$$1 \;>\; \left\langle \frac{1}{N} \sum_{i,j} Z_{i,j} \right\rangle_{\epsilon \to 0} \;>\; 0 \qquad (T_c \;> T \;>\; 0) \tag{6.21}$$

$$\left\langle \frac{1}{N} \sum_{i,j} Z_{i,j} \right\rangle_{\epsilon \to 0} \;=\; 0 \qquad (T \;>\; T_c) \tag{6.22}$$

where T_c is some finite transition temperature, as plotted in Fig. 6-5(a).

One may notice that the total magnetization has some non-zero value as long as the temperature is below the transition temperature T_c. This indicates that the system is stable against thermal fluctuations for $T < T_c$. In particular, the system properties for $T_c > T > 0$ are close to the ground state properties at $T = 0$. However, the system properties change drastically at $T = T_c$, and for $T > T_c$, the total magnetization vanishes. This indicates that the system undergoes a phase transition at $T = T_c$, and is unstable against thermal fluctuations for $T > T_c$.

Now, one can establish the connection between self-correcting properties and the thermal stability. In a coding theoretical language, the computation of the magnetization at finite temperature may be interpreted as follows. We first apply an initial bias and encode a bit 0 to a ground state $|0 \cdots \rangle$. Then, we let the system interact with the external environment at finite temperature, and wait until the system reaches the equilibrium while slowly turning off the initial bias. Finally, we decode the initially encoded bit by measuring the total magnetization. Therefore, self-correcting property

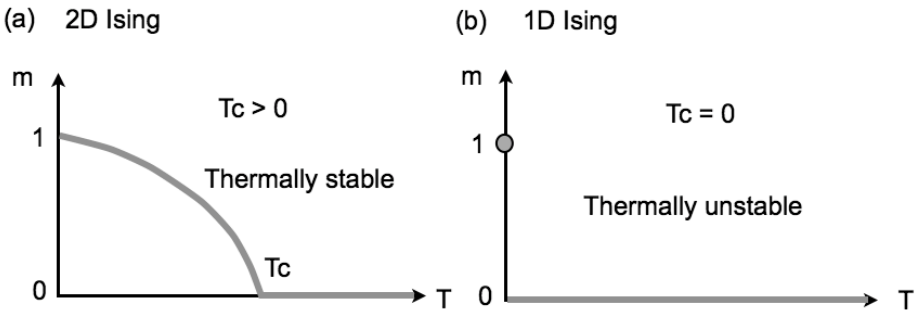

Figure 6-5: Total magnetizations. (a) Two-dimensional Ising model. (b) One-dimensional Ising model.

of two-dimensional Ising model with exponentially long bit storage time is a direct consequence of the thermal stability of ferromagnetic order at finite temperature.

In general, the total magnetization we have used above is called an *order parameter* in condensed matter physics since it can be used to distinguish different phases of matters. On the other hand, quantum coding theoretically, one may view the total magnetization as a symmetric summation of a zero-dimensional logical operator $Z_{i,j}$ with which a classical bit is encoded.

One-dimensional ferromagnet: Next, let us see that one-dimensional Ising model, which does not work as self-correcting classical memory, is not stable against thermal fluctuations. Consider one-dimensional Ising model:

$$H(\epsilon) \;=\; -\sum Z_j Z_{j+1} - \epsilon \sum Z_j \tag{6.23}$$

with an initial bias, and compute the expectation values of the total magnetization. Then, we have

$$\left\langle \; \frac{1}{N} \sum_j Z_j \; \right\rangle_{\epsilon \to 0} \;=\; 1 \qquad (T \;=\; 0) \tag{6.24}$$

$$\left\langle \; \frac{1}{N} \sum_j Z_j \; \right\rangle_{\epsilon \to 0} \;=\; 0 \qquad (T \;>\; 0) \tag{6.25}$$

as plotted in Fig. 6-5(b). One may notice that the total magnetization becomes zero at any finite temperature. This indicates that the system is not stable against thermal fluctuations at any finite temperature, and the system undergoes a phase transition at $T = 0$ as seen from the sudden change of the magnetization at $T = 0$. The system properties for $T = 0$ and for $T > 0$ are significantly different, and the ground state properties are not stable against thermal fluctuations. This is the underlying reason why one-dimensional Ising model has $O(1)$ bit storage time, and does not work as self-correcting classical memory.

Summary of the equivalence: With observations above, one may notice that a large energy barrier, which is essential to self-correcting properties, is the key to the thermal stability of ferromagnetic order. In Fig. 6-6, we give a summary of the equivalence concerning classical memories.

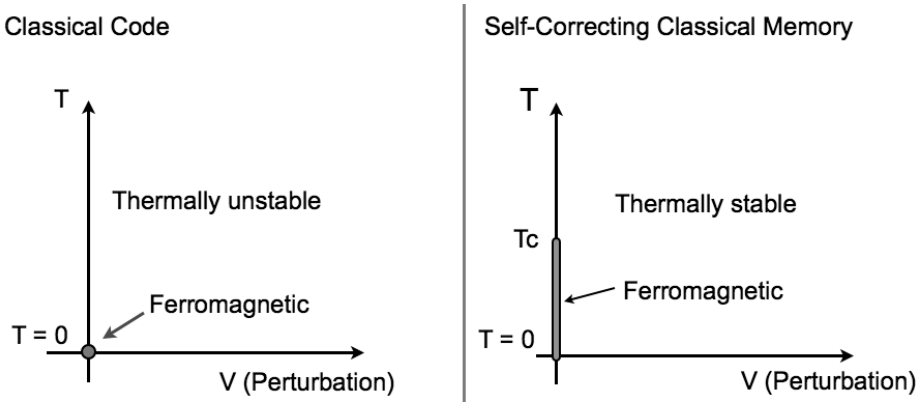

Figure 6-6: A summary of the classical equivalence.

Here, it is worth noting that ferromagnetic systems, such as one-dimensional and two-dimensional Ising model are not stable against perturbations, as described in Fig. 6-6. If one chooses V as the initial bias, one can easily break the ground state degeneracy, and thus, the ground state property is not stable against perturbations. This indicates that ferromagnetic systems are not topologically ordered.

6.3.2 Quantum equivalence

In this subsection, we establish the connection between self-correcting quantum memory and topological order at finite temperature, and analyze the thermal stability of topological order arising in STS models.

Two-dimensional Toric code: Two-dimensional Toric code is topologically ordered since it has a macroscopic code distance: $d \sim O(1)$. Yet, it does not work as self-correcting quantum memory since the energy barrier is $\Delta E \sim O(1)$. This is closely related to the thermal instability of topological order as we shall see below. Let us perform a thermodynamic analysis on two-dimensional Toric code in a way similar to Ising model by adding an initial bias:

$$H_\ell(\epsilon) \;=\; H_{Toric} - \epsilon \sum_{j=1}^{L} T_2^j(\ell) \tag{6.26}$$

$$H_r(\epsilon) \;=\; H_{Toric} - \epsilon \sum_{i=1}^{L} T_1^i(r) \tag{6.27}$$

where ℓ and r are one-dimensional logical operators extending in the $\hat{1}$ and $\hat{2}$ directions

respectively. Here, we define the following "normalized logical operators":

$$m_\ell = \frac{1}{L}\sum_{j=1}^{L} T_2^j(\ell) \tag{6.28}$$

$$m_r = \frac{1}{L}\sum_{i=1}^{L} T_1^i(r) \tag{6.29}$$

by taking symmetric summations of logical operators, as we did for Ising model. Then, we have

$$\langle m_\ell \rangle_{\epsilon\to 0} = \langle m_r \rangle_{\epsilon\to 0} = 1 \qquad (T = 0) \tag{6.30}$$

$$\langle m_\ell \rangle_{\epsilon\to 0} = \langle m_r \rangle_{\epsilon\to 0} = 0 \qquad (T > 0) \tag{6.31}$$

as plotted in Fig. 6-7(a) where $\langle m_\ell \rangle$ is evaluated for $H_\ell(\epsilon)$, and $\langle m_r \rangle$ is evaluated for $H_r(\epsilon)$. This indicates that the system is not stable against thermal fluctuations at any finite temperature, meaning that topological order arising in two-dimensional Toric code is thermally unstable. This implies that one cannot read out initially encoded qubit by measuring m_ℓ and m_r.

Three-dimensional Toric code: Next, let us consider thermodynamic properties of three-dimensional Toric code. While three-dimensional Toric code does not work as self-correcting quantum memory, it works as self-correcting *classical* memory. This is because it has pairs of one-dimensional and two-dimensional logical operators, and as a result, the bit storage time is $\tau \sim \mathrm{EXP}(L)$ while the qubit storage time is $\tau \sim O(1)$. These coding properties are closely related to thermodynamic properties of three-dimensional Toric code, as seen from expectation values of logical operators:

$$m_\ell = \frac{1}{L}\sum_{z=1}^{L} T_3^z(\ell) \tag{6.32}$$

$$m_r = \frac{1}{L^2}\sum_{x,y=1}^{L} T_1^x T_2^y(r) \tag{6.33}$$

where ℓ is a two-dimensional logical operator extending in the $\hat{1}$ and $\hat{2}$ directions, while r is a one-dimensional logical operator extending in the $\hat{3}$ direction. Their expectation values behave as follows:

$$\langle m_\ell \rangle_{\epsilon\to 0} = 1 \qquad (T = 0) \tag{6.34}$$

$$\langle m_\ell \rangle_{\epsilon\to 0} = 0 \qquad (T > 0) \tag{6.35}$$

and

$$\langle m_r \rangle_{\epsilon \to 0} = 1 \qquad (T = 0) \tag{6.36}$$

$$1 > \langle m_r \rangle_{\epsilon \to 0} > 0 \qquad (T_c > T > 0) \tag{6.37}$$

$$\langle m_r \rangle_{\epsilon \to 0} = 0 \qquad (T > T_c) \tag{6.38}$$

where T_c is some finite transition temperature, as plotted in Fig. 6-7(b). This implies that three-dimensional Toric code undergoes phase transitions both at $T = 0$ and $T = T_c$, and the ground state properties are not completely stable against thermal fluctuations at any finite temperature. Yet, the ground state properties partially survive at finite temperature as a direct consequence of being self-correcting classical memory.

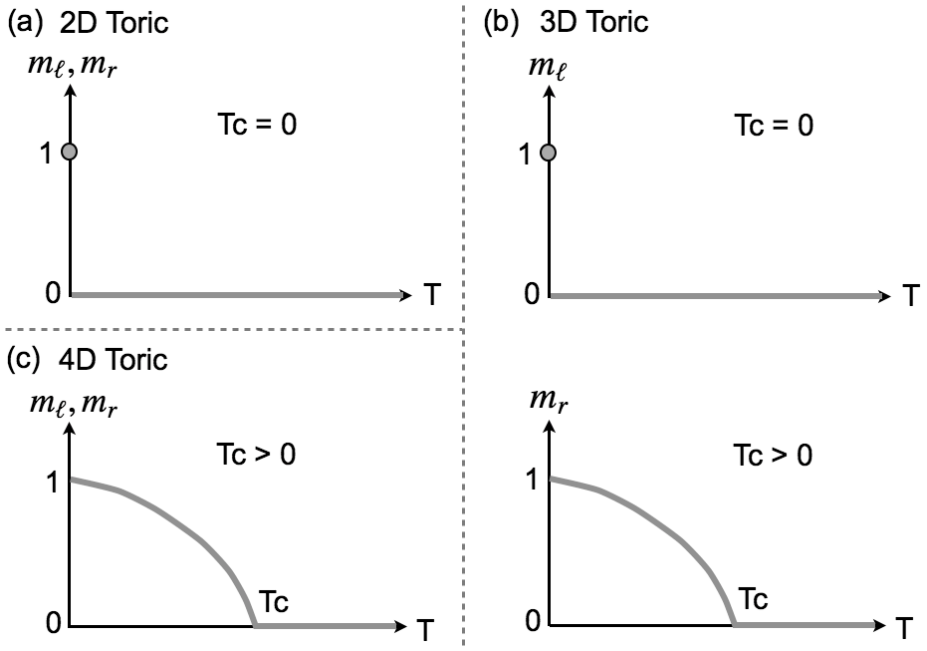

Figure 6-7: Expectation values of logical operators. (a) Two-dimensional Toric code. (b) Three-dimensional Toric code. (c) Four-dimensional Toric code.

Four-dimensional Toric code: Finally, let us see that four-dimensional Toric code, which works as self-correcting quantum memory, is stable against thermal fluctuations. Here, we define

$$m_\ell = \frac{1}{L^2} \sum_{z,w=1}^{L} T_3^z T_4^w(\ell) \tag{6.39}$$

$$m_r = \frac{1}{L^2} \sum_{x,y=1}^{L} T_1^x T_2^y(r) \tag{6.40}$$

where ℓ is a two-dimensional logical operator extending in the $\hat{1}$ and $\hat{2}$ directions, and r is a two-dimensional logical operator extending in the $\hat{3}$ and $\hat{4}$ directions. Then, we have

$$\langle m_\ell \rangle_{\epsilon\to 0} = \langle m_r \rangle_{\epsilon\to 0} = 1 \qquad (T = 0) \tag{6.41}$$

$$1 > \langle m_\ell \rangle_{\epsilon\to 0} = \langle m_r \rangle_{\epsilon\to 0} > 0 \qquad (T_c > T > 0) \tag{6.42}$$

$$\langle m_\ell \rangle_{\epsilon\to 0} = \langle m_r \rangle_{\epsilon\to 0} = 0 \qquad (T > T_c) \tag{6.43}$$

where T_c is some finite transition temperature, as plotted in Fig. 6-7(c). This implies that the ground state properties are stable against thermal fluctuations and topological order arising in four-dimensional Toric code is stable at finite temperature.

Summary of the equivalence: With these observations, one may notice that large energy barrier inside the ground space, which is essential to self-correcting properties, is the key to the thermal stability of topological order. In Fig. 6-8, we give a summary of the equivalence concerning quantum memory.

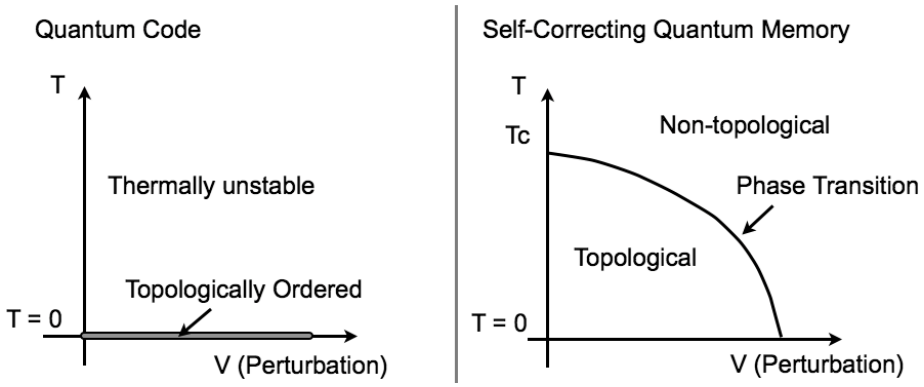

Figure 6-8: The quantum equivalence.

6.4 Three-dimensional STS model

In this subsection, we describe geometric shapes of logical operators in STS models, and discuss the feasibility of self-correcting quantum memory.

6.4.1 Three-dimension

For logical operators in a three-dimensional STS model, the following theorem holds.

Theorem 6.4 (**Dimensional Duality**). *For a three-dimensional STS model, there exists a canonical set of logical operators:*

$$\left\{ \begin{array}{ccc} \ell_1, & \cdots, & \ell_k \\ r_1, & \cdots, & r_k \end{array} \right\} \tag{6.44}$$

whose pair of anti-commuting operators ℓ_j and r_j has one of the following four properties.

- *ℓ_j is a zero-dimensional logical operator defined inside $1 \times 2v \times (2v)^2$, while r_j is a three-dimensional logical operator defined in a periodic way: $T_1(r_j) = r_j$, $T_2(r_j) = r_j$ and $T_3(r_j) = r_j$.*

- *ℓ_j is a one-dimensional logical operator defined inside $n_1 \times 2v \times 1$ in a periodic way: $T_1(\ell_j) = \ell_j$, while r_j is a two-dimensional logical operator defined inside $1 \times n_2 \times n_3$ in a periodic way: $T_2(r_j) = r_j$ and $T_3(r_j) = r_j$.*

- *ℓ_j is a one-dimensional logical operator defined inside $1 \times n_2 \times 2v$ in a periodic way: $T_2(\ell_j) = \ell_j$, while r_j is a two-dimensional logical operator defined inside $n_1 \times 1 \times n_3$ in a periodic way: $T_1(r_j) = r_j$ and $T_3(r_j) = r_j$.*

- *ℓ_j is a one-dimensional logical operator defined inside $2v \times 1 \times n_3$ in a periodic way: $T_3(\ell_j) = \ell_j$, while r_j is a two-dimensional logical operator defined inside $n_1 \times n_2 \times 1$ in a periodic way: $T_1(r_j) = r_j$ and $T_2(r_j) = r_j$.*

It is worth representing geometric shapes of logical operators graphically (Fig. 6-9). Note that logical operators are periodic in the directions in which they are stretched. There is a dimensional duality on geometric shapes of logical operators as follows:

$$\left\{ \begin{array}{ll} 0 \text{ dim}, & 1 \text{ dim} \\ 3 \text{ dim}, & 2 \text{ dim} \end{array} \right\} \tag{6.45}$$

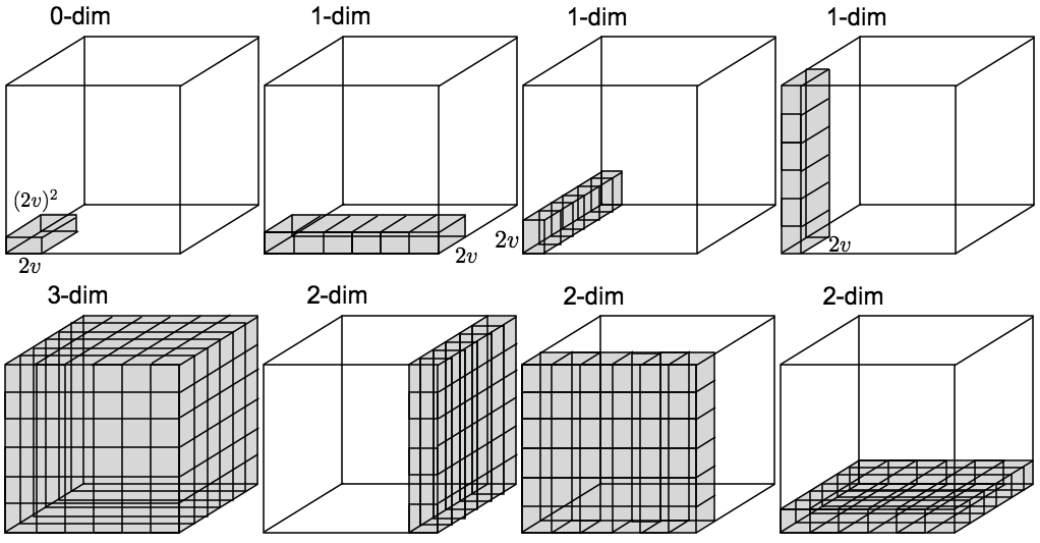

Figure 6-9: Dimensional duality in a three-dimensional system.

As a result of this dimensional duality, one may find the upper bound on the code distance. When $n_1 = n_2 = n_3 = L$, the code distance of a three-dimensional STS

model is upper bounded as follows:

$$d \leq 2vL \sim O(L). \tag{6.46}$$

Note that this bound is tight for the three-dimensional Toric code. The system may have topological order when it is free from zero-dimensional logical operators.

6.4.2 Higher-dimensions

Though our primary interests are in coding properties of three-dimensional STS models, it is worth extending the analysis to higher dimensions. For a D-dimensional STS model ($D \geq 4$), we make the following *conjectures*:

- In a D-dimensional system, m-dimensional and $(D-m)$-dimensional logical operators form anti-commuting pairs where m is an integer.
- The code distance is tightly upper bounded by $O(L^{\frac{D}{2}})$ when D is even and by $O(L^{\frac{D-1}{2}})$ when D is odd.

Note that generalizations of the Toric code to D-dimensional systems have the above dimensional duality for arbitrary integer m. With this connection between the feasibility of self-correcting quantum memory and the thermal stability of topological order, we conclude that topological order arising in STS models is not stable against thermal fluctuations. In other words, for $D \leq 3$, there is no system which is stable against both thermal fluctuations and local perturbations simultaneously. We summarize physical properties of STS models based on dimensions of pairs of logical operators:

Spatial dim	Logical operators	V	T	Memory property
1 dim	0 dim + 1 dim			Classical code
2 dim	0 dim + 2 dim		stable	Classical self-correction
2 dim	1 dim + 1 dim	stable		Quantum code
3 dim	0 dim + 3 dim		stable	Classical self-correction
3 dim	1 dim + 2 dim	stable		Quantum code
4 dim	2 dim + 2 dim	stable	stable	Quantum self-correction

where, for $D = 4$, we presented coding properties of four-dimensional Toric code. V represents stability against local perturbations and T represents thermal stability at finite temperature.

6.4.3 Implications

Finally, we discuss feasibility of self-correcting quantum memory and thermal stability of topological order. Since STS models may have pairs of one-dimensional and two-dimensional logical operators, the energy barrier as a quantum memory is $O(1)$. As a result, the memory time is $O(1)$, and thus, it does not work as a self-correcting

quantum memory. The fact that STS models do not work as a self-correcting quantum memory implies that topological order arising in STS models is not stable at non-zero temperature. Therefore, our analysis gives negative implications to questions concerning feasibility of self-correcting quantum memory and thermal stability of topological order.

While our discussion is limited to the cases where systems possess translation symmetries and continuous scale symmetries, there are interesting proposals which do not utilize translation symmetries or continuous scale symmetries. While we have assumed that the interaction strength in stabilizer Hamiltonians are uniform, one may design spatially random interaction strengths

$$H = -\sum_j c_j S_j \tag{6.47}$$

where c_j are random variables. For a system with random interaction terms, it is known that excitations may be localized due to the Anderson localization effect. These disorder-based quantum memories are shown to enhance the stability of encoding against local perturbations [99, 100, 101]. It may be an interesting future problem to study the stability of such quantum memories against thermal fluctuations.

There are interesting examples of stabilizer Hamiltonians which do not have these continuous scale symmetries, but have discrete scale symmetries. In [10], Haah proposed a beautiful example of quantum codes with discrete scale symmetries, called the cubic code. Surprisingly, the cubic code is known to be free from any of one-dimensional logical operators, and the energy barrier is logarithmically large with respect to the system size [8, 83]. Then, according to the Arrhenius law, one might hope that the memory time goes to infinity as the system size becomes large.

Unfortunately, it has been recently shown that the memory time of the cubic code is upper bounded by some constant at fixed temperature [8]. This is essentially because the model has a large number of ground states and local minima, and there are a large number of possible decoherence paths which invalidates the use of the Arrhenius law for a large system size. Yet, it has been also found that the memory time of cubic code is significantly longer than that of quantum codes with one-dimensional logical operators such as two and three-dimensional Toric code, and the model may be still promising as a quantum memory device as shown in [8]. Therefore, in practice, the cubic code may work as a reliable quantum memory device at sufficiently low temperature.

Regardless of whether it works as a reliable quantum memory device or not in practice, the cubic code is a truly nobel example of quantum phases found from studies of quantum coding theory. Searches and classifications of quantum phases arising in stabilizer Hamiltonians with discrete scale symmetries, including the cubic code, is an important future problem.

6.5 Fate of Schrödinger's cat

Discussion in this chapter shows that, if a system is governed by a stabilizer Hamiltonian with translation and continuous scale symmetries, the energy barrier is $\Delta E \sim O(1)$. Then due to the Arrhenius law, one has

$$\tau \sim O(1) \qquad \text{for} \quad L \to \infty. \tag{6.48}$$

Therefore, such systems do not work as self-correcting quantum memory. This also implies that such systems must undergo phase transitions at $T_c = 0$ if they possess topological order at zero temperature. We believe that this result is universal for arbitrary gapped spin systems with a small number of ground states.

To conclude, we point out that our no-go theorem concerning topological order at $T > 0$ may provide useful insights on a conceptual puzzle concerning the Schrödiner's cat state. According to the superposition principle of quantum mechanics, for a pair of orthogonal quantum states $|A\rangle$ and $|B\rangle$, its superposition state $|A\rangle + |B\rangle$ exists. At a microscopic level, this fundamental principle of quantum mechanics can be experimentally verified. For instance, for a single spin state $|\downarrow\rangle$, one obtains the superposition state $|\downarrow\rangle + |\uparrow\rangle$ by applying a $\pi/4$ rotation.

This superposition principle of quantum mechanics must hold for macroscopic states too. Yet, at the macroscopic level, the superposition principle looks very counterintuitive as an argument on the Schrödiner's cat state implies. Since a cat can be either alive or dead, two quantum states denoted by $|\text{alive}\rangle$ and $|\text{dead}\rangle$ exist. Then, due to the superposition principle, the Schrödiner's cat state $|\text{alive}\rangle + |\text{dead}\rangle$ also may exist. However the Schrödiner's cat state $|\text{alive}\rangle + |\text{dead}\rangle$ has not been observed or created in real physical systems while a microscopic superposition state $|\downarrow\rangle + |\uparrow\rangle$ can be easily created. What is the reason behind this puzzle on the superposition principle at the microscopic and macroscopic levels in terms of the experimental realizability?

The reason for this apparent discrepancy concerning the superposition principle becomes clear by considering the time scale of these events. If the coherence time of $|\downarrow\rangle + |\uparrow\rangle$ is much longer than the time required for a $\pi/4$ rotation, which is typically the case at a low temperature, a microscopic superposition $|\downarrow\rangle + |\uparrow\rangle$ can be experimentally created easily. On the other hand, since the cat state is a macroscopic superposition state, the time $\tau_{creation}$ required to create $|\text{alive}\rangle + |\text{dead}\rangle$ grows proportionally with respect to the system size L (or the size of a cat): $\tau_{creation} \sim O(L)$. This heuristic argument on the creation time of a macroscopic superposition state can be made more rigorous by using the Lieb-Robinson bound [70]. Therefore, as the system size increases, it gets more and more difficult to create a macroscopic superposition state.

It is more illuminating when we model the problem of the coherence time of $|\text{alive}\rangle + |\text{dead}\rangle$ as the memory time of quantum information storage device. Suppose a "system Hamiltonian" H has two ground states $|\text{alive}\rangle$ and $|\text{dead}\rangle$ and assume that $|\text{alive}\rangle$ and $|\text{dead}\rangle$ are both thermally stable in a sense that coherence time of $|\text{alive}\rangle$ and $|\text{dead}\rangle$ are very long with respect to our time scale. Then one is interested in the memory time of a macroscopic superposition state $|\text{alive}\rangle + |\text{dead}\rangle$. However, as our no-go theorem implies, $|\text{alive}\rangle + |\text{dead}\rangle$ is not thermally stable in three-

dimensional systems, and the memory time τ is upper bounded by some constant. On the other hand, the creation time for $|\text{alive}\rangle + |\text{dead}\rangle$ grows at least proportionally to L. Therefore, it is impossible to create $|\text{alive}\rangle + |\text{dead}\rangle$ in three-dimensional systems for large L.

On the other hand, in four-dimensional systems, such a macroscopic superposition state may be thermally stable as in the four-dimensional Toric code. Our argument is summarized in the following observation:

Observation 6.5. *In a three-dimensional system, if two macroscopic states $|A\rangle$ and $|B\rangle$ are thermally stable, then $|A\rangle + |B\rangle$ will not be thermally stable and its coherence time will be upper bounded by some constant as $L \to \infty$. Thus, it will be not possible to create $|A\rangle + |B\rangle$ for large L.*

We emphasize that the above observation should not be considered as a mathematical theorem, but should be considered as a physical observation. Our claim here is as simple as saying that a macroscopic superposition state is difficult to create and easily decays at finite temperature. And the underlying reason behind this instability is because $D = 3$.

6.6 Discussion

Here we summarize the main findings in this chapter as follows.

(a) Feasibility of self-correcting memory is fundamentally akin to thermal stability of topological order.

(b) When a system is topologically ordered at $T = 0$, it is stable against local perturbations. When a system is topologically ordered at $T > 0$, it is also stable against thermal fluctuations.

(c) A solution of three-dimensional STS models suggests that stabilizer Hamiltonians are not likely to work a self-correcting memory.

(d) In three-dimensional systems, a superposition of macroscopic states is thermally unstable.

While our discussion on three-dimensional stabilizer Hamiltonians is limited to the cases with continuous scale symmetries, there are interesting systems with discrete scale symmetries. See [16, 50, 102, 103] for such models.

Chapter 7

Information storage capacity of discrete spin systems

Having finished analyzing quantum phases arising in STS models, stabilizer Hamiltonians at fixed points with continuous scale symmetries, we turn to another main problem of this thesis concerning information storage capacity of discrete spin systems.

7.1 Introduction

Understanding the limits imposed on information storage capacity of physical systems is a problem of fundamental and practical importance which bridges physics and information science [104]. This problem has been answered for continuum systems by Bekenstein where he showed that it is impossible to store an infinite amount of information on a finite system and derived the well-celebrated bound on the number of logical bits that can be stored inside a finite region [105]:

$$S \leq \frac{2\pi k_B L E}{\hbar c} \tag{7.1}$$

where S is the amount of information stored, L is the linear length of the region, and E is the total energy.

The most beautiful outcome concerning the Bekenstein bound is that black holes saturate this theoretical limit [106]. This essentially follows from the observation that an object with a large amount of information (entropy) tends to have high energy, and will eventually turn into a black hole once its energy exceeds a critical value. This surprising connection between information theory and black hole physics is at the heart of the thermodynamic treatment of black holes and the holographic principle [107].

Recently, a similar question on information storage capacity for discrete systems, concerning how much information can be reliably stored in discrete spin systems, has been addressed [32]. This is a problem of practical importance since such a local code would be the best error-correcting code that is physically realizable with local

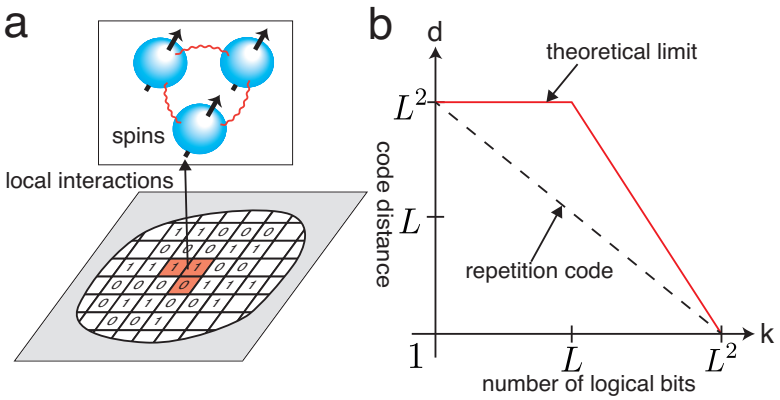

Figure 7-1: (a) Storage of information in discrete spin systems via local interactions. (b) A theoretical upper bound on information storage capacity for $D = 2$. The graph is shown in a logarithmic scale. The dotted line represents a family of repetition codes.

Hamiltonians. This problem is also of fundamental importance since such a local code may be viewed as an analog of a black hole for discrete spin systems, and may be useful for further establishing the connection between continuum and discrete descriptions of space-time and quantum gravity [108, 109].

To be more precise, consider discrete spin systems defined on a D-dimensional lattice which is governed by a local frustration-free Hamiltonian where D is the spatial dimension. Then, the following bound is found to hold by Bravyi, Terhal and Poulin [32]:

$$kd^{1/D} \leq O(n) \tag{7.2}$$

where k is the number of encoded logical bits, d is the code distance, and n is the total number of spins when the energy ground space of the Hamiltonian is viewed as the codeword space of a classical error-correcting code. Such spin systems, called *local codes*, cover a large class of physically realizable error-correcting codes.

Then, one may be naturally led to an analogous question on information storage capacity of discrete spin systems, concerning local codes which saturate the bound in Eq. (7.2). However, finding a local code which saturates the bound turned out to be a challenging problem. In particular, previously found local codes were far below the bound as seen in Fig. 7-1(b). To gain some insights on the problem, let us look at a prototypical example of local codes on a two-dimensional lattice ($D = 2$). A repetition code encodes 0 and 1 into repetitions of zeros and ones; $000\cdots$ and $111\cdots$, and can be physically realized as a local code through ferromagnetic interactions. Since a repetition code encodes a single logical bit and the Hamming distance (i.e. the number of different spin values) between two codewords is n, it has $k = 1$ and $d = n$. On the other hand, for $D = 2$, the bound is $k\sqrt{d} \leq O(n)$, and thus, the repetition code is far below the theoretical limit. One may modify a repetition code by splitting the entire lattice into smaller subparts and using them as individual repetition codes.

However, such a construction gives a family of local codes with $kd = n$ as shown with a dotted line in Fig. 7-1(b), which is still below the bound. So far, there have been no example of local codes with provably better coding properties than those of repetition codes.

In this chapter, we present a construction of local codes, called *fractal codes*, which saturate the bound asymptotically as summarized in the following theorem.

Theorem 7.1. *There exists a local code which can approach the theoretical limit arbitrarily close:*

$$k \sim O(L^{D-1}), \qquad O(L^{D-\epsilon}) < d \leq O(L^D) \tag{7.3}$$

for $D \geq 2$ where ϵ is an arbitrary small positive number, L is the linear length of the lattice and $n = L^D$.

Therefore, our construction gives the best physically realizable error-correcting code that is currently known. In this chapter, we illustrate the construction for $D = 2$ and present the proof of theorem 7.1.

7.2 Fractal spin configurations

Our construction of local codes borrows an idea from a well-known example of fractal geometries. The Sierpinski triangle has self-similar properties where the same patterns appear repeatedly at different length scales as shown in Fig. 7-2(a). This peculiar geometric nature of the triangle is reflected in its non-integer dimensionality where the number of filled elements $L^{\log 3/\log 2}$ grows as if the spatial dimension is $\frac{\log 3}{\log 2} \sim 1.585$.

While it had been long thought that the Sierpinski triangle is a mathematical object, it became apparent that it can be physically realized as a ground state of interacting spin systems via three-body terms [9]. Fig 7-2(a) shows a physical realization of Sierpinski triangle on a square lattice where interaction terms are minimized when local constraints $a + b = c \pmod 2$ on three neighboring spins are satisfied. It has been pointed out that such a fractal system may be useful as an error-correcting code with an efficient decoder [110]. Recently, coding properties of this fractal code have been predicted as follows [32]

$$k \sim O(L), \qquad d \sim O(L^{\frac{\log 3}{\log 2}}) \tag{7.4}$$

based on numerical simulations. Therefore, this fractal spin system may be significantly better than previously found local codes such as repetition codes.

Despite a remarkable idea of constructing a local code based on the Sierpinski triangle, previous works have two serious drawbacks. First, this fractal code is still far below the theoretical limit as seen in Fig. 7-1(b). Second, in order to prove the prediction of $d \sim O(L^{\frac{\log 3}{\log 2}})$, one needs to analyze Hamming distances between all the $O(2^L)$ ground states and find the minimal Hamming distance, which is a formidable challenge both from analytical and computational perspectives.

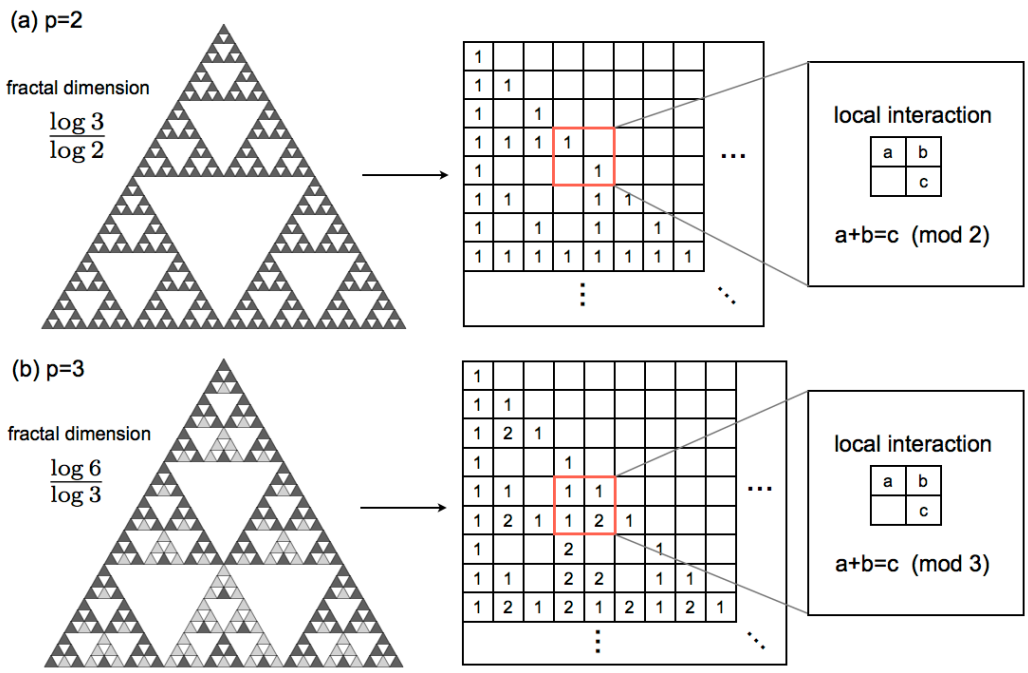

Figure 7-2: (a) Sierpinski triangle and its physical realization on a square lattice ($p = 2$). Filled elements are mapped to 1s while unfilled elements are mapped to 0s. Interaction terms are three-body. (b) A generalization of Sierpinski triangle ($p = 3$). Black elements are mapped to 1s, grey elements are mapped to 2s, and unfilled elements are mapped to 0s.

We start by presenting the resolution of the first challenge. Our construction of fractal codes utilizes a generalization of the Sierpinski triangle with higher-dimensional spins. To begin with, let us discuss fractal properties of the Sierpinski triangle with three-dimensional spins where possible spin values are $0, 1, 2$ as shown in Fig. 7-2(b). The number of non-zero spins in this generalized Sierpinski triangle is $L^{\frac{\log 6}{\log 3}}$, and its fractal dimension is $\frac{\log 6}{\log 3} \sim 1.631$, which is larger than $\frac{\log 3}{\log 2} \sim 1.585$. Then, one may naturally expect that this generalization gives a fractal code with $k \sim O(L)$ and $d \sim O(L^{\frac{\log 6}{\log 3}})$ where k is the number of encodable three-dimensional logical spins.

The key observation here is that the fractal dimension of the Sierpinski triangle grows as the inner dimension of spins increases. In particular, at the limit where p goes to infinity, we notice

$$\mathcal{D}_p^{(2)} = \frac{\log(\frac{p(p+1)}{2})}{\log p} \to 2 \qquad \text{for} \quad p \to \infty. \tag{7.5}$$

Therefore, by taking sufficiently large p, one can construct a fractal code with $k \sim O(L)$ and $d \geq O(L^{2-\epsilon})$ for an arbitrary small $\epsilon > 0$ where k is the number of encodable p-dimensional spins. This family of fractal codes based on generalized Sierpinski triangle will saturate the bound in Eq. (7.2) asymptotically. While our construction of fractal codes uses p-dimensional spins with $p > 2$, one can simulate these fractal

codes only through two-dimensional spins.

Then, what about the bound on higher-dimensional systems with $D > 2$? Fortunately, there exist higher-dimensional generalizations of the Sierpinski triangle constructed on a D-dimensional hypercubic lattice (see [111] for example). For D-dimensional Sierpinski triangle with p-dimensional spins, its fractal dimension is given by

$$\mathcal{D}_p^{(D)} = \log\left(\frac{p(p+1)\cdots(p+D-1)}{D!}\right)/\log(p) \tag{7.6}$$

which approaches to D as p goes to infinity: $\mathcal{D}_p^{(D)} \to D$ for $p \to \infty$. A fractal code based on D-dimensional Sierpinski triangle has $k \sim O(L^{D-1})$ and $d \sim O(L^{\mathcal{D}_p^{(D)}})$, and one can construct fractal codes which saturate the bound asymptotically in any spatial dimension.

Discussion above is valid only if the assumption that the fractal dimension of the code distance is equal to the fractal dimension of the Sierpinski triangle is true.

Theorem 7.2 (Fractal dimension of code distance)**.** *In fractal codes, the fractal dimension of the code distance d is equal to the fractal dimension of the Sierpinski triangle:*

$$k \sim O(L^{D-1}) \qquad d \sim O(L^{\mathcal{D}_p^{(D)}}) \tag{7.7}$$

where $\mathcal{D}_p^{(D)}$ is the fractal dimension of D-dimensional Sierpinski triangle constructed with p-dimensional spins, and k is the number of encodable logical p-dimensional spins.

The rest of this chapter is dedicated to the proof of theorem 7.2 for $D = 2$.

7.3 Two-dimensional fractal code

We begin by giving a precise definition of fractal codes in two-dimensional systems. Consider a two-dimensional square lattice with $n = L \times 2L$ spins where spins are p-dimensional and spin values are $0, \cdots, p-1$. We assume that p is a *prime number*, and $L = p^m$ with arbitrary positive integer m. Each spin is labeled by "time" t and "position" r where $t = 0, \cdots, L-1$ and $t = 0, \cdots, 2L-1$. We set periodic boundary conditions along the time axis, and set open boundary conditions along the position axis (see Fig. 7-3).

The admissible spin configurations of the system obeys the following local constraint:

$$x(t+1)_r = x(t)_{r-1} + x(t)_r \pmod p \qquad 0 \le t \le L-2 \tag{7.8}$$

where $x(t)_r = 0, \cdots, p-1$ represents the spin value at (t, r). Notice that such spin configurations can be physically realized as ground states of the following three-body

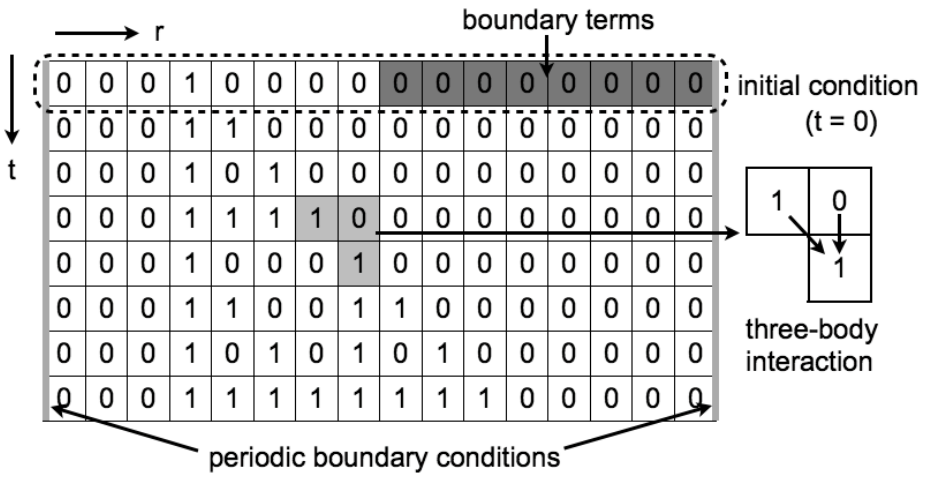

Figure 7-3: The construction of fractal codes. The example above shows the case with $p = 2$ and $L = 8$ ($m = 3$). Periodic boundary conditions are set along the time axis. Admissible spin configurations of a fractal code can be realized as ground states of a three-body Hamiltonian. The first raw at $t = 0$ is called an initial condition. Eight spins on the right hand side of the first raw are zero due to boundary terms.

local Hamiltonian:

$$H_{fractal} = \sum_{t,r} \Pi(t)_r, \qquad \Pi(t)_r = x(t+1)_r - x(t)_{r-1} - x(t)_r \qquad (\text{mod } p) \qquad (7.9)$$

with a finite energy gap. There are p^L admissible spin configurations which can be specified by the "initial condition" $(x(0)_0, \cdots, x(0)_{2L-1})$ for $t = 0$ on the first raw of a square lattice (see Fig. 7-3).

The constraint given in Eq. (7.8) is very simple, involving only three neighboring spins at once, and is translationally symmetric except at the boundary. Yet, the arising spin configurations have highly non-trivial patterns as seen in Fig. 7-3. Our main idea is to utilize such non-trivial structures of spin configurations for reliable encoding of information. Here, the entire system can be viewed as a "computational machine" which computes a vector $x(t) = (x(t)_0, \cdots, x(t)_{2L-1})$ at time t for a given initial condition $x(0) = (x(0)_0, \cdots, x(0)_{2L-1})$ after the time evolution according to the rule in Eq. (7.8). In this light, our code may be considered as a physical realization of the time evolution of one-dimensional cellular automaton [111].

Now, we construct the fractal codes based on admissible spin configurations obeying Eq. (7.8). Here, we further limit ourselves to spin configurations which satisfy the following initial condition:

$$x(0)_r = 0 \qquad \text{for} \quad r \geq L. \qquad (7.10)$$

This constraint may be physically realized by setting additional terms on the bound-

ary of the lattice:

$$H_{boundary} = \sum_{r \geq L} x(0)_r. \tag{7.11}$$

We denote a space of spin configurations specified by Eq. (7.8) and Eq. (7.10) as $\mathcal{C}_p^{(2)}$, and call it the *codeword space* of a fractal code. Then, coding properties of fractal codes are summarized in the following theorem.

Theorem 7.3 (Two-dimensional fractal code)**.** *For the codeword space $\mathcal{C}_p^{(2)}$ specified by Eq. (7.8) and Eq. (7.10), let k be the number of encodable p-dimensional spins and d be the code distance of the code (i.e. the minimal Hamming distance among all the possible spin configurations). Then, we have*

$$k = L, \qquad d = L^{\mathcal{D}_p^{(2)}}. \tag{7.12}$$

where

$$\mathcal{D}_p^{(2)} = \log\left(\frac{p(p+1)}{2}\right) / \log(p). \tag{7.13}$$

Here, we notice that $\mathcal{D}_p^{(2)}$ increases as p increases. In particular, since $\mathcal{D}_p^{(2)} \to 2$ for $p \to \infty$, we can construct a code which asymptotically saturates the bound $k\sqrt{d} \leq O(n)$ in Eq. (7.2). Theorem 7.3 leads to the proof of theorem 7.1.

The reason why we limit our considerations to spin configurations obeying Eq. (7.10) comes from a technical difficulty which is not particularly interesting. For $p = 2$ and an initial condition $(x(0)_0, \cdots, x(0)_{2L-1}) = (1, \cdots, 1)$, the resulting spin configurations are $(x(t)_0, \cdots, x(t)_{2L-1}) = (0, \cdots, 0)$ for $t > 0$ which would lead to $d = 2L$. To avoid this difficulty, we need Eq. (7.10). This issue is closely related to the irreversibility of cellular automaton.

7.4 Principal vectors and fractal dimensions

We begin by analyzing a spin configuration specified by the following initial condition (see Fig. 7-4):

$$x(0)_0 = 1, \qquad x(0)_r = 0 \quad (r \neq 0). \tag{7.14}$$

which generates the Sierpinski triangle. While our fractal codes are constructed with $L \times 2L$ spins on a square lattice which is stretched in the position direction, it is convenient to start our analysis for fractal codes constructed with $L \times L$ spins on a regular square lattice. The entire discussion of this subsection is given for fractal codes with $L \times L$ spins.

Principal vectors: We denote spin values of the t-th row in a spin configuration

(the Sierpinski triangle) arising from $x(r)_0 = (1, 0, \cdots)$ as $B(t)$ where

$$B(t) = (x(t)_0, \cdots, x(t)_{L-1})$$

and call them *principal vectors*. For example, with $m = 2$ and $p = 2$, we have the following principal vectors:

$$B(0) = (1, 0, 0, 0), \quad B(1) = (1, 1, 0, 0), \quad B(2) = (1, 0, 1, 0), \quad B(3) = (1, 1, 1, 1).$$

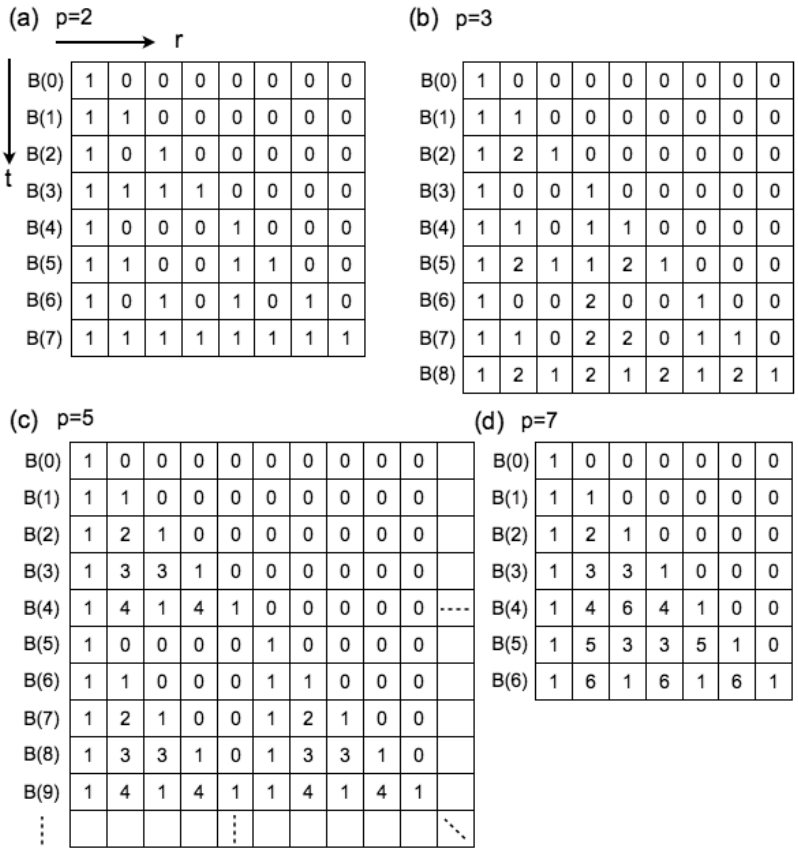

Figure 7-4: Examples of principal vectors $B(t)$ and the Pascal matrices $\mathbf{B}$. (a) $p = 2$ and $m = 3$. (b) $p = 3$ and $m = 2$. (c) $p = 5$. (d) $p = 7$ and $m = 1$.

We represent the spin configuration associated with the initial condition in Eq. (7.14) as an $L \times L$ matrix, and denote it by $\mathbf{B}$. For example, with $m = 2$ and $p = 2$, we have

$$\mathbf{B} = \begin{bmatrix} 1, & 0, & 0, & 0 \\ 1, & 1, & 0, & 0 \\ 1, & 0, & 1, & 0 \\ 1, & 1, & 1, & 1 \end{bmatrix}.$$

We show several other examples of $\mathbf{B}$ and $B(t)$ in Fig 7-4. We call $\mathbf{B}$ the *Pascal*

matrix modulo p due to its resemblance to Pascal's triangle which is also known as Sierpinski triangle.

It is worth observing basic properties of the Pascal matrix $\mathbf{B}$. As seen in Fig. 7-4, the Pascal matrices $\mathbf{B}$ have *fractal properties* with self-similar structures. In particular, as shown in Fig. 7-5(a), similar patterns of spin values appear repeatedly at various length scales. Such self-similar structures are summarized as follows:

Fact 7.4 (Self-similarity)**.** *We denote the Pascal matrix for $L = p^m$ as $\boldsymbol{B}^{(m)}$. Then, we have*

$$\boldsymbol{B}^{(m)} = \begin{bmatrix} \boldsymbol{B}^{(1)}_{0,0} \cdot \boldsymbol{B}^{(m-1)}, & \boldsymbol{B}^{(1)}_{1,0} \cdot \boldsymbol{B}^{(m-1)}, & \cdots, & \boldsymbol{B}^{(1)}_{p-1,0} \cdot \boldsymbol{B}^{(m-1)} \\ \boldsymbol{B}^{(1)}_{0,1} \cdot \boldsymbol{B}^{(m-1)}, & \boldsymbol{B}^{(1)}_{1,1} \cdot \boldsymbol{B}^{(m-1)}, & \cdots, & \boldsymbol{B}^{(1)}_{p-1,1} \cdot \boldsymbol{B}^{(m-1)} \\ \vdots & \vdots & \vdots & \ddots \\ \boldsymbol{B}^{(1)}_{0,p-1} \cdot \boldsymbol{B}^{(m-1)}, & \boldsymbol{B}^{(1)}_{0,0} \cdot \boldsymbol{B}^{(m-1)}, & \cdots, & \boldsymbol{B}^{(1)}_{p-1,p-1} \cdot \boldsymbol{B}^{(m-1)} \end{bmatrix}. \tag{7.15}$$

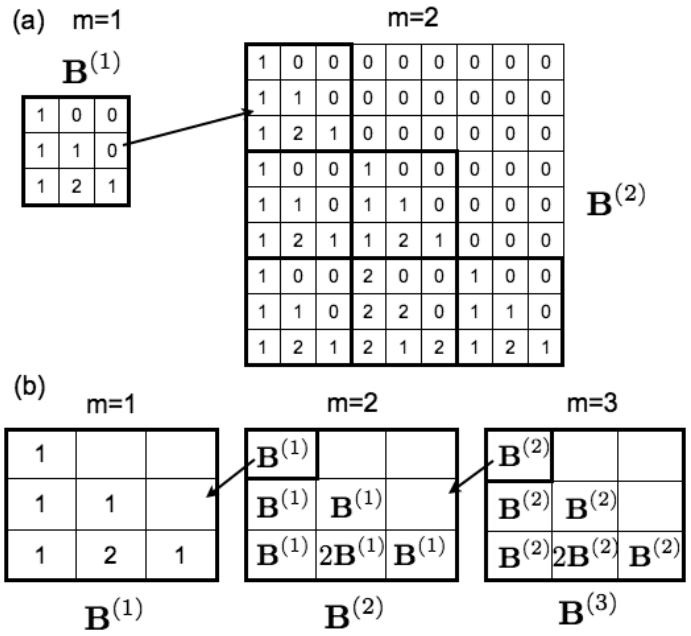

Figure 7-5: (a) An example of a self-similar property for $p = 3$. $\mathbf{B}^{(1)}$ appears repeatedly as submatrices of $\mathbf{B}^{(2)}$. (b) Self-similar properties at different length scales.

Therefore, $\mathbf{B}^{(m-1)}$ appear repeatedly as submatrices of $\mathbf{B}^{(m)}$. It is worth looking at an example for $p = 2$. Then, we notice that

$$\mathbf{B}^{(1)} = \begin{bmatrix} 1, & 0 \\ 1, & 1 \end{bmatrix}, \qquad \mathbf{B}^{(m)} = \begin{bmatrix} \mathbf{B}^{(m-1)}, & 0 \\ \mathbf{B}^{(m-1)}, & \mathbf{B}^{(m-1)} \end{bmatrix} \tag{7.16}$$

where 0 represents a $2^{m-1} \times 2^{m-1}$ matrix whose entries are all zeros. An example for $p = 3$ is shown in Fig. 7-5.

Fractal dimensions: Entries in principal vectors and the Pascal matrix can be derived easily from a simple formula. The lemma below summarizes how to compute the r-th entry of a principal vector $B(t)$, denoted as $B(t)_r$, for arbitrary t and r.

Lemma 7.5 (Entries of the Pascal matrix)**.** *Let us represent t and r in p-adic forms:*

$$r = (r_m, r_{m-1}, \cdots, r_1)_p, \qquad r = \sum_{m'=1}^{m} p^{m'-1} r_{m'}$$

$$t = (t_m, t_{m-1}, \cdots, t_1)_p, \qquad t = \sum_{m'=1}^{m} p^{m'-1} t_{m'}$$

where r_j and t_j are positive integers with $0 \le r_j, t_j \le p-1$.

(a) We have

$$B(t)_r = {}_tC_r \qquad (mod\ p) \tag{7.17}$$

where ${}_tC_r = 0$ for $r > t$.

(b) We have

$${}_tC_r \neq 0 \qquad (mod\ p) \qquad iff \qquad t_{m'} \ge r_{m'} \qquad for\ all\ m'. \tag{7.18}$$

(c) We have

$${}_tC_r = \prod_{m'=1}^{m} {}_{t_{m'}}C_{r_{m'}}. \tag{7.19}$$

Some examples are shown in Fig. 7-6. As a direct consequence of the lemma above, we have the following corollary on the weight of the Pascal matrix $\mathbf{B}$ (See Fig. 7-7):

Corollary 7.6 (Fractal dimension)**.** *For principal vectors $B(t)$, we denote its Hamming weights (the number non-zero entries) as $W(B(t))$. Similarly, we denote the Hamming weight of a the Pascal matrix $\boldsymbol{B}$ as $W(\boldsymbol{B})$. Then, the number of spins with non-zero entries is*

$$W(\boldsymbol{B}) = \sum_{t=0}^{L-1} W(B(t)) = \left(\frac{p(p+1)}{2}\right)^m. \tag{7.20}$$

Thus, the fractal dimension of the Pascal matrix $\boldsymbol{B}$ is

$$W(\boldsymbol{B}) = L^{\mathcal{D}_p^{(2)}} \qquad where \qquad \mathcal{D}_p^{(2)} = \log\left(\frac{p(p+1)}{2}\right) / \log p. \tag{7.21}$$

Proof. When $p = 2$, the number of non-zero entries corresponds to the number of

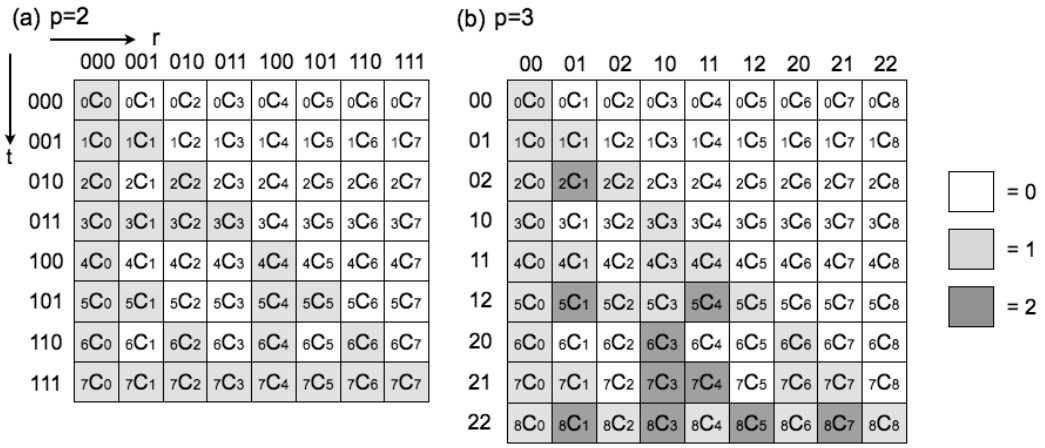

Figure 7-6: Entries of the Pascal matrix. t and r are represented in p-adic forms. (a) $p = 2$ and $m = 3$. Shaded entries represent one, while unfilled entries represent zero. (b) $p = 3$ and $m = 2$. Shaded entries represent one, black entries represent two, while unfilled entries represent zero.

pairs of t and r such that

$$t_{m'} \geq r_{m'} \qquad \text{for all } m'$$

from lemma 7.5. Then, we notice that only the following three pairs of $t_{m'}, r_{m'}$ are allowed:

$$(t_{m'}, r_{m'}) = (0,0), (1,0), (1,1).$$

Therefore, in total, there are 3^m non-zero entries. For $p > 2$, there are $\frac{p(p+1)}{2}$ possible pairs of $t_{m'}$ and $r_{m'}$. Therefore, in total, there are $\left(\frac{p(p+1)}{2}\right)^m$ non-zero entries. □

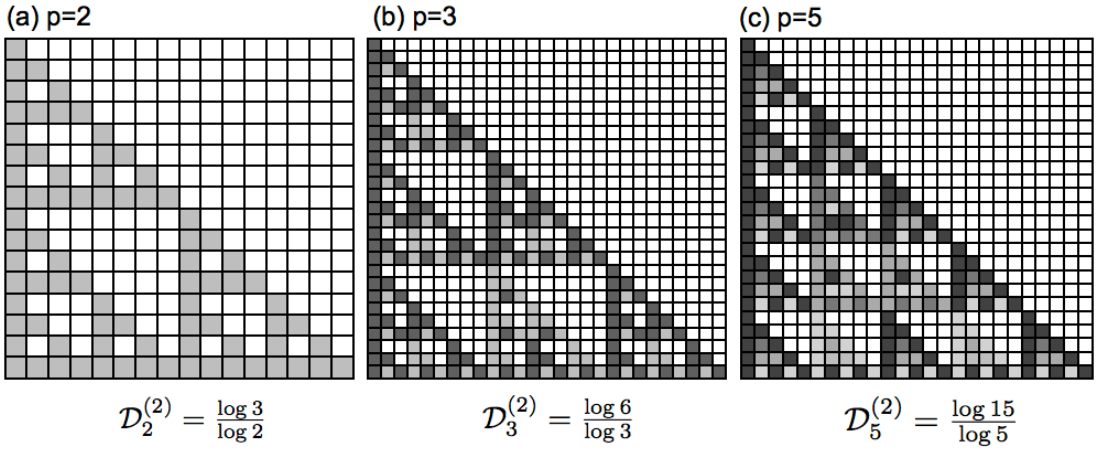

Figure 7-7: Examples of fractal dimensions for $p = 2, 3, 5$ represented in a gray scale.

7.5 Inequality on principal vectors

We have analyzed a spin configuration **B** arising from an initial condition $B(0)$. In this subsection, we extend our analysis to spin configurations arising from arbitrary initial conditions.

Time evolution of principal vectors: Let us denote an arbitrary initial condition as $V(0)$ and its t-th raw as $V(t)$. Since principal vectors $B(t)$ are independent, one can decompose $V(0)$ as a linear combination of $B(t)$:

$$V(0) = \sum_{t=0}^{L-1} c(t)B(t) \tag{7.22}$$

where $c(t) = 0, \cdots, p-1$. Then, our goal is to find an expression for $V(t)$ in terms of principal vectors $B(\tau)$ for arbitrary t.

Lemma 7.7 (Time evolution)**.** *We define $B(L+a) = 2B(a)$ for $a \geq 0$. Then, when $V(0) = \sum_\tau c(\tau)B(\tau)$, we have*

$$V(t) = \sum_{\tau} c(\tau)B(\tau + t). \tag{7.23}$$

When $V(0) = B(\tau)$ ($\tau \neq 0$), the time evolution is

$$B(\tau) \to B(\tau+1) \to \cdots \to B(L-1) \to 0 \to \cdots \to 0$$

for $p = 2$, while

$$B(\tau) \to B(\tau+1) \to \cdots \to B(L-1) \to 2B(0) \to \cdots \to 2B(\tau-1)$$

for $p > 2$.

While we are primarily interested in fractal codes with periodic boundary conditions, one may generalize the analysis to fractal codes with open boundary conditions. In such cases, the time evolution is slightly modified since $B(L-1)$ always evolves into $B(0)$ regardless of p: $B(L-1) \to B(0)$. A similar discussion holds for codes with open boundary conditions, and one can obtain a similar bound on the code distance.

Inequality on principal vectors: Finally, we prove theorem 7.3. Our proof relies on the following lemma on the weights of vectors represented in terms of principal vectors:

Lemma 7.8 (Inequality on principal vectors)**.** *Consider the following linear combination of principal vectors:*

$$V(0) = \sum_{t=0}^{L-1} c(t)B(t)$$

and denote the smallest positive integer t such that $c(t) \neq 0$ as t_{min}. Then, for the Hamming weight of $V(0)$, we have

$$W(V(0)) \geq W(B(t_{min})). \tag{7.24}$$

This is one of the most important technical tools obtained in this work. See the original paper for the proof [14]. It is worth looking at an example. Let us consider the case where $p = 3$ and $m = 2$:

$$\begin{aligned} &B(2) = (1,2,1,0,0,0,0,0,0), \quad B(5) = (1,2,1,1,2,1,0,0,0) \\ &B(7) = (1,1,0,2,2,0,1,1,0), \quad B(2) + B(5) + B(7) = (0,2,2,0,1,1,1,1,0). \end{aligned}$$

Then, we notice

$$W(B(2) + B(5) + B(7)) \geq W(B(2))$$

and the lemma holds.

The proof of theorem 7.3 also requires the following fact on the self-similar properties of principal vectors:

Fact 7.9. *We have*

$$W(B(t + b \cdot p^{m-1})) = (b+1)W(B(t)) \tag{7.25}$$

for $0 \leq b < p$ and $0 \leq t < p^{m-1}$.

We are now ready to prove theorem 7.3. We consider a spin configuration generated by an initial condition $V(0)$:

$$V(0) = \sum_{\tau=0}^{2L-1} c(\tau) B(\tau).$$

Since the initial condition obeys Eq. (7.10), one has

$$c(\tau) = 0 \qquad \tau \geq L. \tag{7.26}$$

Then, the tth raw of this spin configuration can be represented as

$$V(t) = \sum_{\tau=0}^{L-1} c(\tau) B(\tau + t).$$

Here, we denote the smallest τ such that $c(\tau) \neq 0$ as $\tau_{\min}$. The total spin weight

of this spin configuration is tightly lower bounded as follows

$$W = \sum_{t=0}^{L-1} W(V(t)) \geq \sum_{t=0}^{L-1} W(B(\tau_{\min} + t)) \tag{7.27}$$

$$\geq \sum_{t=0}^{L-1} W(B(t)) = L^{\mathcal{D}_p^{(2)}} \tag{7.28}$$

which completes the proof of theorem 7.3.

7.6 Discussion

While our fractal codes utilize the simplest example of fractal geometries (i.e. the Sierpinski triangle), one can physically realize arbitrary cellular automaton based on linear update rules in principle.

Recall that one can represent a spin configuration of the Sierpinski triangle as a polynomial over finite fields F_p [111]. In particular, the tth raw of the Sierpinski triangle can be generated by f^t where $f = 1 + x$. For instance,

$$f^0 \ = \ 1 \quad f^1 \ = \ 1 + x \quad f^2 \ = \ 1 + x^2 \quad f^3 \ = \ 1 + x + x^2 + x^3 \tag{7.29}$$

for $p = 2$, and

$$f^0 \ = \ 1 \quad f^1 \ = \ 1 + x \quad f^2 \ = \ 1 + 2x + x^2 \quad f^3 \ = \ 1 + x^3 + x^3 \tag{7.30}$$

for $p = 3$ where coefficients of polynomials represent spin configurations. Periodic boundary conditions are set by assuming $x^L = 1$.

One may generate fractal geometries by choosing an arbitrary polynomial f as long as f is non-trivial ($f \neq x^c$). The system Hamiltonian can be obtained as follows. Assume f is given by

$$f \ = \ c_0 + c_1 x + c_2 x^2 + c_3 x^3 + \cdots . \tag{7.31}$$

Then, local terms in the Hamiltonian is given by

$$\begin{bmatrix} \cdots & Z^{-c_3} & Z^{-c_2} & Z^{-c_1} & Z^{-c_0} \\ \cdots & I & I & I & Z \end{bmatrix} \tag{7.32}$$

and its powers where Z is a generalized Pauli matrix for p-dimensional spins:

$$Z|j\rangle \ = \ e^{ij2\pi/p}|j\rangle. \tag{7.33}$$

Note that we must add powers of the above interaction terms such that the system Hamiltonian is hermitian.

Discrete scale symmetries: Fractal codes do not have continuous scale symme-

tries, but have discrete scale symmetries. While detailed demonstrations of discrete scale symmetries are beyond the scope of this thesis, one may see that spin configurations generated by f are fractal since

$$f^p \;=\; c_0 + c_1 x^p + c_2 x^{2p} + c_3 x^{3p} + \cdots . \tag{7.34}$$

Therefore, a similar patter repeats when we change the scale of the system by a factor of p. In fractal codes discussed in this chapter, dimensions of the code distances are the same as the fractal dimensions of corresponding fractal geometries. An interesting open future problem may be to ask if this is true for other classes of fractal codes or not.

Generally, it is extremely difficult to obtain the number of logical bits for arbitrary system sizes L especially when the system has periodic boundary conditions in both directions of the lattice. Yet, one may easily see that the number of logical bits k behaves "analytically" only under global scale transformations $L \to pL$. As a result, one can see that spin configurations arising in fractal codes exhibit behaviors like limit cycles under RG transformations. In the future work, we will address a systematic characterization of limit cycles arising in fractal codes.

A particularly interesting observation is that fractal codes are beyond STS models, and are probably beyond descriptions of topological field theory. For instance, fractal codes have anti-commuting pairs of zero-dimensional and $\mathcal{D}_p^{(2)}$-dimensional logical operators, and do not have the dimensional duality which appeared in STS models. As a result, one cannot continuously deform geometric shapes of logical operators which implies the notion of topology is not sufficient to characterize quantum phases arising in fractal code, and effective theory of fractal codes is beyond topological field theory.

Finally, we mention that there have been considerable interests on limit cycle behaviors arising in cold atoms. In particular, it has been pointed out that the Efimov effect, a few-body bound state with discrete scale symmetries, is a rare manifestation of limit cycles under RG transformations [112, 113, 114]. While renormalization approaches used in the analysis on the Efimov effect is fairly different from RG transformations used in the analysis on lattice systems, it is fascinating to observe possibilities of nobel quantum phases of matters which may correspond to limit cycles. Compared with studies of systems at fixed points, studies on systems at limit cycles have been less addressed, which may be an important future problem in theoretical physics community.

Area law: To conclude, we point out that an area law naturally arises on coding properties of fractal codes: the number of encoded bits k is area-like with $k \sim O(L^{D-1})$, while the code distance d is asymptotically volume-like with $d \sim O(L^{D-\epsilon})$. However, a connection between fractal codes and black holes has not been established, with further work needed. To proceed, one needs to establish the connection between the Bekenstein bound and the bound on information storage capacity of discrete spin systems in Eq. (7.2) which may be an exciting future problem.

Chapter 8

Higher-dimensional fractal code

The construction of two-dimensional fractal codes can be generalized to higher-dimensional systems too. In this chapter, we introduce the three-dimensional version of fractal codes and prove theorem 7.1 for $D = 3$.

8.1 Three-dimensional fractal codes and principal matrix

We consider a three-dimensional cubic lattice with $n = L \times L \times 2L$ spins where spins are p-dimensional and $L = p^m$. Each spin is labeled by "time" t and two "positions" $r^{(1)}$ and $r^{(2)}$ with $t, r^{(1)} = 0, \cdots, L-1$ and $r^{(2)} = 0, \cdots, 2L-1$. We set periodic boundary conditions on all the surfaces which are parallel to the time axis (see Fig. 8-1). The admissible spin configurations obeys the following constraint:

$$x(t+1)_{r^{(1)},r^{(2)}} = x(t)_{r^{(1)}-1,r^{(2)}} + x(t)_{r^{(1)},r^{(2)}-1} + x(t)_{r^{(1)},r^{(2)}} \qquad (\mathrm{mod}\ p) \tag{8.1}$$

where $x(t)_{r^{(1)},r^{(2)}} = 0, \cdots, p-1$ represents the spin value at $(t, r^{(1)}, r^{(2)})$. Spin configurations may be uniquely specified by "initial conditions" $x(0)$ with $x(0)_{r^{(1)},r^{(2)}} = 0, \cdots, p-1$, which may be considered as $2L \times 2L$ matrices.

We further limit ourselves to spin configurations which satisfy the following initial condition (see Fig. 8-1(c)):

$$x(0)_{r^{(1)},r^{(2)}} = 0 \qquad \text{for} \quad r^{(2)} \geq L, \tag{8.2}$$

and denote a space of spin configurations specified by this condition as $C_p^{(3)}$. Then, our main result is summarized in the following theorem:

Theorem 8.1 (Three-dimensional fractal code)**.** *For the codeword space $C_p^{(3)}$, let k be the number of encodable p-dimensional spins and d be the code distance of the code. Then, we have*

$$k = L^2, \qquad d = L^{\mathcal{D}_p^{(3)}} \tag{8.3}$$

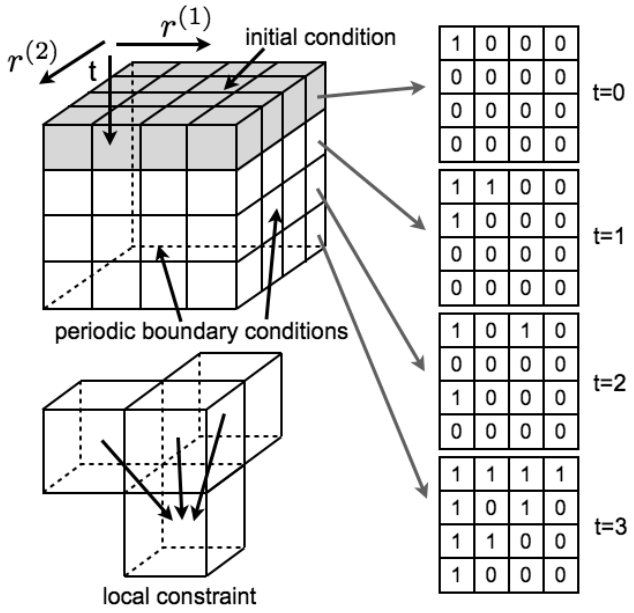

Figure 8-1: The construction of three-dimensional fractal codes. The example above shows the case with $p = 2$ and $m = 2$.

where

$$\mathcal{D}_p^{(3)} = \log\left(\frac{p(p+1)(p+2)}{6}\right) / \log(p). \tag{8.4}$$

When $D = 3$, the fractal dimension goes to three: $\mathcal{D}_p^{(3)} \to 3$ for $p \to \infty$. Therefore, the code saturates the bound $kd^{1/3} \leq O(n)$ in Eq. (7.2) for $D = 3$ asymptotically. Below, we present the proof of theorem 8.1.

8.2 Principal matrix

As in the case for $D = 2$, we start our analysis with fractal codes constructed with $L \times L \times L$ spins. Let us begin by analyzing a spin configuration specified by the following initial condition:

$$x(0)_{0,0} = 1, \qquad x(0)_{r^{(1)},r^{(2)}} = 0 \qquad \text{for} \quad (r^{(1)}, r^{(2)}) \neq (0,0) \tag{8.5}$$

which may be represented in the following matrix form:

$$B(0,0) \equiv \begin{bmatrix} 1, & 0, & \cdots & 0 \\ 0, & 0, & \cdots & 0 \\ \vdots & \vdots & \ddots & \vdots \\ 0, & 0, & \cdots & 0 \end{bmatrix} \tag{8.6}$$

We denote the spin configuration tensor, generated by the initial condition $B(0,0)$, as $\mathbf{B}$, and call it the *Pascal tensor*. We also denote a matrix representing a spin configuration on the t-th layer of the Pascal tensor $\mathbf{B}$ as $B(0,t)$, and call them *principal matrices*. Therefore, the time evolution of the initial condition $B(0,0)$ may be represented as follows:

$$B(0,0) \to B(0,1) \to \cdots \to B(0,L-1). \tag{8.7}$$

When $p=2$ and $m=2$, principal matrices are

$$B(0,0) \equiv \begin{bmatrix} 1, & 0, & 0, & 0 \\ 0, & 0, & 0, & 0 \\ 0, & 0, & 0, & 0 \\ 0, & 0, & 0, & 0 \end{bmatrix} \quad B(0,1) \equiv \begin{bmatrix} 1, & 1, & 0, & 0 \\ 1, & 0, & 0, & 0 \\ 0, & 0, & 0, & 0 \\ 0, & 0, & 0, & 0 \end{bmatrix}$$
$$B(0,2) \equiv \begin{bmatrix} 1, & 0, & 1, & 0 \\ 0, & 0, & 0, & 0 \\ 1, & 0, & 0, & 0 \\ 0, & 0, & 0, & 0 \end{bmatrix} \quad B(0,3) \equiv \begin{bmatrix} 1, & 1, & 1, & 1 \\ 1, & 0, & 1, & 0 \\ 1, & 1, & 0, & 0 \\ 1, & 0, & 0, & 0 \end{bmatrix}.$$

Other examples are shown in Fig. 8-2.

Now, we derive a formula to find spin configurations of principal matrices $B(0,t)$. For $0 \le t, r^{(1)}, r^{(2)} \le L-1$, we define

$$\begin{aligned} {}_tC_{r^{(1)},r^{(2)}} &= \frac{t!}{r^{(1)}!r^{(2)}!(t-r^{(1)}-r^{(2)})!} \\ &= {}_tC_{r^{(1)}} \cdot {}_{t-r^{(1)}}C_{r^{(2)}}. \end{aligned} \tag{8.8}$$

The lemma below summarizes how to compute the entry at $(r^{(1)}, r^{(2)})$ in $B(0,t)$, denoted as $B(0,t)_{r^{(1)},r^{(2)}}$, for arbitrary t, $r^{(1)}$ and $r^{(2)}$:

B(0,0)

1	0	0	0	0
0	0	0	0	0
0	0	0	0	0
0	0	0	0	0
0	0	0	0	0

B(0,1)

1	1	0	0	0
1	0	0	0	0
0	0	0	0	0
0	0	0	0	0
0	0	0	0	0

B(0,2)

1	2	1	0	0
2	2	0	0	0
1	0	0	0	0
0	0	0	0	0
0	0	0	0	0

B(0,3)

1	3	3	1	0
3	1	3	0	0
3	3	0	0	0
1	0	0	0	0
0	0	0	0	0

B(0,4)

1	4	1	4	1
4	2	2	4	0
1	2	1	0	0
4	4	0	0	0
1	0	0	0	0

Figure 8-2: Examples of principal matrices $B(0,t)$ for $p=5$ and $m=1$.

Lemma 8.2 (Entries of the Pascal tensor)**.** *Let us represent t, $r^{(1)}$ and $r^{(2)}$ in p-adic forms:*

$$\begin{aligned} r^{(1)} &= (r_m^{(1)} r_{m-1}^{(1)} \cdots r_1^{(1)}), \qquad & r &= \sum_{m'=1} p^{m'-1} r_{m'} \\ r^{(2)} &= (r_m^{(2)} r_{m-1}^{(2)} \cdots r_1^{(2)}), \qquad & r &= \sum_{m'=1} p^{m'-1} r_{m'} \\ t &= (t_m t_{m-1} \cdots t_1), & t &= \sum_{m'=1} p^{m'-1} t_{m'}. \end{aligned}$$

(a) We have

$$B(0,t)_{r^{(1)},r^{(2)}} = {}_tC_{r^{(1)},r^{(2)}} \qquad (mod\ p). \tag{8.9}$$

(b) We have

$${}_tC_{r^{(1)},r^{(2)}} \neq 0 \qquad (mod\ p) \qquad iff \qquad t_{m'} \geq r_{m'}^{(1)} + r_{m'}^{(2)} \qquad for\ all\ m'. \tag{8.10}$$

(c) We have

$${}_tC_{r^{(1)},r^{(2)}} = \prod_{m'} {}_{t_{m'}}C_{r_{m'}^{(1)},r_{m'}^{(2)}}. \tag{8.11}$$

An example is shown in Fig. 8-3. The proof is skipped.

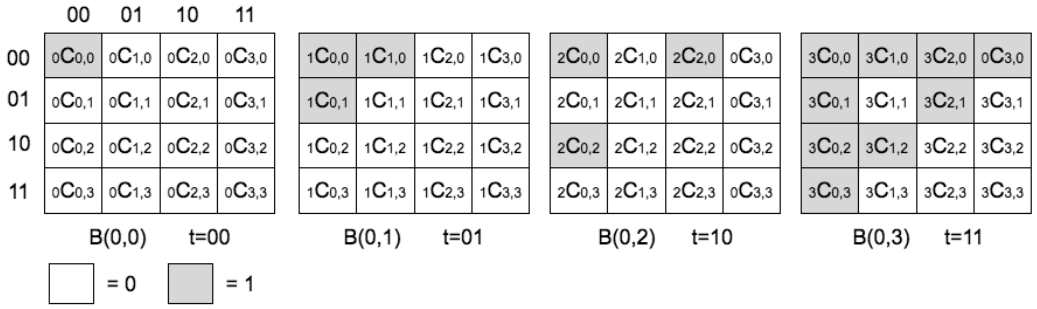

Figure 8-3: Entries of principal matrices for $p = 2$ and $m = 2$.

As a direct consequence of the lemma above, we have the following corollary on the weight of the Pascal tensor $\mathbf{B}$:

Corollary 8.3 (Fractal dimension)**.** *The number of non-zero entries in the Pascal tensor is*

$$W(\boldsymbol{B}) = \sum_{t=0}^{L-1} W(B(0,t)) = \left(\frac{p(p+1)(p+2)}{6}\right)^m. \tag{8.12}$$

Thus, the fractal dimension is

$$W(\boldsymbol{B}) = L^{D_p^{(3)}} \qquad \textit{where} \qquad \mathcal{D}_p^{(3)} = \log\left(\frac{p(p+1)(p+2)}{6}\right)/\log p. \tag{8.13}$$

Proof. In order for $B(0,t)_{r^{(1)},r^{(2)}}$ to be non-zero, $(t_{m'}, r_{m'}^{(1)}, r_{m'}^{(2)})$ must satisfy $t_{m'} \geq r_{m'}^{(1)} + r_{m'}^{(2)}$ for all m'. The number of such choices for each m' is

$$\sum_{j=1}^{p} \frac{j(j+1)}{2} = \frac{p(p+1)(p+2)}{6}.$$

□

Principal matrix and principal vector: We continue an analyze on basic properties of principal matrices $B(0,t)$. We introduce the following shorthand notation of principal matrices $B(0,t)$:

$$B(0,t) = \begin{bmatrix} B(0,t)_0 \\ B(0,t)_1 \\ \vdots \\ B(0,t)_{L-1} \end{bmatrix} \tag{8.14}$$

where $B(0,t)_j$ are L-component vectors with

$$B(0,t)_j = (B(0,t)_{0,j}, B(0,t)_{1,j}, \cdots, B(0,t)_{L-1,j}). \tag{8.15}$$

For example, when $p = 2$ and $m = 2$, we have

$$B(0,3) = \begin{bmatrix} 1, & 1, & 1, & 1 \\ 1, & 0, & 1, & 0 \\ 1, & 1, & 0, & 0 \\ 1, & 0, & 0, & 0 \end{bmatrix},$$

and

$$\begin{aligned} B(0,3)_0 &= (1,1,1,1), \quad B(0,3)_1 = (1,0,1,0) \\ B(0,3)_2 &= (1,1,0,0), \quad B(0,3)_3 = (1,0,0,0). \end{aligned}$$

Therefore, one may represent $B(0,3)$ as follows:

$$B(0,3) = \begin{bmatrix} B(3) \\ B(2) \\ B(1) \\ B(0) \end{bmatrix}$$

where $B(0)$, $B(1)$, $B(2)$ and $B(3)$ are principal vectors used in analyzing two-dimensional

fractal codes. We also have

$$B(0,2) = \begin{bmatrix} 1, & 0, & 1, & 0 \\ 0, & 0, & 0, & 0 \\ 1, & 0, & 0, & 0 \\ 0, & 0, & 0, & 0 \end{bmatrix} = \begin{bmatrix} B(2) \\ 0 \\ B(0) \\ 0 \end{bmatrix}.$$

As examples above show, principal matrices $B(0,t)$ can be concisely represented in terms of principal vectors $B(t)$. Other examples are shown in Fig. 8-4 too. One may represent principal matrices $B(0,t)$ in terms of principal vectors $B(t)$ as follows:

Lemma 8.4 (Principal matrix)**.** *A principal matrix $B(0,t)$ can be represented as*

$$B(0,t) = \begin{bmatrix} B(t)_0 \cdot B(t) \\ B(t)_1 \cdot B(t-1) \\ \vdots \\ B(t)_{L-1} \cdot B(t-L+1) \end{bmatrix} \tag{8.16}$$

As an example, let us represent $B(0,6)$ for $p = 2$ and $m = 3$ in this shorthand representation (see Fig. 8-4):

$$B(6) = (1,0,1,0,1,0,1,0), \qquad B(0,6) = (B(6),0,B(4),0,B(2),0,B(0),0)^T$$

where 0 represents vectors with zero entries. Similarly, we can represent $B(0,7)$ for $p = 3$ and $m = 2$ as follows:

$$\begin{aligned} &B(7) = (1,1,0,2,2,0,1,1,0) \\ &B(0,7) = (B(7),B(6),0,2B(4),2B(3),0,B(1),B(0),0)^T. \end{aligned}$$

It is worth representing all the principal matrices $B(0,t)$ at once as in Fig. 8-4(b). Therefore, in a principal matrix $B(0,t)$, principal vectors $B(0),\cdots,B(t)$ are distributed with weights corresponding to a principal vector $B(t)$.

8.3 Inequality on principal matrices

So far, we have analyzed the spin configuration generated by the following initial condition:

$$B(0,0) \equiv \begin{bmatrix} B(0) \\ 0 \\ 0 \\ 0 \end{bmatrix}. \tag{8.17}$$

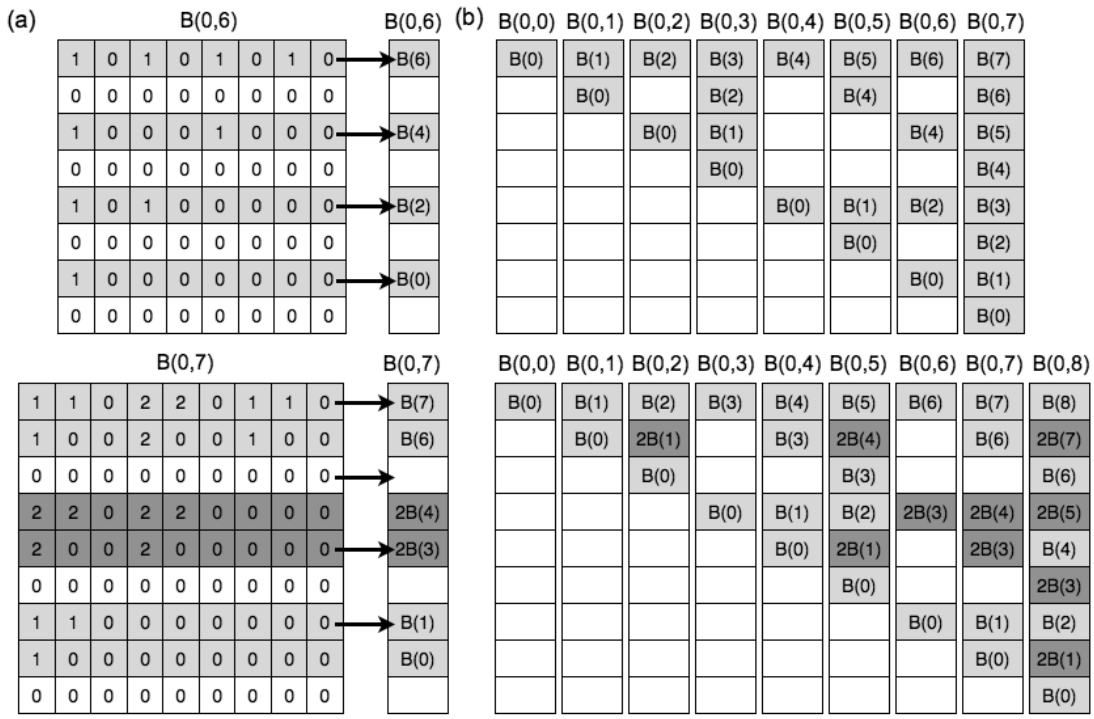

Figure 8-4: (a) Shorthand notations of $B(0,6)$ for $p=2$ and $m=3$, and $B(0,7)$ for $p=3$ and $m=2$. (b) Principle matrices and principal vectors.

Here, we start by generalizing our analyses and consider spin configurations generated by other initial conditions:

$$B(a,0) \equiv \begin{bmatrix} B(a) \\ 0 \\ 0 \\ 0 \end{bmatrix} \qquad (\text{for } a = 0, \cdots, L-1). \tag{8.18}$$

We denote the t-th layer of the spin configuration generated by $B(a,0)$ as $B(a,t)$. For simplicity, we will call $B(a,t)$ for *both* $a=0$ and $a \neq 0$ *principal matrices* from now on.

One may represent $B(a,t)$ explicitly as follows:

Lemma 8.5 (Generalized principal matrix)**.** *A principal matrix $B(a,t)$ can be represented as*

$$B(a,t) = \begin{bmatrix} B(t)_0 \cdot B(t+a) \\ B(t)_1 \cdot B(t+a-1) \\ \vdots \\ B(t)_{L-1} \cdot B(t+a-L+1) \end{bmatrix} \tag{8.19}$$

where $B(\tau + L) = 2B(\tau)$.

The proof of the lemma is similar to the one for lemma 8.4, so we skip it. Below,

we show some examples. For $p = 2$ and $m = 2$, we have:

$$B(0,0) = \begin{bmatrix} B(0) \\ 0 \\ 0 \\ 0 \end{bmatrix}, \quad B(0,1) = \begin{bmatrix} B(1) \\ B(0) \\ 0 \\ 0 \end{bmatrix}, \quad B(0,2) = \begin{bmatrix} B(2) \\ 0 \\ B(0) \\ 0 \end{bmatrix}, \quad B(0,3) = \begin{bmatrix} B(3) \\ B(2) \\ B(1) \\ B(0) \end{bmatrix}$$

$$B(1,0) = \begin{bmatrix} B(1) \\ 0 \\ 0 \\ 0 \end{bmatrix}, \quad B(1,1) = \begin{bmatrix} B(2) \\ B(1) \\ 0 \\ 0 \end{bmatrix}, \quad B(1,2) = \begin{bmatrix} B(3) \\ 0 \\ B(1) \\ 0 \end{bmatrix}, \quad B(1,3) = \begin{bmatrix} 0 \\ B(3) \\ B(2) \\ B(1) \end{bmatrix}$$

$$B(2,0) = \begin{bmatrix} B(2) \\ 0 \\ 0 \\ 0 \end{bmatrix}, \quad B(2,1) = \begin{bmatrix} B(3) \\ B(2) \\ 0 \\ 0 \end{bmatrix}, \quad B(2,2) = \begin{bmatrix} 0 \\ 0 \\ B(2) \\ 0 \end{bmatrix}, \quad B(2,3) = \begin{bmatrix} 0 \\ 0 \\ B(3) \\ B(2) \end{bmatrix}$$

$$B(3,0) = \begin{bmatrix} B(3) \\ 0 \\ 0 \\ 0 \end{bmatrix}, \quad B(3,1) = \begin{bmatrix} 0 \\ B(3) \\ 0 \\ 0 \end{bmatrix}, \quad B(3,2) = \begin{bmatrix} 0 \\ 0 \\ B(3) \\ 0 \end{bmatrix}, \quad B(3,3) = \begin{bmatrix} 0 \\ 0 \\ 0 \\ B(3) \end{bmatrix}.$$

For $p = 3$ and $m = 1$, we have

$$B(0,0) = \begin{bmatrix} B(0) \\ 0 \\ 0 \end{bmatrix}, \quad B(0,1) = \begin{bmatrix} B(1) \\ B(0) \\ 0 \end{bmatrix}, \quad B(0,2) = \begin{bmatrix} B(2) \\ 2B(1) \\ B(0) \end{bmatrix}$$

$$B(1,0) = \begin{bmatrix} B(1) \\ 0 \\ 0 \end{bmatrix}, \quad B(1,1) = \begin{bmatrix} B(2) \\ B(1) \\ 0 \end{bmatrix}, \quad B(1,2) = \begin{bmatrix} 2B(0) \\ 2B(2) \\ B(1) \end{bmatrix}$$

$$B(2,0) = \begin{bmatrix} B(2) \\ 0 \\ 0 \end{bmatrix}, \quad B(2,1) = \begin{bmatrix} 2B(0) \\ B(2) \\ 0 \end{bmatrix}, \quad B(2,2) = \begin{bmatrix} 2B(1) \\ B(0) \\ B(2) \end{bmatrix}.$$

Now, let us analyze the time evolution of principal matrices. Recall that $B(a, 0)$ evolves as follows:

$$B(a,0) \to B(a,1) \to \cdots \to B(a, L-1). \tag{8.20}$$

Here, we are interested in the time evolution of $B(a, \tau)$:

Lemma 8.6 (Periodic boundary conditions)**.** *We define $B(a, L+t) = 3B(a, t)$. When the initial condition is $V(0) = B(a, \tau)$, we have*

$$V(t) = B(a, \tau + t). \tag{8.21}$$

Here we derive some inequality concerning the weights of principal matrices. We begin by noticing that there are L^2 principal matrices and they are all independent.

Then, one can decompose an arbitrary initial condition $V(0)$ in terms of principal matrices $B(a,t)$:

$$V(0) = \sum_{a,t} c(a,t)B(a,t). \tag{8.22}$$

We define the following sets:

$$\begin{aligned} R_0(V(0)) &= \{(a,t) : c(a,t) \neq 0\} \\ R_1(V(0)) &= \{(a,t) \in R_0 : a+t \leq a'+t' \text{ for all } (a',t') \in R_0\} \\ R_2(V(0)) &= \{(a,t) \in R_1 : t \leq t' \text{ for all } (a',t') \in R_1\}. \end{aligned} \tag{8.23}$$

Note that $R_2 \subseteq R_1 \subseteq R_0$, and there is only one element in R_2. Examples of R_0, R_1 and R_2 are shown in Fig. 8-5. Then, for the weight of the initial condition, we have the following inequality:

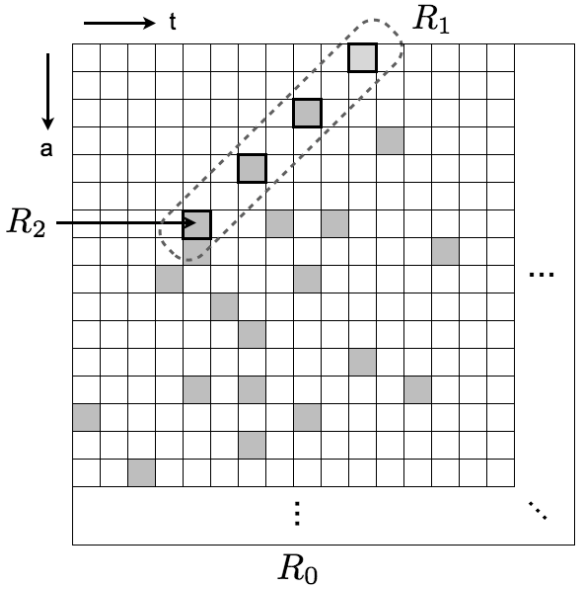

Figure 8-5: Examples of R_0, R_1 and R_2. R_0 is a set of all shaded sites. R_1 is a set of sites with minimal $a+t$. R_2 is a subset of R_1 with minimal t.

Lemma 8.7 (Inequality on principal matrices)**.** *Consider a matrix*

$$V(0) = \sum_{a,t} c(a,t)B(a,t) \tag{8.24}$$

where $c(a,t) = 0$ *for all* (a,t) *with* $a+t \geq L$. *Let* $(a',t') \in R_2(V(0))$. *Then, we have*

$$W(V(0)) \geq W\left(B(0,t')\right). \tag{8.25}$$

We do not include the proof in this thesis since it is lengthy. The proof is presented in the original paper. As an example, let us consider the following linear

decomposition:

$$V(0) = B(2,3) + B(5,3) + B(1,4) + B(0,8).$$

Then, we have

$$R = \{(2,3),(5,3),(1,4),(0,8)\}, \qquad R_1 = \{(2,3),(1,4)\}, \qquad R_2 = \{(2,3)\}$$

and

$$W(V(0)) \geq W(B(0,3)).$$

Now, we prove theorem 8.1. Since spins on tth layer are represented by an $L \times 2L$ matrix in fractal codes, we extend our definition of principal matrices to $t = 0, \cdots, 2L-1$. By noticing self-similar properties of fractal codes, one has

$$B^*(a,t) = \begin{bmatrix} B(a,t) \\ 0 \end{bmatrix} \qquad B^*(a,t+L) = \begin{bmatrix} 2B(a,t) \\ B(a,t) \end{bmatrix} \tag{8.26}$$

for $0 \geq t < L$ where $B^*(a,t)$ are $L \times 2L$ matrices and $B(a,t)$ are original principal matrices.

Since $B^*(a,t)$ are independent, one can decompose the initial condition $V(0)$ as

$$V(0) = \sum_{a,t=0}^{2L-1} c(a,t) B(a,t). \tag{8.27}$$

Since the initial condition $V(0)$ obeys Eq. (8.2), one has

$$c(a,t) = 0 \qquad \text{for} \quad t \geq L. \tag{8.28}$$

Let $(a',t') = R_2(V(0))$. From some speculations, one notices that

$$\begin{aligned} W(V(t)) &\geq W(B(0,t'+t)) \qquad \text{for} \quad t'+t < L \\ W(V(t)) &\geq W(B(0,t'+t-L)) \qquad \text{for} \quad t'+t \geq L. \end{aligned}$$

Therefore, one has

$$\sum_t W(V(t)) \geq \sum_t B(0,t) = L^{\mathcal{D}_p^{(3)}} \tag{8.29}$$

which completes the proof.

Bibliography

[1] A. Yu. Kitaev. Fault-tolerant quantum computation by anyons. *Ann. Phys.*, 303:2–30, 2003.

[2] Michael A. Levin and Xiao-Gang Wen. String-net condensation: A physical mechanism for topological phases. *Phys. Rev. B*, 71:045110, 2005.

[3] Nicolas Sourlas. Spin-glass models as error-correcting codes. *Nature*, 339:693, 1989.

[4] P. W. Shor. Fault-tolerant quantum computation. In *Proceedings of the 37th Annual Symposium on Foundations of Computer Science (FOCS)*, page 56. IEEE Computer Society, Los Alamitos, CA, 1996.

[5] Daniel Gottesman. Class of quantum error-correcting codes saturating the quantum hamming bound. *Phys. Rev. A*, 54:1862, 1996.

[6] Charles H. Bennett, David P. DiVincenzo, John A. Smolin, and William K. Wootters. Mixed-state entanglement and quantum error correction. *Phys. Rev. A*, 54:3824, 1996.

[7] Raymond Laflamme, Cesar Miquel, Juan Pablo Paz, and Wojciech Hubert Zurek. Perfect quantum error correcting code. *Phys. Rev. Lett.*, 77:198, 1996.

[8] Sergey Bravyi and Jeongwan Haah. On the energy landscape of 3d spin hamiltonians with topological order. *Phys. Rev. Lett.*, 107:150504, 2011.

[9] M. E. J. Newman and Cristopher Moore. Glassy dynamics and aging in an exactly solvable spin model. *Phys. Rev. E*, 60:5068, 1999.

[10] Jeongwan Haah. Local stabilizer codes in three dimensions without string logical operators. *Phys. Rev. A*, 83:042330, 2011.

[11] Beni Yoshida and Isaac L. Chuang. Framework for classifying logical operators in stabilizer codes. *Phys. Rev. A*, 81:052302, 2010.

[12] Beni Yoshida. Classification of quantum phases and topology of logical operators in an exactly solved model of quantum codes. *Ann. Phys.*, 326:15–95, 2011.

[13] Beni Yoshida. Feasibility of self-correcting quantum memory and thermal stability of topological order. *Ann. Phys.*, 326:2566–2633, 2011.

[14] Beni Yoshida. Information storage capacity of discrete spin systems. arXiv:1111.3275.

[15] H. Bombin. Structure of 2d topological stabilizer codes. arXiv:1107.2707, 2011.

[16] Jeongwan Haah. Commuting pauli hamiltonians as maps between free modules. arXiv:1204.1063.

[17] G. Vidal, J. I. Latorre, E. Rico, and A. Kitaev. Entanglement in quantum critical phenomena. *Phys. Rev. Lett.*, 90:227902, 2003.

[18] Tobias J. Osborne and Michael A. Nielsen. Entanglement in a simple quantum phase transition. *Phys. Rev. A*, 66:032110, 2002.

[19] Pasquale Calabrese and John Cardy. Entanglement entropy and quantum field theory. *J. Stat. Phys.*, 2004:P06002, 2004.

[20] Eduardo Fradkin and Joel E. Moore. Entanglement entropy of 2d conformal quantum critical points: Hearing the shape of a quantum drum. *Phys. Rev. Lett.*, 97:050404, 2006.

[21] Shinsei Ryu and Tadashi Takayanagi. Holographic derivation of entanglement entropy from the anti–de sitter space/conformal field theory correspondence. *Phys. Rev. Lett.*, 96:181602, 2006.

[22] Hui Li and F. D. M. Haldane. Entanglement spectrum as a generalization of entanglement entropy: Identification of topological order in non-abelian fractional quantum hall effect states. *Phys. Rev. Lett.*, 101:010504, 2008.

[23] Alexei Kitaev and John Preskill. Topological entanglement entropy. *Phys. Rev. Lett.*, 96:110404, 2006.

[24] Michael Levin and Xiao-Gang Wen. Detecting topological order in a ground state wave function. *Phys. Rev. Lett.*, 96:110405, 2006.

[25] M. Hein, J. Eisert, and H. J. Briegel. Multiparty entanglement in graph states. *Phys. Rev. A*, 69:062311, 2004.

[26] David Fattal, Toby S. Cubitt, Yoshihisa Yamamoto, Sergey Bravyi, and Isaac L. Chuang. Entanglement in the stabilizer formalism. arXiv:0406168, (2004).

[27] Mark Wilde and David Fattal. Nonlocal quantum information in bipartite quantum error correction. *Quant. Inf. Proc.*, 9:591, 2010.

[28] Sergey Bravyi, Matthew Hastings, and Spyridon Michalakis. Topological quantum order: Stability under local perturbations. *J. Math. Phys*, 51:093512, 2010.

[29] X. G. Wen and Q. Niu. Ground-state degeneracy of the fractional quantum hall states in the presence of a random potential and on high-genus riemann surfaces. *Phys. Rev. B*, 41:9377, 1990.

[30] A Yu Kitaev. Quantum computations: algorithms and error correction. *Russ. Math. Surv.*, 52:1191, 1997.

[31] Sergey Bravyi and Barbara Terhal. A no-go theorem for a two-dimensional self-correcting quantum memory based on stabilizer codes. *New. J. Phys.*, 11:043029, 2009.

[32] Sergey Bravyi, David Poulin, and Barbara Terhal. Tradeoffs for reliable quantum information storage in 2d systems. *Phys. Rev. Lett.*, 104:050503, 2010.

[33] Emanuel Knill and Raymond Laflamme. Theory of quantum error-correcting codes. *Phys. Rev. A*, 55:900–911, 1997.

[34] Mark Hillery, Vladimír Bužek, and André Berthiaume. Quantum secret sharing. *Phys. Rev. A*, 59:1829–1834, 1999.

[35] Daniel Gottesman. Theory of quantum secret sharing. *Phys. Rev. A*, 61:042311, 2000.

[36] David Poulin. Stabilizer formalism for operator quantum error correction. *Phys. Rev. Lett.*, 95:230504, 2005.

[37] Dave Bacon. Operator quantum error-correcting subsystems for self-correcting quantum memories. *Phys. Rev. A*, 73:012340, 2006.

[38] Panos Aliferis and Andrew W. Cross. Subsystem fault tolerance with the bacon-shor code. *Phys. Rev. Lett.*, 98:220502, 2007.

[39] Román Orús, Andrew C. Doherty, and Guifré Vidal. First order phase transition in the anisotropic quantum orbital compass model. *Phys. Rev. Lett.*, 102:077203, 2009.

[40] Y. Tokura and N. Nagaosa. Orbital physics in transition-metal oxides. *Science*, 288:462, 2000.

[41] Jeongwan Haah and John Preskill. Logical operator tradeoff for local quantum codes. arXiv:1011.3529, (2011).

[42] Sergey Bravyi. Subsystem codes with spatially local generators. *Phys. Rev. A*, 83:012320, 2011.

[43] Eric Dennis, Alexei Kitaev, Andrew Landahl, and John Preskill. Topological quantum memory. *J. Math. Phys.*, 43:4452–4505, 2002.

[44] Ian Affleck, Tom Kennedy, Elliott H. Lieb, and Hal Tasaki. Rigorous results on valence-bond ground states in antiferromagnets. *Phys. Rev. Lett.*, 59:799, 1987.

[45] Ian Affleck, Tom Kennedy, Elliott H. Lieb, and Hal Tasaki. Valence bond ground states in isotropic quantum antiferromagnets. *Commun. Math. Phys.*, 115:477–528, 1988.

[46] Alexei Kitaev. Anyons in an exactly solved model and beyond. *Ann. Phys.*, 321:2–111, 2006.

[47] A. Y. Kitaev, A. H. Shen, and M. N. Vyalyi. *Classical and quantum computation*. AMS, Providence, RI, 2002.

[48] Sergey Bravyi. Efficient algorithm for a quantum analogue of 2-sat. quant-ph/0602108.

[49] Robert Raussendorf, Daniel E. Browne, and Hans J. Briegel. Measurement-based quantum computation on cluster states. *Phys. Rev. A*, 68:022312, 2003.

[50] Claudio Chamon. Quantum glassiness in strongly correlated clean systems: An example of topological overprotection. *Phys. Rev. Lett.*, 94:040402, 2005.

[51] Alastair Kay and Roger Colbeck. Quantum self-correcting stabilizer codes. arXiv:0810.3557, (2008).

[52] S. Sachdev. *Quantum Phase Transitions*. Cambridge University Press, Cambridge, 1999.

[53] M. B. Hastings and Xiao-Gang Wen. Quasiadiabatic continuation of quantum states: The stability of topological ground-state degeneracy and emergent gauge invariance. *Phys. Rev. B*, 72:045141, 2005.

[54] Xie Chen, Zheng-Cheng Gu, and Xiao-Gang Wen. Local unitary transformation, long-range quantum entanglement, wave function renormalization, and topological order. *Phys. Rev. B*, 82:155138, 2010.

[55] Sergey Bravyi, Libor Caha, Ramis Movassagh, Daniel Nagaj, and Peter Shor. Criticality without frustration for quantum spin-1 chains. arxiv:1203.5801, 2012.

[56] Elliott Lieb, Theodore Schultz, and Daniel Mattis. Two soluble models of an antiferromagnetic chain. *Ann. Phys. (NY)*, 16:407–466, 1961.

[57] Michael M. Wolf, Gerardo Ortiz, Frank Verstraete, and J. Ignacio Cirac. Quantum phase transitions in matrix product systems. *Phys. Rev. Lett.*, 97:110403, 2006.

[58] Stein Olav Skrvseth and Stephen D. Bartlett. Phase transitions and localizable entanglement in cluster-state spin chains with ising couplings and local fields. *Phys. Rev. A*, 80:022316, 2009.

[59] Chetan Nayak, Steven H. Simon, Ady Stern, Michael Freedman, and Sankar Das Sarma. Non-abelian anyons and topological quantum computation. *Rev. Mod. Phys.*, 80:1083, 2008.

[60] G. E. Volovik. *The Universe in a Helium Droplet.* Oxford University Press, New York, 2003.

[61] Edward Witten. Quantum field theory and the jones polynomial. *Commun. Math. Phys.*, 121:351–399, 1989.

[62] I. M. Lifshitz. Anomalies of electron characteristics of a metal in the high pressure region. *Sov. Phys. JETP*, 11:1130, 1960.

[63] Alioscia Hamma. Berry phases and quantum phase transitions. quant-ph/0602091, 2006.

[64] Steven White. Density matrix formulation for quantum renormalization groups. *Phys. Rev. Lett.*, 69:2863, 1992.

[65] F. Verstraete, J. J. García-Ripoll, and J. I. Cirac. Matrix product density operators: Simulation of finite-temperature and dissipative systems. *Phys. Rev. Lett.*, 93:207204, 2004.

[66] F. Verstraete and J. I. Cirac. Matrix product states represent ground states faithfully. *Phys. Rev. B*, 73:094423, 2006.

[67] M. Hastings. Solving gapped hamiltonians locally. *Phys. Rev. B*, 73:085115, 2006.

[68] G. Vidal. Entanglement renormalization. *Phys. Rev. Lett.*, 99:220405, 2007.

[69] Sergey Bravyi, David P. DiVincenzo, Roberto I. Oliveira, and Barbara M. Terhal. The complexity of stoquastic local hamiltonian problems. *Quant. Inf. Comp.*, 8:0361, 2008.

[70] S. Bravyi, M. B. Hastings, and F. Verstraete. Lieb-robinson bounds and the generation of correlations and topological quantum order. *Phys. Rev. Lett.*, 97:050401, 2006.

[71] Norbert Schuch, David Pérez-García, and Ignacio Cirac. Classifying quantum phases using matrix product states and projected entangled pair states. *Phys. Rev. B*, 84:165139–, 2011.

[72] Salman Beigi. Classification of the phases of 1d spin chains with commuting hamiltonians. *J. Phys. A: Math. Gen.*, 45, 2012.

[73] Xie Chen, Zheng-Cheng Gu, and Xiao-Gang Wen. Classification of gapped symmetric phases in one-dimensional spin systems. *Phys. Rev. B*, 83:035107, 2011.

[74] H. Bombin and M. A. Martin-Delgado. Topological quantum distillation. *Phys. Rev. Lett.*, 97:180501, 2006.

[75] Tobias J. Osborne. Simulating adiabatic evolution of gapped spin systems. *Phys. Rev. A*, 75:032321, 2007.

[76] Tosio Kato. On the adiabatic theorem of quantum mechanics. *J. Phys. Soc. Jpn.*, 5:435, 1950.

[77] A Messiah. *Quantum Mechanics*, volume 2. North-Holland, Amsterdam, 1962.

[78] Zohar Nussinov and Gerardo Ortiz. Autocorrelations and thermal fragility of anyonic loops in topologically quantum ordered systems. *Phys. Rev. B*, 77:064302, 2008.

[79] R Alicki, M Fannes, and M Horodecki. On thermalization in kitaev's 2d model. *J. Phys. A: Math. Gen.*, 42:065303, 2009.

[80] R. Alicki, M. Horodecki, P. Horodecki, and R. Horodecki. On thermal stability of topological qubit in kitaev's 4d model. *Open Syst. Inf. Dyn.*, 17:1, 2010.

[81] Matthew B. Hastings. Topological order at nonzero temperature. *Phys. Rev. Lett.*, 107:210501, 11 2011.

[82] Isaac H. Kim. Stability of topologically invariant order parameters at finite temperature. arXiv:1109.3496.

[83] Sergey Bravyi and Jeongwan Haah. Analytic and numerical demonstration of quantum self-correction in the 3d cubic code, 2011.

[84] Peter W. Shor. Scheme for reducing decoherence in quantum computer memory. *Phys. Rev. A*, 52:2493, 1995.

[85] A. R. Calderbank and Peter W. Shor. Good quantum error-correcting codes exist. *Phys. Rev. A*, 54:1098–1105, 1996.

[86] Fernando Pastawski, Alastair Kay, Norbert Schuch, and Ignacio. Cirac. Limitations of passive protection of quantum information. *Quantum Inf. Comput.*, 10:580, 2010.

[87] Koujin Takeda and Hidetoshi Nishimori. Self-dual random-plaquette gauge model and the quantum toric code. *Nucl. Phys. B*, 686:377–396, 2004.

[88] Alioscia Hamma, Claudio Castelnovo, and Claudio Chamon. Toric-boson model: Toward a topological quantum memory at finite temperature. *Phys. Rev. B*, 79:245122, 2009.

[89] R. B. Laughlin. Anomalous quantum hall effect: An incompressible quantum fluid with fractionally charged excitations. *Phys. Rev. Lett.*, 50:1395, 1983.

[90] G. Misguich, D. Serban, and V. Pasquier. Quantum dimer model on the kagome lattice: Solvable dimer-liquid and ising gauge theory". *Phys. Rev. Lett.*, 89:137202, 2002.

[91] C. L. Kane and E. J. Mele. Z_{2} topological order and the quantum spin hall effect. *Phys. Rev. Lett.*, 95:146802, 2005.

[92] Liang Fu, C. L. Kane, and E. J. Mele. Topological insulators in three dimensions. *Phys. Rev. Lett.*, 98:106803, 2007.

[93] Claudio Castelnovo and Claudio Chamon. Entanglement and topological entropy of the toric code at finite temperature. *Phys. Rev. B*, 76:184442, 2007.

[94] S. Iblisdir, D. Pérez-García, M. Aguado, and J. Pachos. Scaling law for topologically ordered systems at finite temperature. *Phys. Rev. B*, 79:134303, 04 2009.

[95] Sergei V. Isakov, Matthew B. Hastings, and Roger G. Melko. Topological entanglement entropy of a bose-hubbard spin liquid. arxiv:1102.1721, (2011).

[96] Isaac H. Kim. 3d local qupit quantum code without string logical operator. arXiv:1202.0052.

[97] Claudio Castelnovo and Claudio Chamon. Topological order in a three-dimensional toric code at finite temperature. *Phys. Rev. B*, 78:155120, 2008.

[98] Zohar Nussinov and Gerardo Ortiz. A symmetry principle for topological quantum order. *Ann. Phys. (NY)*, 324:977–1057, 2009.

[99] Cyril Stark, Lode Pollet, Ataç Imamoğlu, and Renato Renner. Localization of toric code defects. *Phys. Rev. Lett.*, 107:030504, 07 2011.

[100] James R. Wootton and Jiannis K. Pachos. Bringing order through disorder: Localization of errors in topological quantum memories. *Phys. Rev. Lett.*, 107:030503, 07 2011.

[101] Sergey Bravyi and Robert Koenig. Disorder-assisted error correction in majorana chains. arXiv:1108.3845.

[102] Sergey Bravyi, Bernhard Leemhuis, and Barbara M. Terhal. Topological order in an exactly solvable 3d spin model. *Ann. Phys.*, 326:839–866, 2011.

[103] Isaac H. Kim. Local non–calderbank-shor-steane quantum error-correcting code on a three-dimensional lattice. *Phys. Rev. A*, 83(5):052308–, 05 2011.

[104] R. Landauer. Dissipation and noise immunity in computation and communication. *Nature*, 335:779, 1988.

[105] Jacob D. Bekenstein. Universal upper bound on the entropy-to-energy ratio for bounded systems. *Phys. Rev. D*, 23:287, 1981.

[106] S. Hawking. Particle creation by black holes. *Commun. Math. Phys.*, 43:199–220, 1975.

[107] Leonard Susskind. The world as a hologram. *J. Math. Phys.*, 36:6377, 1995.

[108] Roger Penrose. Angular momentum: an approach to combinatorial space-time. In *Quantum Theory and Beyond*. Cambridge Univertity Press, 1971.

[109] Carlo Rovelli and Lee Smolin. Spin networks and quantum gravity. *Phys. Rev. D*, 52:5743–5759, 1995.

[110] D. Roy Chowdhury, S. Basu, I. Sen Gupta, and P. Pal Chaudhuri. Design of caecc - cellular automata based error correcting code. *IEEE Transactions on Computers*, 43:759–764, 1994.

[111] Stephen Wolfram. *A new kind of science*. Wolfram Media Inc. Champaign., 2002.

[112] V. Efimov. Energy levels arising from resonant two-body forces in a three-body system. *Physics Letters B*, 33:563–564, 1970.

[113] V. Efimov. Energy levels of three resonantly interacting particles. *Nucl. Phys. A*, 210:157–188, 1973.

[114] P. F. Bedaque, H. W. Hammer, and U. van Kolck. Renormalization of the three-body system with short-range interactions. *Phys. Rev. Lett.*, 82:463, 1999.